8-1-2009

Concrete Deck Cracking Investigation SR309 over Church Road, Montgomery County, PA

Ian C. Hodgson

Stephen Pessiki

Concrete Deck Cracking Investigation
SR309 over Church Road
Montgomery County, Pennsylvania

Final Report

by

Stephen Pessiki

Ian C. Hodgson

ATLSS Report No. 09-07

August 2009

ATLSS is a National Center for Engineering Research
on Advanced Technology for Large Structural Systems

117 ATLSS Drive
Bethlehem, PA 18015-4729

Phone: (610)758-3525
Fax: (610)758-5902

www.atlss.lehigh.edu
Email: inatl@lehigh.edu

Concrete Deck Cracking Investigation
SR309 over Church Road
Montgomery County, Pennsylvania

Final Report

by

Stephen Pessiki
Professor and Chairperson
Department of Civil and Environmental Engineering

Ian C. Hodgson
Research Engineer
ATLSS Engineering Research Center

ATLSS Report No. 09-07

August 2009

ATLSS is a National Center for Engineering Research
on Advanced Technology for Large Structural Systems

117 ATLSS Drive
Bethlehem, PA 18015-4729

Phone: (610)758-3525
Fax: (610)758-5902

www.atlss.lehigh.edu
Email: inatl@lehigh.edu

TABLE OF CONTENTS

LIST OF FIGURES

LIST OF TABLES

ABSTRACT

This report concerns the investigation into the cause of cracking in the concrete deck of the bridge carrying SR 309 over Church Road in Montgomery County, Pennsylvania. Similar cracking has been observed on two other bridges that were recently constructed. The focus of this report is the SR309 bridge over Church Road, though the findings of this study may apply to the other bridges as well.

The primary goal of this investigation was to assess the observed cracking and determine the likely cause of the cracking. This assessment has been based on a review of pertinent project data, field investigations, and computer analyses. Previous forensic petrographic testing reports, design drawings, concrete mix design, construction materials utilized, and construction procedures and specifications for the placement of the deck concrete were provided by PennDOT and were reviewed. Additionally, a number of site visits to the bridge were performed. During these visits, detailed photographs were taken at selected areas of the cracked deck to document the nature of the cracks. Three core samples were removed from the bridge deck and subjected to detailed petrographic analyses. The petrographic analysis was used to assess the composition of the concrete and make a determination whether the characteristics of the material itself contributed to the observed cracking. The petrographic analysis was also used to provide insight into the age of the concrete when the cracking occurred. Digital image correlation testing was performed to assess whether the existing cracks in the deck are opening and/or closing under traffic loading. In addition to the field studies, computer modeling of the deck slab was performed. Both elastic stress analyses and thermal analyses of the deck were performed.

The study concluded that: (1) The observed cracking is not caused by any inherent material property defect in the concrete mixture. The concrete appears to have been batched, placed and cured properly. The cement used to make the concrete did exhibit a high fineness more like a Type III cement; (2) The observed transverse cracking likely occurred early in the life of the concrete, when the concrete was plastic, semi-plastic, or shortly thereafter. This is based upon the observation that the transverse cracking circumscribes aggregate particles and thus occurred when the concrete had very little strength; (3) The observed transverse cracking in the structure is most likely due to thermal gradients in the slab early in the life of the concrete caused by heat generated by hydration of the cement and slag in the concrete. An increase in the rate of heat generation caused by an increase in cement fineness as reported in the petrography analysis will increase the thermal gradient present in the slab; (4) The observed longitudinal cracking occurred later in the life of the concrete when the concrete had gained some appreciable strength. This is based on the observation that the longitudinal cracking transects aggregate particles and thus occurred when the concrete had some appreciable strength, and relatively greater strength than when the transverse cracking formed; (5) The observed longitudinal cracking may be due in part to early-age construction loading, but more likely includes significant contributions of other effects including drying shrinkage and possibly stress concentrations due to the mild steel reinforcing and / or other stress concentrations in the deck.

Recommendations from the study are: (1) To prevent similar cracking in future similar concrete deck placements (whether replacement decks or new decks), consideration should be given to factors that influence the temperature distribution in the deck and a thermal management plan should be implemented. This thermal management plan should consider all factors that influence the temperature distribution in the deck at early ages. Implementation of the thermal management plan may include the need for additional specifications that govern the construction of the decks; (2) To gain further insight in to current practice, the following is recommended: (a) concrete decks currently under construction should be instrumented with thermocouples to measure the temperature distribution in the slabs at early ages, (b) the constituent materials used in the actual concrete mixtures used for these same decks should be further quantified to understand the properties of the cement that influence heat generation, and (c) careful inspection of these same decks for cracking should be performed to better identify when cracking occurs should it occur. This, combined with thermocouple data as described above, may provide additional insight into the early-age cracking phenomenon; (3) An experimental program should be undertaken to study in a controlled manner the issue of thermal cracking in concrete bridge decks at early ages. Such a program would provide information that may be gained from monitoring actual bridge decks under construction, but would be done in a controlled manner that would allow a systematic variation in key parameters to provide detailed insight into the cracking phenomenon and thus would inform the development of any thermal management plan and changes in specifications for the construction of new or replacement concrete bridge decks.

Engineers from Michael Baker, Inc. reviewed five options for remediation of the observed cracking in the concrete deck of this bridge. These options included (1) do nothing; (2) apply a deck/crack sealer; (3) install an asphalt overlay with membrane waterproofing; (4) install a concrete overlay; and (5) replace the deck. BAKER recommends that a methyl methacrylate (MMA) deck sealer be used to repair the observed cracking. Two commercially available products are suggested.

1. INTRODUCTION

1.1 Background

This report concerns the investigation into the cause of cracking in the concrete deck of the bridge carrying SR 309 over Church Road in Montgomery County, Pennsylvania. Figure 1.1 shows a photograph of the bridge during the recent rehabilitation project. The existing bridge was widened and redecked as a part of this project.

Unexpected cracking was first observed in the deck of this bridge in October 2006, just before the bridge was opened to traffic. It is not clear when the cracking may actually have occurred. Similar cracking has been observed on two other bridges that were recently constructed. The focus of this report is the SR309 bridge over Church Road, though the findings of this study may apply to the other bridges as well.

Figure 1.1 – Aerial view of SR309 over Church Road Bridge during widening construction looking northwest (Stage 5 under construction) [PennDOT 2007]

1.2 Bridge Description

The original bridge comprised twelve riveted steel girders supporting a non-composite concrete deck, with three spans (77 ft.-136 ft.-77 ft.) carrying SR309 over Church Road. Each girder line was configured with pin and hangers at two locations in the center span creating two back spans and a central suspended span. Each girder is approximately 6 ft. 4 in. deep. The bridge is skewed approximately 35 degrees.

In 2005-2006, the bridge underwent a major rehabilitation. The existing concrete deck was removed. The bridge was widened on both sides through the addition of two continuous welded steel plate girders on each side (a total of four new girders in the cross-section). These new girders are approximately 4 ft. deep. Each of the existing riveted plate girders was made continuous through the removal of all pin and hangers and the addition of bolted splice plates across both flanges and the web. The new 8-1/4 in.

concrete deck was placed compositely with the existing and new steel girders. The concrete was placed on steel stay-in-place (SIP) forms (2 in. deep, 8-1/2 in. flute spacing). The form flutes were filled with polystyrene foam to reduce weight. Sound barriers were installed on both sides of the bridge. Photographs of the completed bridges are shown in Figures 1.2 and 1.3.

Figure 1.2 – View of SR309 bridge over Church Road looking east

Figure 1.3 – View of SR309 bridge over Church Road looking northwest at Abutment 2

1.3 Construction Staging

The bridge rehabilitation proceeded in five stages. Traffic was maintained across the bridge during each stage. Stages 3, 4, and 5 entailed the successive demolition of existing deck slab and placement of the new deck slab. Figure 1.4 is a schematic drawing of the original cross-section of the bridge. As shown, there were originally 12 steel girders (spaced at 6 ft. 5 in. on center with 4 ft. between the two center girders).

Stage 3 of construction was completed first, followed by Stage 4 and 5. Figure 1.5 presents two schematic drawings of the bridge cross-section during Stage 3 of rehabilitation. The upper drawing shows the cross-section after deck demolition while the lower drawing presents the cross-section after placement of the new deck. Similar drawings are presented for construction Stages 4 and 5 in Figure 1.6 and Figure 1.7, respectively.

The design drawings for the bridge indicate that the deck placement was to proceed in three pours. The first was specified in the positive moment regions at the ends of the bridge. The second was to be at the positive moment region in Span 2. The final pour was to be in the negative moment regions over the two piers. This pour sequence was used for Stage 4.

The contractor submitted an alternate pour sequence which was approved by PennDOT and used for Stages 3 and 5. With this sequence, deck placement proceeded in two steps. First, concrete was placed in the positive moment regions at the ends of the bridge. The second step entailed a continuous pour of the remaining deck. A summary of the placement sequence is presented in Figure 1.8. This figure also provides the dates of concrete placement. It can be seen that Stage 3 was completed first in March/April 2005. This was followed by Stage 4 (October 2005) and Stage 5 (May 2006).

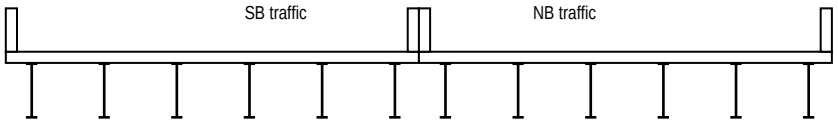

Figure 1.4 – As-built condition (pre-rehabilitation)

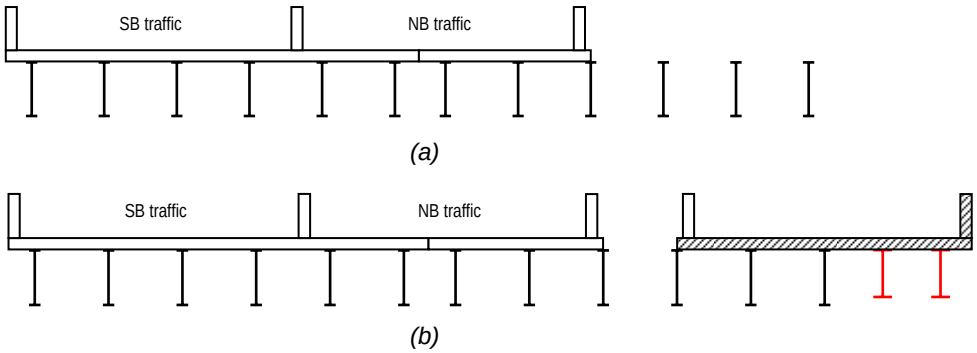

Figure 1.5 – Stage 3 of rehabilitation - (a) after deck demolition; (b) after placement of new deck

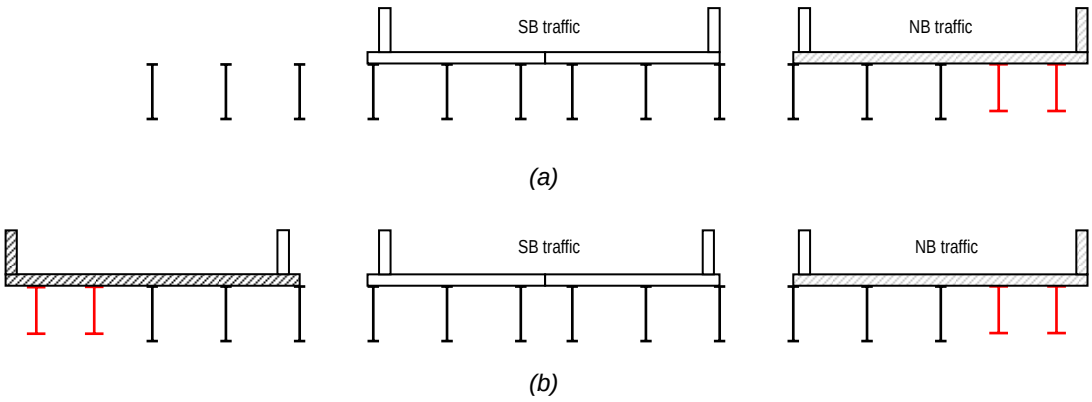

Figure 1.6 – Stage 4 of rehabilitation - (a) after deck demolition; (b) after deck placement

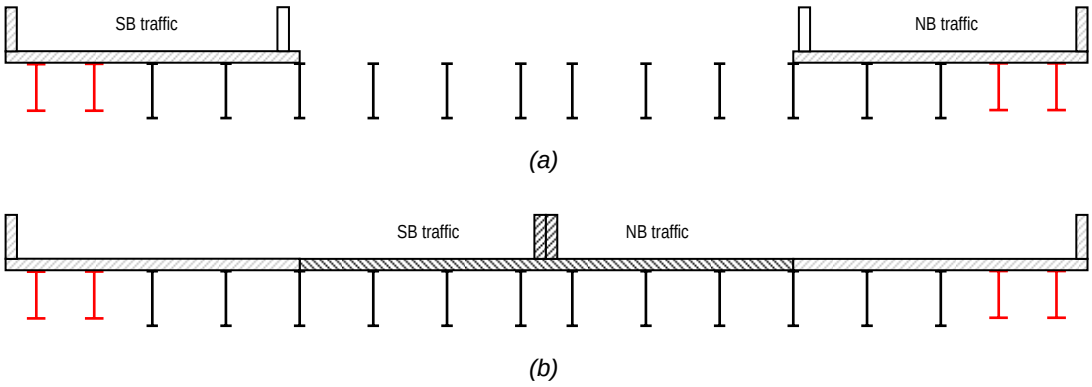

Figure 1.7 – Stage 5 of rehabilitation - (a) after deck demolition; (b) after deck placement

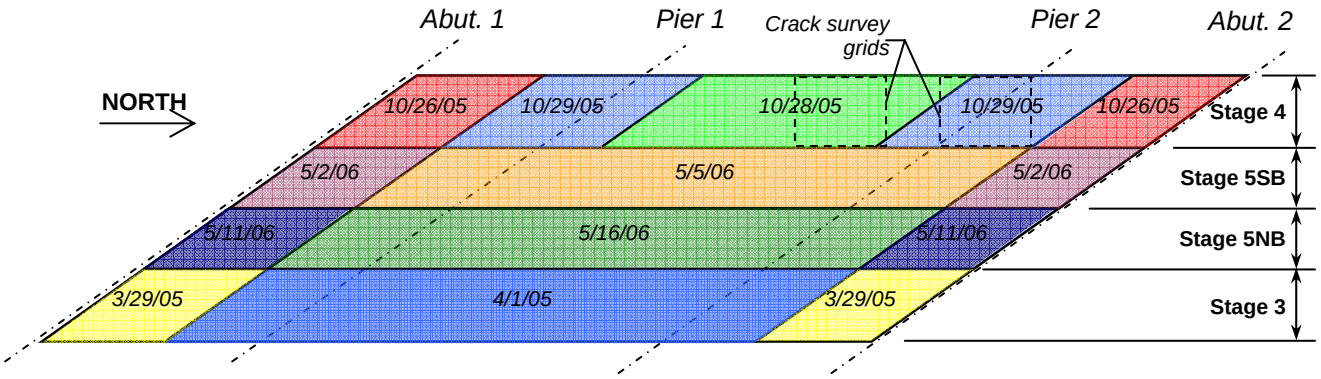

Figure 1.8 – Plan view of rehabilitated bridge deck indicating locations and dates of concrete placement

1.4 Deck Curing

After concrete placement, the deck surface was sprayed with an approved curing compound. Subsequently the deck was covered with wet burlap and white polyethylene sheeting for the duration of the cure period. Soaker hoses connected to a water tank/truck were used to maintain the saturation of the wet burlap.

1.5 Objectives and Approach

The primary goal of this investigation was to assess the observed cracking and determine the likely cause of the cracking. This assessment has been based on a review of pertinent project data, field investigations, and computer analyses.

Previous forensic petrographic testing reports, design drawings, concrete mix design, construction materials utilized, and construction procedures and specifications for the placement of the deck concrete were provided by PennDOT and were reviewed.

Additionally, a number of site visits to the bridge were performed. During these visits, detailed photographs were taken at selected areas of the cracked deck to document the nature of the cracks. In these areas, a grid pattern was laid out on the bridge deck where cracks were found. Photographs were taken of each area of the grid and were subsequently merged into a single composite image of the bridge deck.

Three core samples were removed from the bridge deck. These core samples were sent out for petrographic analyses. The petrographic analysis was used to assess the composition of the concrete and make a determination whether the characteristics of the material itself contributed to the observed cracking. The petrographic analysis was also used to provide insight into the age of the concrete when the cracking occurred.

Digital image correlation testing was performed assess whether the existing cracks in the deck are opening and/or closing under traffic loading. The equipment used comprises two cameras. Reference images are taken of the deck surface without traffic nearby. A fully loaded tri-axle test truck was supplied by PennDOT and used to load the bridge in the vicinity of the test area. A second set of images were taken of the deck under load. By comparing the two images, measurements of the displacements and strains were obtained. These measurements can be used to assess whether existing cracks are opening/closing as a result of load on the deck surface.

In addition to the field studies, computer modeling of the deck slab was performed. Both elastic stress analyses and thermal analyses of the deck were performed.

From the analytical and testing results, a determination of the likely causes of the cracking, and recommendations for acceptance, remediation or replacement of the concrete decks are made.

1.6 Summary of Findings

1. The observed cracking is not caused by any inherent material property defect in the concrete mixture. The concrete appears to have been batched, placed and cured properly. The cement used to make the concrete did exhibit a high fineness more like a Type III cement.
2. The observed transverse cracking likely occurred early in the life of the concrete, when the concrete was plastic, semi-plastic, or shortly thereafter. This is based upon the observation that the transverse cracking circumscribes aggregate particles and thus occurred when the concrete had very little strength.
3. The observed transverse cracking in the structure is most likely due to thermal gradients in the slab early in the life of the concrete caused by heat generated by hydration of the cement and slag in the concrete. An increase in the rate of heat

generation caused by an increase in cement fineness as reported in the petrography analysis will increase the thermal gradient present in the slab.

4. The observed longitudinal cracking occurred later in the life of the concrete when the concrete had gained some appreciable strength. This is based on the observation that the longitudinal cracking transects aggregate particles and thus occurred when the concrete had some appreciable strength, and relatively greater strength than when the transverse cracking formed.
5. The observed longitudinal cracking may be due in part to early-age construction loading, but more likely includes significant contributions of other effects including drying shrinkage and possibly stress concentrations due to the mild steel reinforcing and / or other stress concentrations in the deck.

1.7 Summary of Remediation Recommendations

Engineers from Michael Baker, Inc. reviewed five options for remediation of the observed cracking in the concrete deck of this bridge. These options included (1) do nothing; (2) apply a deck/crack sealer; (3) install an asphalt overlay with membrane waterproofing; (4) install a concrete overlay; and (5) replace the deck. BAKER recommends that a methyl methacrylate (MMA) deck sealer be used to repair the observed cracking. Two commercially available products are suggested.

1.8 Organization of this Report

Section 2 presents results of the field investigations. Section 3 presents the findings of the petrographic analysis of three core samples removed from the bridge. Section 4 presents an analysis to investigate the possibility of load-induced longitudinal cracking. Section 5 presents an analysis to investigate the possibility of thermal-induced transverse cracking. Section 6 presents a discussion of the results. A summary of the recommendations for remediation is presented in Section 7. Conclusions and recommendations from the investigation are presented in Section 8.

2. FIELD INVESTIGATIONS

2.1 Summary of Field Visits

A number of field visits were performed. The purpose of these field visits was to inspect and document the deck cracking, to remove core samples, and to perform digital image correlation testing. Section 2.2 presents the findings of the documentation of the deck cracking that was performed. The digital image correlation testing that was performed is presented in Section 2.3. The results of the petrographic examination of the core samples is presented in Section 3.

An initial site visit was performed on June 3, 2008. The purpose of this visit was to make an initial assessment of the nature of the cracks and to become familiarized with the bridge. The bridge was examined from the shoulder with assistance from PennDOT (no lane closures were set up).

A second visit to the bridge was performed on October 9, 2008. During this visit several tasks were performed. First, a crack survey grid was laid out on the bridge deck in the southbound shoulder and right lane in the negative moment region centered over Pier 2. Photographs were taken of each square of the grid. Second, an initial trial of the digital image correlation system was performed in the southbound shoulder in Span 1. The southbound right lane was closed for the duration of the work under the direction of PennDOT.

A third visit to the bridge was performed on October 23, 2009. During this visit, three core samples were removed from the bridge deck for petrographic testing. The cores were extracted from three locations within the crack survey grid over Pier 2 (negative moment region). The cores were taken through transverse and longitudinal cracks. The southbound right lane was closed for the duration of the work under the direction of PennDOT.

A final visit to the bridge was conducted on March 18, 2009. During this visit, a second crack survey grid was laid out with identical dimensions but located within Span 2 in the positive moment region. The southbound right lane was closed under the direction of PennDOT for the duration of the work.

2.2 Documentation of Deck Cracking

Two crack survey grids were laid out on the bridge. Both grids were located in the southbound shoulder and right lane (Stage 4 concrete placement), with one grid located over Pier 2 in the negative moment region and one grid at midspan of Span 2 in the positive moment region. Each grid comprised 3 ft. by 3 ft. squares, with ten squares (a total of 30 ft.) in the direction of traffic and eight squares (a total of 24 ft.) transversely starting from the face of the west parapet.

Figure 2.1 is a schematic drawing of the bridge deck (Stage 4 placement). The figure indicates where the positive and negative moment region crack survey grids were placed.

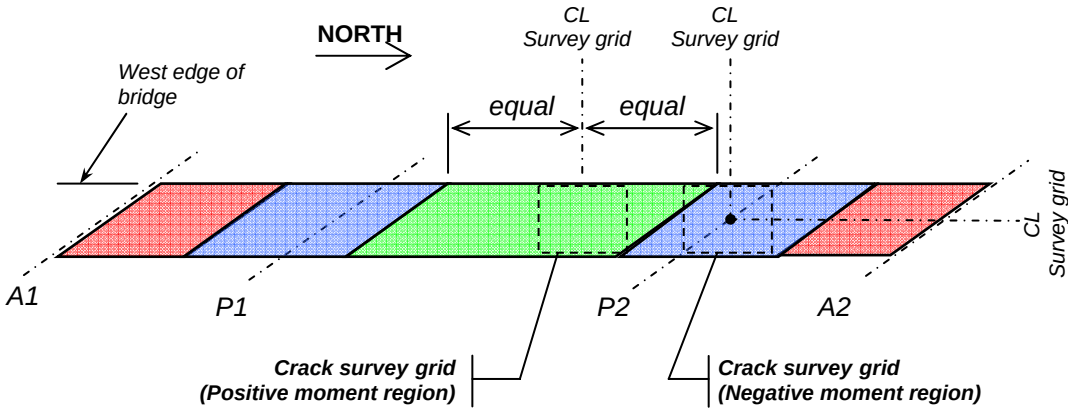

Figure 2.1 – Location plan of the two crack survey grids of the Stage 4 deck

Each grid square is identified by its row and column number. Figure 2.2 presents the numbering system used for the two crack survey grids. A photograph of each square was taken with a camera mounted to a tripod. Care was taken to ensure that each photograph was taken from the same position relative to each square. Adobe Photoshop was used to correct each photograph for perspective yielding a square image. As an example, Figure 2.3 shows the raw image of Square 6-7 in the negative moment region. This image was cropped and corrected for perspective using Photoshop. The resulting image is shown in Figure 2.4. The images were then combined to form a composite image of the survey area.

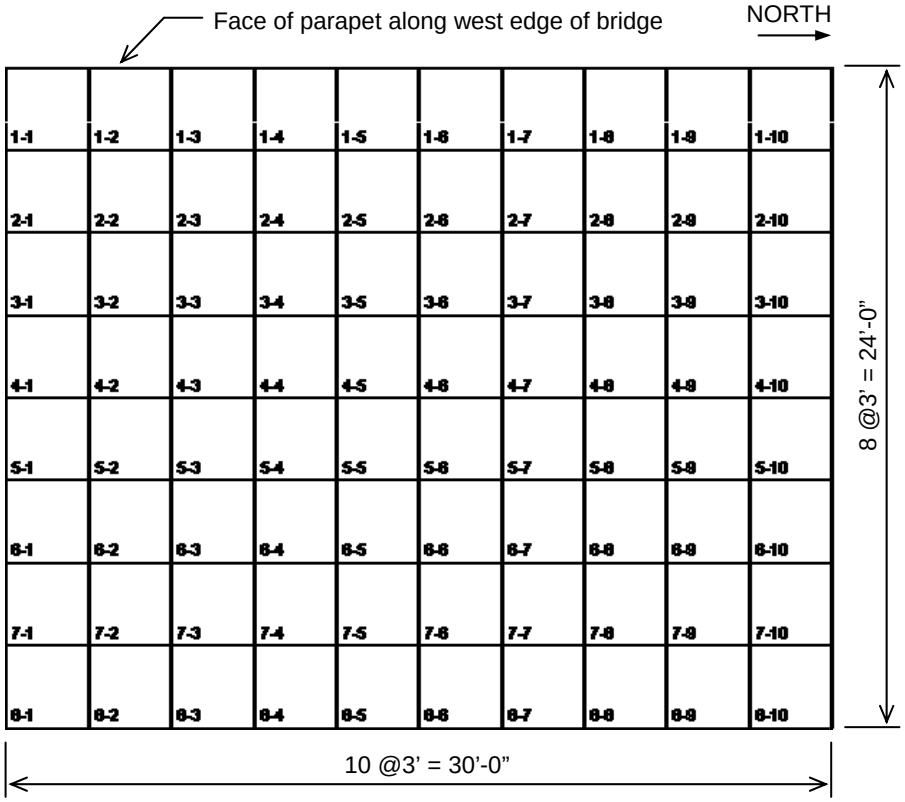

Figure 2.2 – Layout and numbering of crack survey grids located in the southbound shoulder and right lane

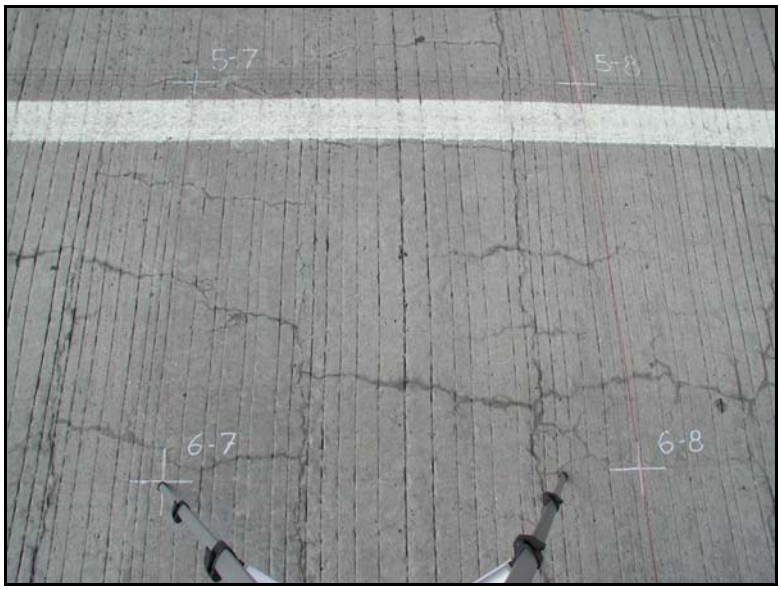

Figure 2.3 – Raw image of Square 6-7 in negative moment region

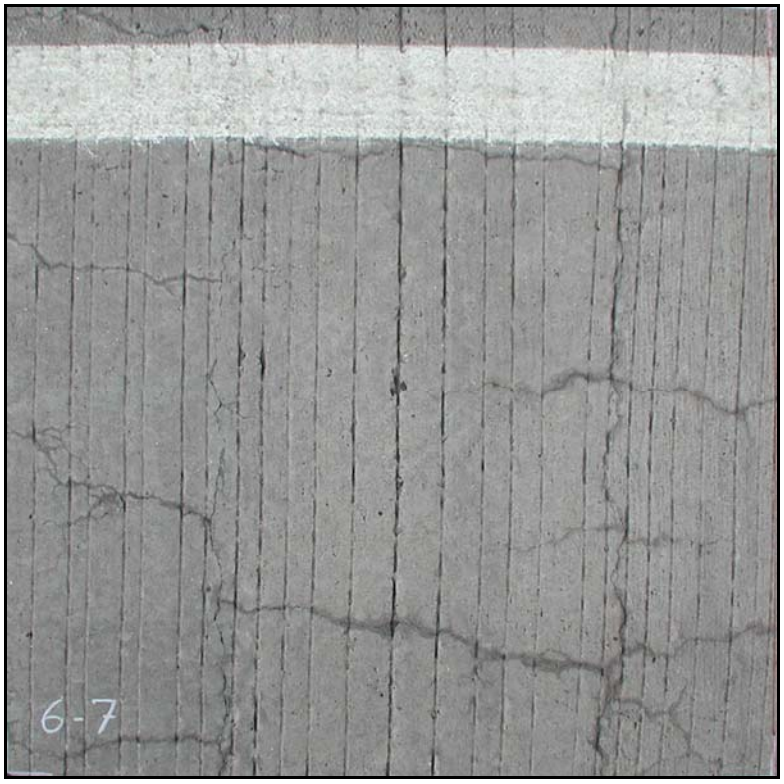

Figure 2.4 – Image of Square 6-7 in negative moment region after correction for perspective using Photoshop

2.2.1 Negative Moment Crack Survey

Figure 2.5 is the composite image of the negative moment crack survey grid. The crack locations have been highlighted in the composite image for clarity. The transverse locations of Girders G1 through G5 are indicated in the figure. Girders G1 and G2 are the new welded steel plate girders while Girders G3, G4, and G5 are original riveted plate girders. Locations of the diaphragms are also shown in the figure. A number of diaphragms exist and are either perpendicular to the girders or parallel with the pier. The roadway stripe separating the shoulder (upper portion of the image) from the southbound right lane (lower portion of the image) can be seen between Girders G3 and G4.

It can be seen that both transverse and longitudinal cracks exist in the deck. The transverse cracks appear to be fairly regularly spaced between 12 and 24 in. There are a series of longitudinal cracks along Girders G3 and G4, and to a somewhat lesser extent along Girder G5. In general, the transverse cracking is more extensive as compared to the longitudinal cracking.

In this region, the top mat of reinforcement comprises transverse and longitudinal #5 bars at 6 in. spacing. The transverse bars rest atop the longitudinal bars. The slab is specified as being 8-1/4 in. thick with 2-1/2 in. clear cover to the transverse bars.

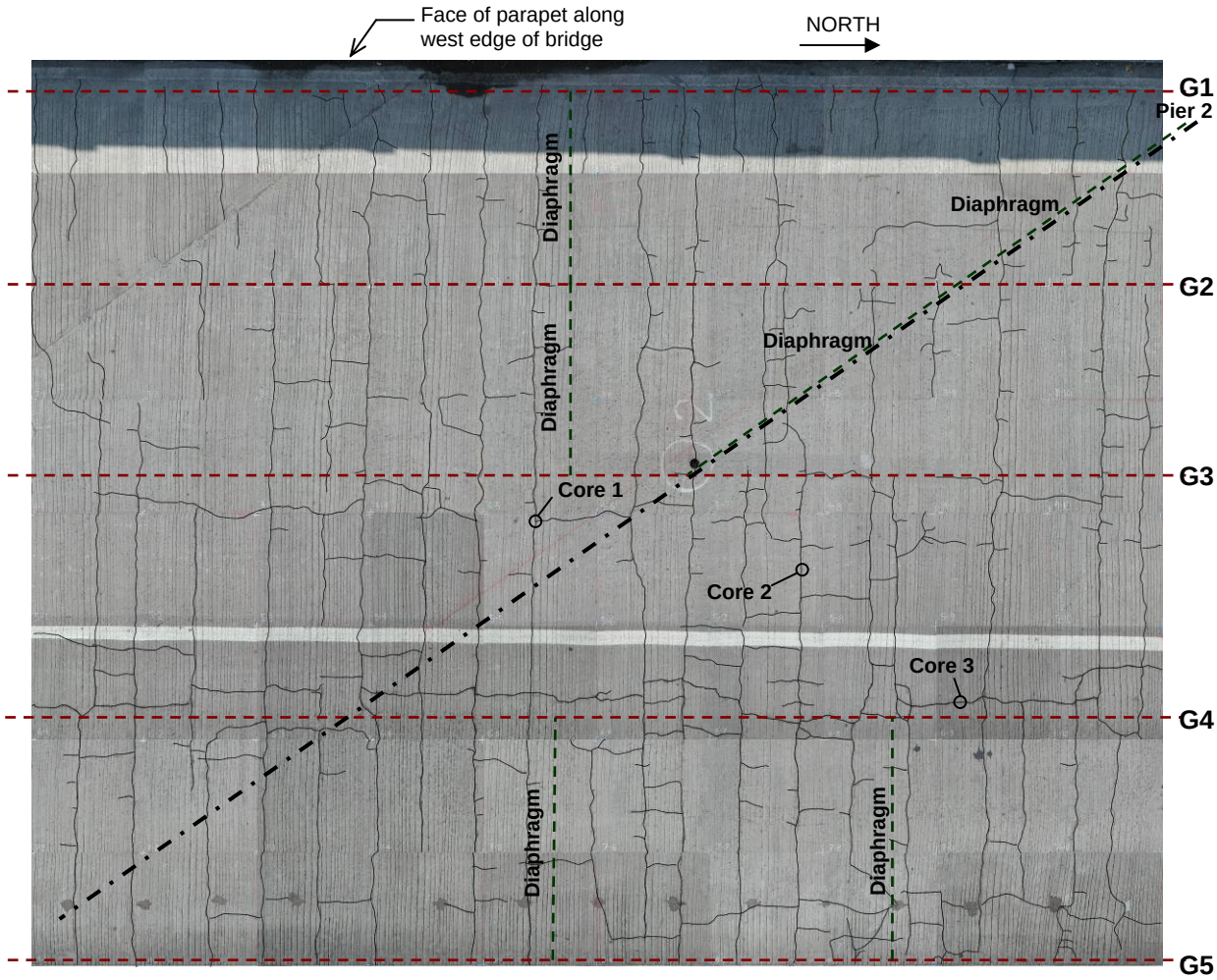

Figure 2.5 – Composite image of cracking in negative moment crack survey grid

Figure 2.6 is an image of the negative moment crack survey grid with an overlay showing the grid identification numbers.

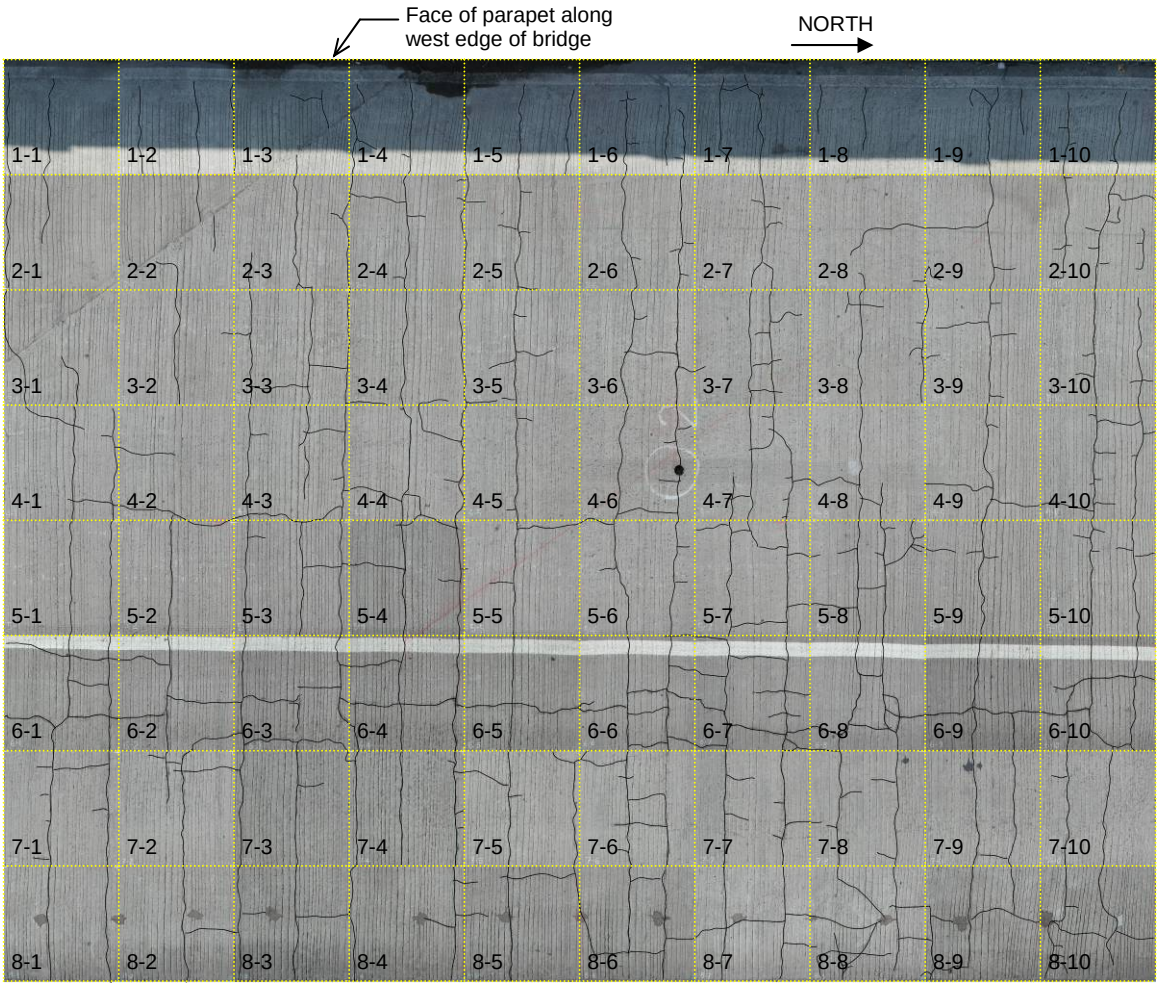

Figure 2.6 – Composite image of cracking in negative moment crack survey grid with grid numbering overlay

2.2.2 Positive Moment Crack Survey

Figure 2.7 is the composite image of the positive moment crack survey grid. The crack locations have been highlighted for clarity. Again, the locations of Girders G1 through G5 are indicated in the figure. The roadway stripe separating the shoulder (upper portion of the image) from the southbound right lane (lower portion of the image) can be seen between Girders G3 and G4.

It can be seen that similar to the negative moment survey region, both transverse and longitudinal cracks exist in the deck. The transverse cracks have a larger spacing than in the negative moment region, with a spacing of approximately 36 in. There are a series of longitudinal cracks along Girder G4. Similar to the negative moment region, in general the transverse cracking is more extensive as compared to the longitudinal cracking.

In this region, the top mat of reinforcement comprises transverse #5 bars at 6 in. spacing and longitudinal #4 bars at 12 in. spacing. The transverse bars rest atop the longitudinal bars. The slab is specified as being 8-1/4 in. thick with 2-1/2 in. clear cover to the transverse bars.

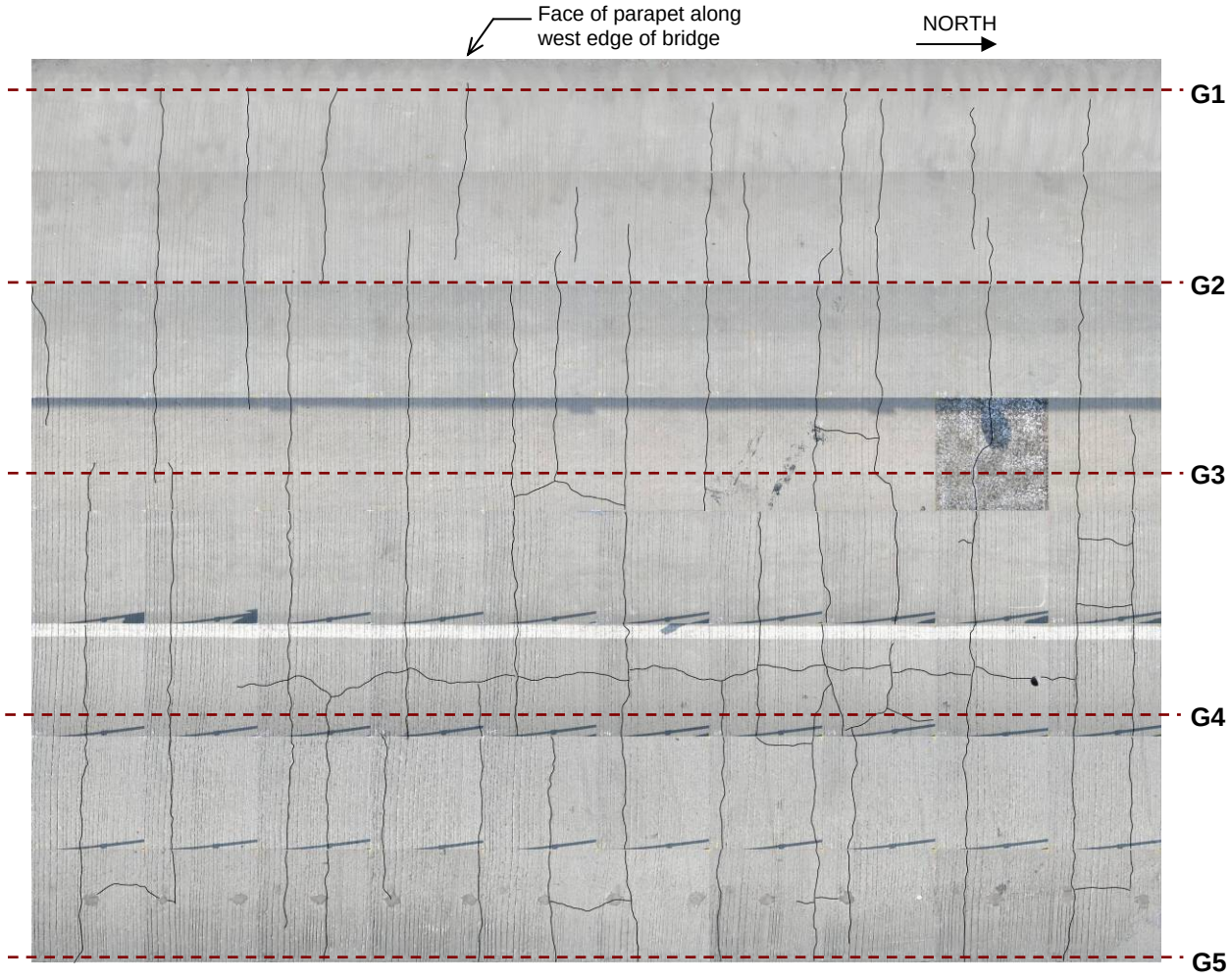

Figure 2.7 – Composite image of cracking in positive moment crack survey grid

Figure 2.8 is the crack survey grid from the positive moment region with an overlay showing the grid identification numbering.

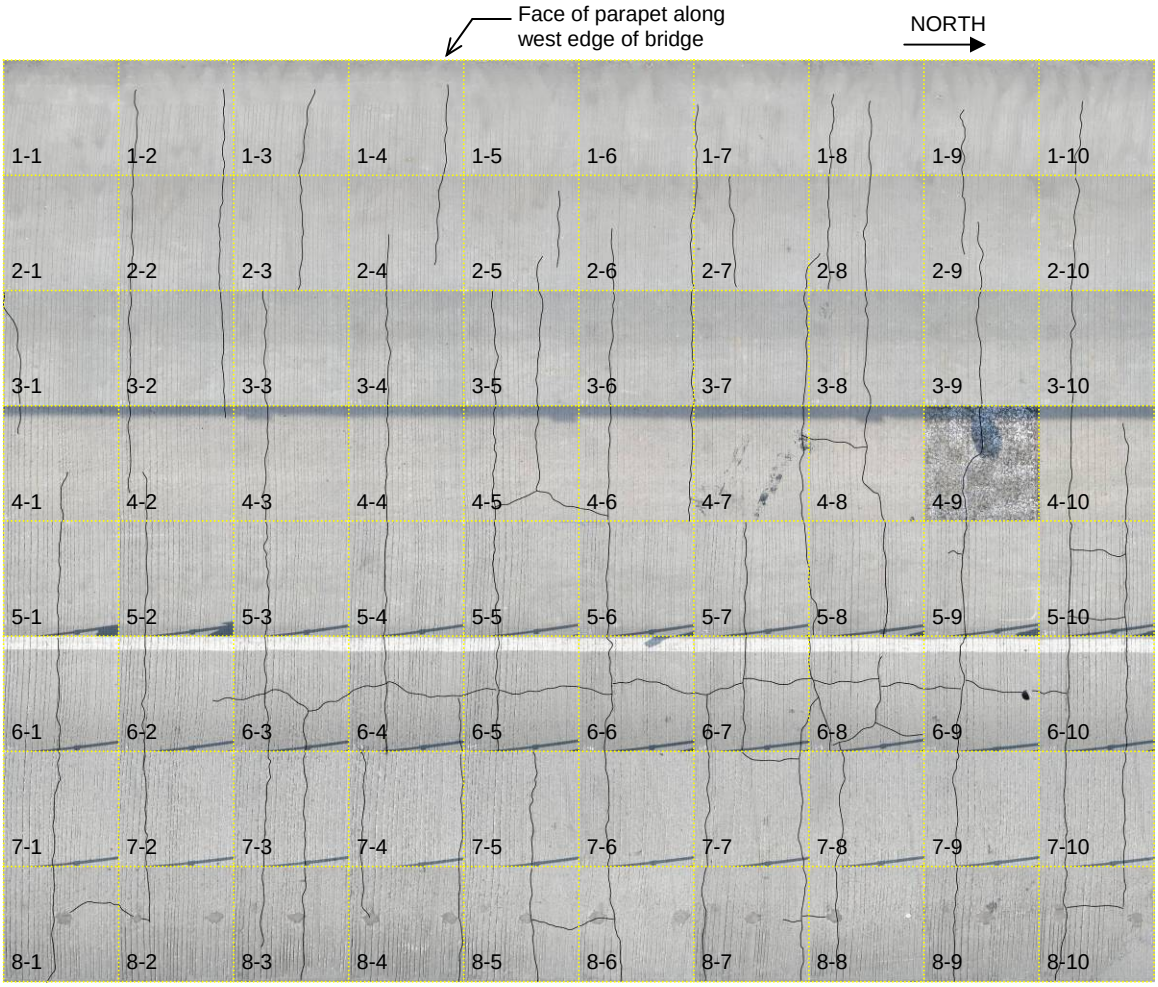

Figure 2.8 – Composite image of cracking in positive moment crack survey grid with grid numbering overlay

2.3 Digital Image Correlation Testing

Digital image correlation testing was performed using a digital image correlation system manufactured by Trilion Optical Test Systems. The purpose of this testing was to evaluate whether the application of traffic load to the deck causes the cracks to open and/or close. The test system uses a pair of specialized camera to take simultaneous images of a test specimen (in this case the concrete deck surface) to which a random speckle pattern has been applied. A second set of images are taken after load has been applied altering the strain field in the test specimen. By comparing the two sets of images, the test system produces a displacement or strain contour of the surface of the test specimen.

An initial exploratory test was performed during a site visit of October 9, 2008. During this test, an existing crack monitored in the closed right-hand lane while traffic was present in the left-hand lane. This testing was performed primarily to evaluate the feasibility of the testing. Results of the exploratory tests suggested that the method was feasible and a decision was made to conduct further tests under controlled loading conditions.

2.3.1 Test Details

A second set of tests were performed on March 18, 2009 with a fully loaded tri-axle dump truck provided by PennDOT. The testing was performed in the positive moment region within the crack survey grid (Stage 4 deck placement). A photograph of the test truck used is presented in Figure 2.9. The truck had three main axles and a fourth floating rear axle which remained in the up position for all tests. The test truck was fully loaded with stone and had a gross vehicle weight (GVW) of 68,040 pounds (tare weight of 27,780 with 40,260 pounds of stone). The truck was weighed on scales at the loading facility immediately before departing for the bridge. The individual axles of the truck were not measured. However, the individual axle weights were estimated based on past test truck geometry and weight data. Table 2.1 contains the weight at each axle. Table 2.2 provides the key dimensions of the test truck.

Figure 2.9 – Test truck used during controlled load tests

Test Description	Rear Axle Type	Front Axle Load (lb)	Rear Axle Group Load (lb)	GVW[1] (lb)	Date of Tests
Controlled Load Tests	Tandem[2]	18,960[3]	49,080[3]	68,040	March 18, 2009

Note:
1. GVW = Gross Vehicle Weight
2. Floating third rear axle was in the up position for all tests.
3. Only GVW was measured. Individual axle loads are estimated based on past similar test truck weights and dimensions.

Table 2.1 – Test truck axle load data

Rear Axle	L1 (in)	L2 (in)	W_f (in)	W_r (in)	A (in)	B (in)	C (in)
Tandem	179	50	83	71	13	8.5	22

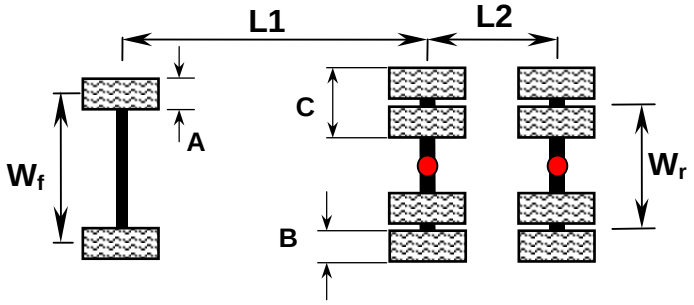

Table 2.2 – Geometry of test truck used for controlled load tests

Prior to performing these tests, a random speckle pattern was applied to the deck surface with black and white paint using rollers and sponges (see Figure 2.10). Subsequently a reference image was taken. This reference image was taken when no traffic was on the bridge. The truck was backed into position until it was as close to the field of view of the cameras as possible as shown in Figure 2.11 (generally 5 to 7 ft. from the rear axle). After the truck was stopped at this position, a second set of images were taken representing the loaded condition. Table 2.3 presents a summary of the load tests performed with the digital image correlation system. This table also shows the position of the test truck with respect to the view of the camera and the bridge.

Figure 2.10 – Application of random speckle pattern to concrete deck surface

Figure 2.11 – Position of test truck during load test

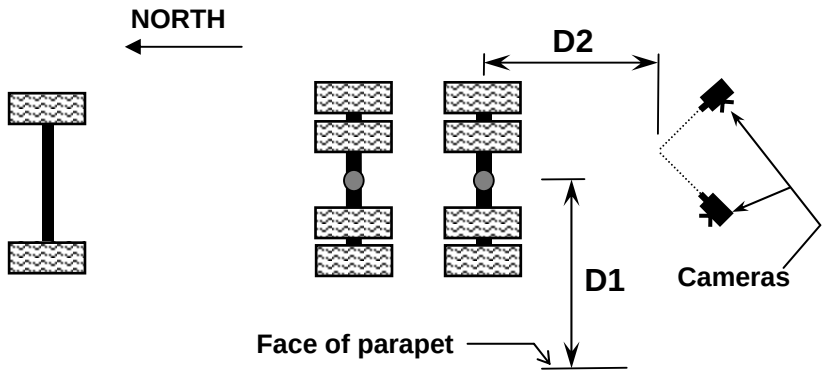

Test No.	Grid Location	D1	D2	Crack Type
1	6-8, 6-9	15’-0”	6’-6”	Longitudinal
2	6-8, 6-9	14’-0”	6’-8”	Longitudinal
3	4-9	10’-0”	5’-0”	Transverse
4	6-9	16’-0”	5’-0”	Longitudinal & Transverse
5	6-7	16’-6”	3’-6”	Transverse

Table 2.3 – Summary of load tests performed during digital image correlation testing. Note that tests were performed in the positive moment crack survey grid.

2.4 Findings

The results of this testing appear to indicate that bridge traffic will not lead to opening and/or closing of the cracks. Crack movements measured during the load tests were very low, with magnitudes of less than 1 mil.

3. PETROGRAPHIC INVESTIGATION

3.1 Introduction

Three core samples were removed from the bridge in October 2008 (see Figure 3.1). Complete petrographic examinations of each core were performed by Mr. Bernard Erlin of The Erlin Company. The complete petrography report is presented in Appendix A.

The purpose of these petrographic examinations was to assess whether the composition of the concrete was a factor in the development of the cracking observed in the surface of the deck, and to provide insight into the age of the concrete when the cracking occurred.

3.2 Core Sample Removal

As noted above, three core samples were removed from the deck and identified as Core #1, #2, and #3. Each core was taken through the full depth of the slab. The cores have 3-3/4 inch diameters and respective lengths of 8-3/4, 8-3/8, and 8-1/2 in. Top core ends are tined surfaces with impressions spaced variably but usually 1-3/4 to 2 in. apart; bottom core ends are formed surfaces. All cores were removed from within the negative moment crack survey grid located in Stage 4 slab over Pier 2 (southbound SR309 shoulder and right lane). A layout of the three cores with respect to the crack survey grid is presented in Figure 3.2.

Core #1 was taken at the intersection of a transverse and longitudinal crack, located within Grid 5-5, in the southbound shoulder. A detailed photograph of Grid 5-5 showing the location of Core #1 is presented in Figure 3.3. Finally, three photographs of Core #1 are shown in Figure 3.4.

Core #2 was taken through a transverse crack, located within Grid 5-7, in the southbound shoulder. A detailed photograph of Grid 5-7 showing the location of Core #2 is presented in Figure 3.5. Finally, three photographs of Core #2 are shown in Figure 3.6.

Core #3 was taken through a longitudinal crack, located within Grid 6-9, in the southbound right-hand lane. A detailed photograph of Grid 6-9 showing the location of Core #3 is presented in Figure 3.7. Finally, three photographs of Core #3 are shown in Figure 3.8.

Sections of green epoxy-coated No. 5 bars are present in the upper and lower part of Cores #1 and #2 and the upper half of Core #3. Associated with bars in Cores #1 and #2 are yellow epoxy-coated tie-wires. Sections of 7/32- and 3/16-inch diameter mesh are present in Core #1.

Each core was saw-cut to provide cross-sections for petrographic examinations. One-half inch-thick sections from the top and middle of each core were saw-cut for chloride analyses. Concrete remaining was broken up and used for more detailed petrographic examinations and depth of carbonation analyses as detailed in the petrography report presented in Appendix A.

Figure 3.1 – Coring operation during removal of Core #1

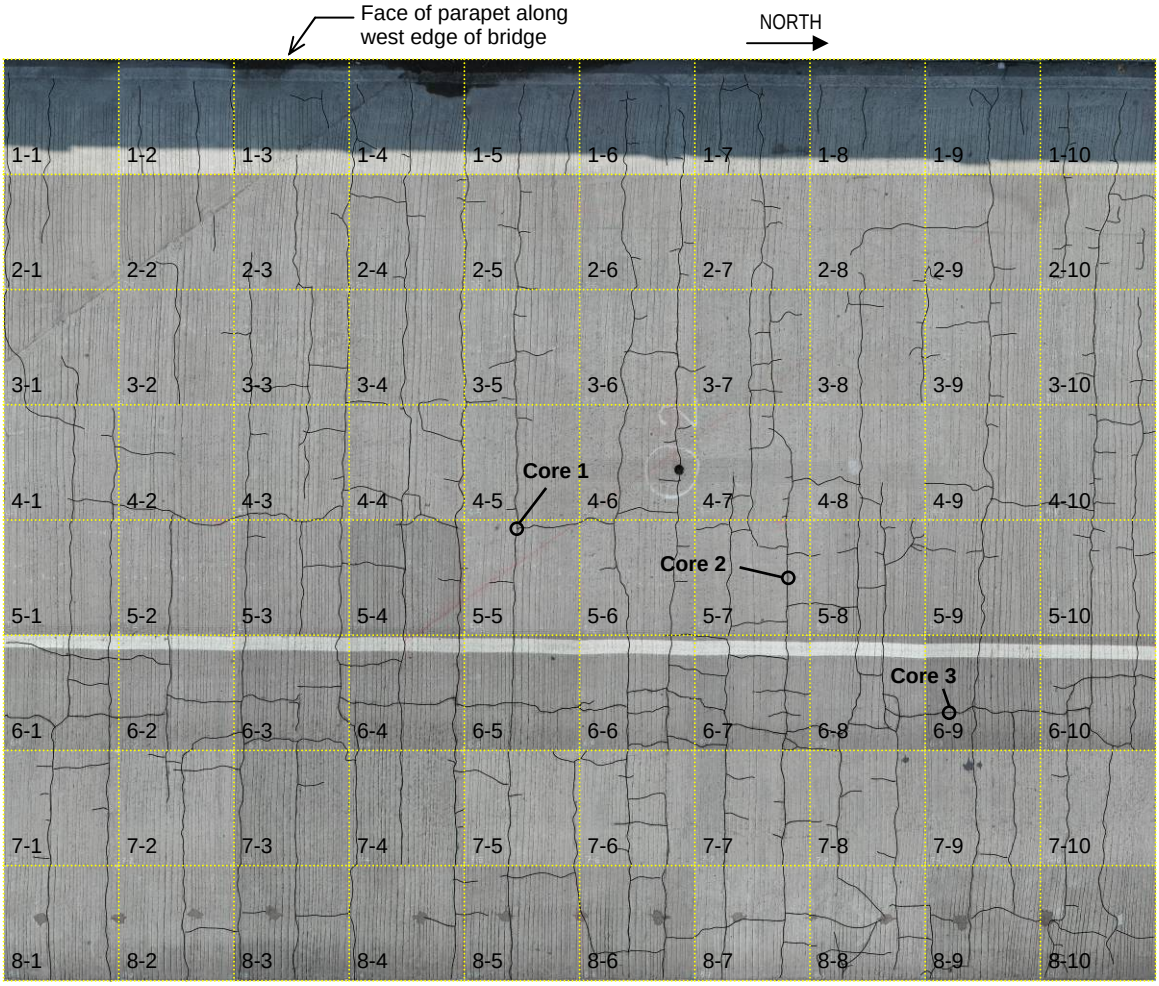

Figure 3.2 – Composite image of cracking in negative moment crack survey grid over Pier 2 in southbound shoulder and right-hand lane with grid numbering overlay

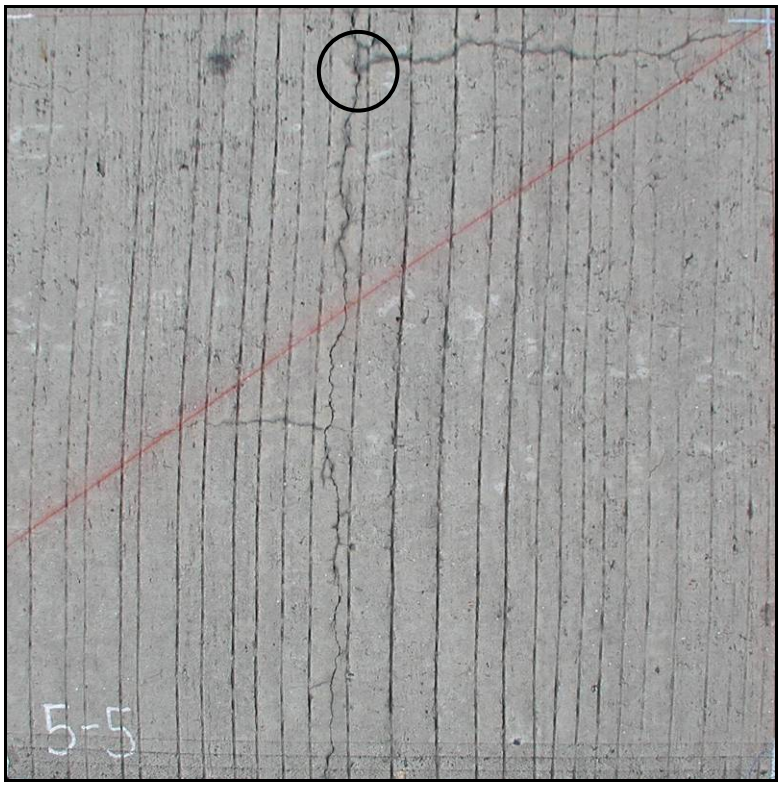

Figure 3.3 – Negative moment crack survey grid area 5-5 showing location of Core #1

(a) (b)

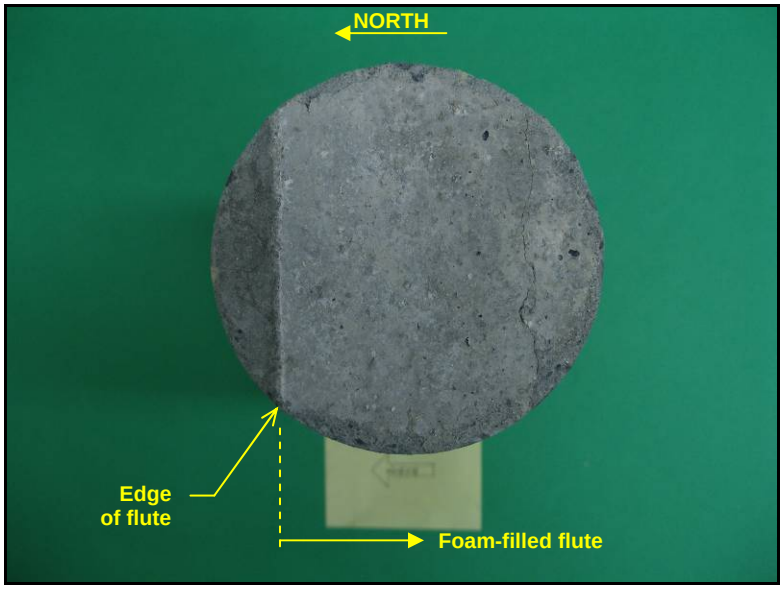

(c)

Figure 3.4 – Photographs of Core #1; (a) overall, (b) from the west side, (c) underside

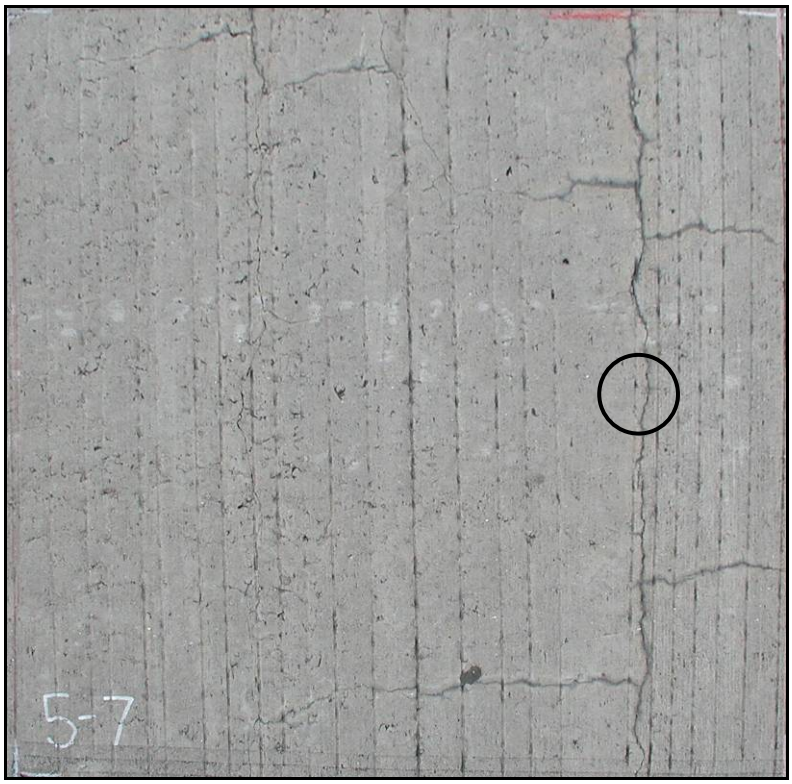

Figure 3.5 – Negative moment crack survey grid area 5-7 showing location of Core #2

(a) (b)

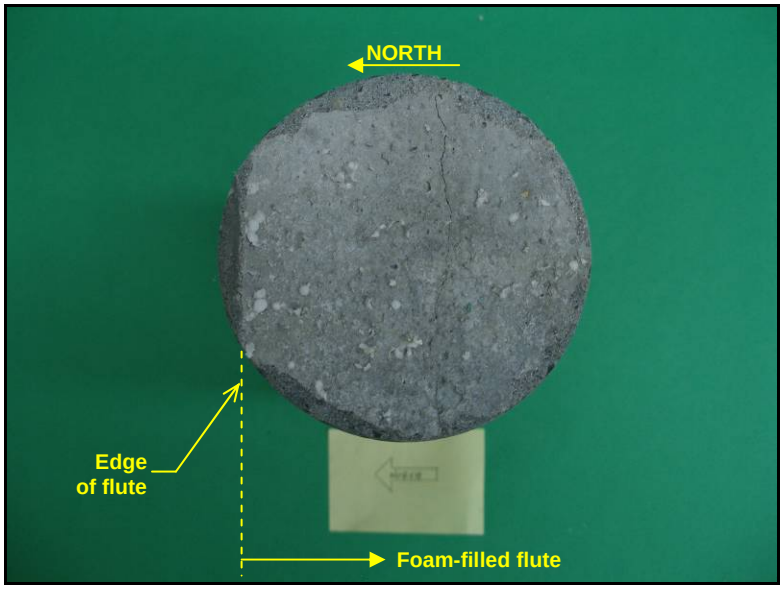

(c)

Figure 3.6 – Photographs of Core #2; (a) overall, (b) from the west side, (c) underside

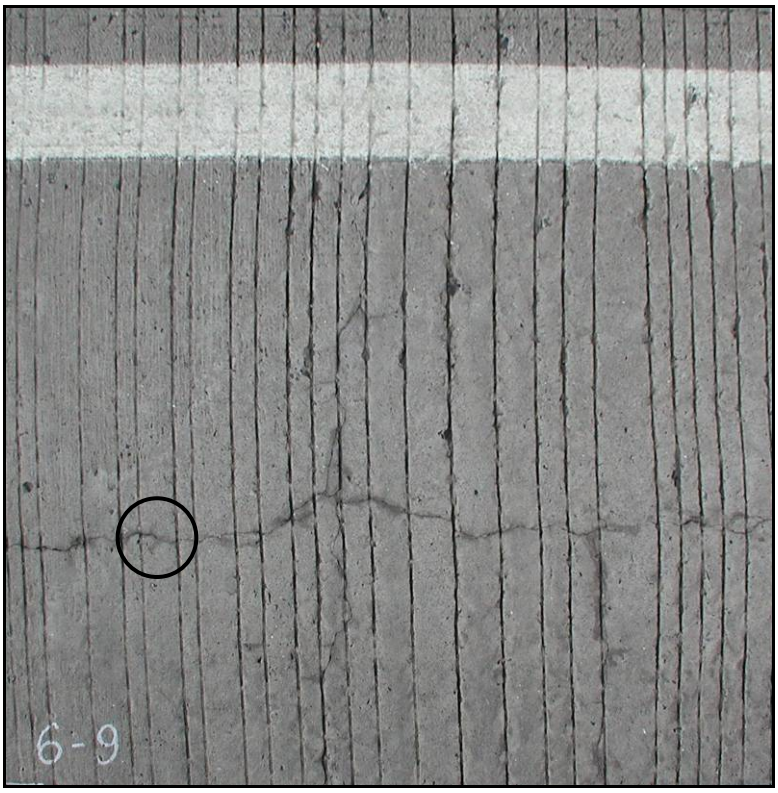

Figure 3.7 – Negative moment crack survey grid area 6-9 showing location of Core #3

(a) (b)

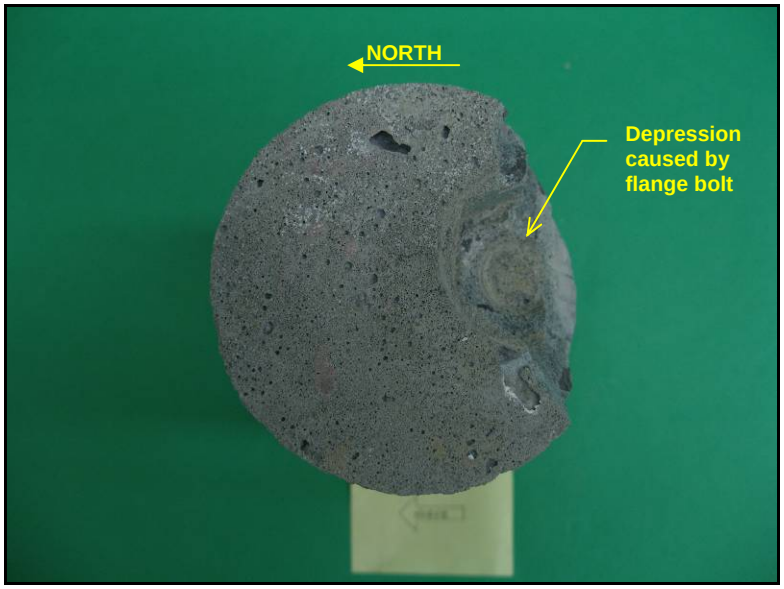

(c)

Figure 3.8 – Photographs of Core #3; (a) overall, (b) from the north side, (c) underside

3.3 Findings from Petrographic Analysis

Important findings from the petrographic analysis are as follows:

1. There do not appear to be any inherent problems with the material properties of the concrete. The components used to make the concrete, and their proportions, conform to the reported mix design. Hydration of the portland cement and slag are normal. Air content is adequate to provide freeze-thaw resistance. The depth of carbonation is shallow (1/16-inch or less) which indicates low-water cement ratio, adequate handling, placement and curing.

2. The cement used was found to have particles exhibiting high fineness more like a Type III cement which may have resulted in a faster heat generation rate.

3. A major vertical crack in Cores #1 and #2 extends the full depth of each core. The cracks circumscribe aggregate particles and occurred very early in the life of the concrete (e.g. when the concrete was plastic, semi-plastic, or shortly thereafter). These are transverse cracks in the bridge deck. Thus the transverse cracking in the bridge deck was caused by effects early in the life of the concrete.

4. A major vertical crack in Core #3 tightens with depth and terminates 2.5 in. from the bottom of the core. The crack transects numerous aggregate particles in contrast to the cracks that essentially circumscribe aggregate particles in the other two cores and, thus, occurred after there was significant aggregate-paste bond strength. The crack in Core #3 is a longitudinal crack in the bridge deck. Thus the longitudinal cracking in the bridge deck occurred later than the transverse cracking in the life of the concrete.

5. The observed cracking does not appear to be caused by alkali-silica aggregate reactivity.

6. There is evidence that concrete has been exposed to deicing salts but there is no evidence that the salts have caused any deterioration in the concrete.

7. There is no evidence of corrosion in the sections of reinforcing steel contained in the cores.

8. Dirt has infiltrated the cracks to depths of 4-1/2 in. in Core #1, 6 in. in Core #2, and 3 in. in Core #3. The presence of this dirt may influence attempts to repair the cracks.

4. ANALYSIS OF POSSIBLE LOAD-INDUCED LONGITUDINAL CRACKING

4.1 Background

Analyses were performed to investigate whether the longitudinal cracking may be due in part to construction loads on the deck prior to completion of the bridge. Figure 4.1 is a schematic drawing showing the moment diagram resulting from the placement of a set of rear truck axles centered over the first interior girder from the longitudinal construction joint during Stage 3 or 4 of construction. This configuration of the load results in a negative moment over the girder that induces tensile stresses in the top surface of the slab. This moment is higher than the moment induced after the deck has been completed due to the fact at this location the load is in an end span. After completion of the deck, the deck would be made continuous across the construction joint. The cracking pattern shown in Figure 2.5 appears to correspond to this theory as most of the longitudinal cracking occurs over Girder G4, the first interior support.

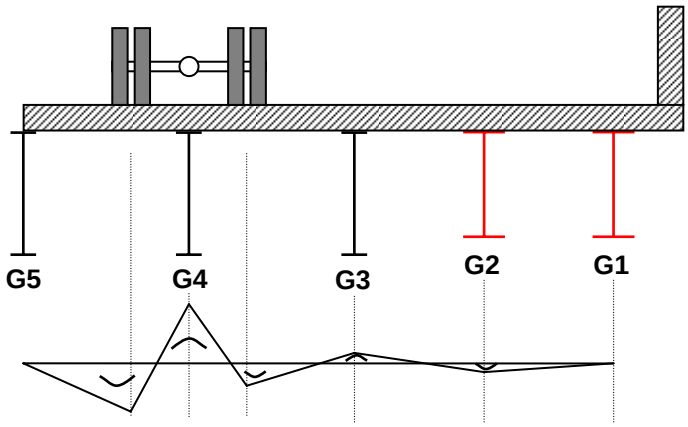

Figure 4.1 – Stage 4 of deck placement with heavy vehicle inducing negative moment over Girder 4 causing tension stresses in the top surface of the deck (Stage 3 placement similar)

4.2 SAP 2000 Analysis

To investigate whether the longitudinal cracking could have been caused by an overweight vehicle during construction, a simple static stress analysis was performed using SAP2000 Plus version 7.40. A model of the deck slab was created using four-noded elastic shell elements (see Figure 4.2).

Four spans of the deck were modeled similar to the schematic drawing of Figure 4.1. As shown, the girders are spaced at 6 ft.-5 in. (between original riveted girders) and 5 ft.-2 in. (between new welded girders). The slab elements were assigned a thickness of 8-1/4 in., and a modulus of elasticity 3600 ksi, equal to $57(f'_c)^{1/2}$, where f'_c is equal to approximately 4000 psi. The results were found to be insensitive to the assumed modulus.

A set of four point loads were applied downward on the deck surface. These four point loads represent a rear tandem axle of a heavy truck. Each point load is 15 kips, for a total load of 60 kips (two 30 kips axles). The loads were centered over the first interior girder. Note that the left hand side of Figure 4.2 represents the free construction joint while the right hand edge represents the barrier side of the bridge. Traffic travels parallel to the global Z direction shown in the figure. The loads were spaced at 54 in. longitudinally (a typical spacing for tandems axles), and 6 ft.-5 in. transversely (slightly larger than the typical spacing of 6 ft.-0 in., but selected to be centered in the spans).

Also noted in the figure are the supports. Nodal restraints were applied along each girder line. At the leftmost girder line, vertical and transverse translations were restrained. At all other girder lines, only vertical translations were restrained.

Note that the model is a simplified representation of the structure. It does not account for any influence of girder deflections or relative deflections on the stresses.

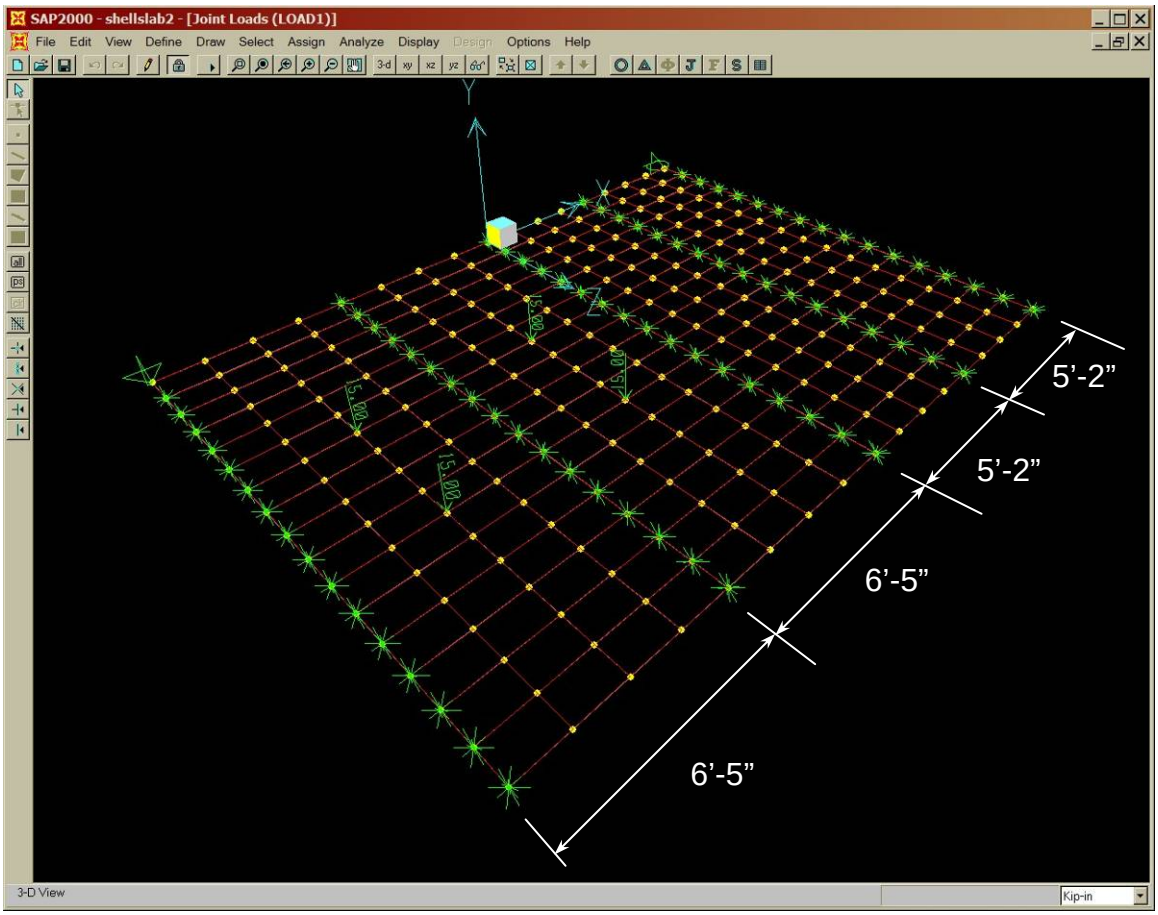

Figure 4.2 – Two-dimensional SAP2000 model of concrete deck with four 15 kip point loads representing a rear tandem axle of a heavy truck (two 30 kip axle loads)

Figure 4.3 is the transverse (X-dir) stress contour at the top surface of the deck slab for the loading described above. The slab is shown in its deformed shape. As expected the maximum transverse tensile stresses in the top surface occur over first interior girder (gray shaded area), and are equal to approximately 320 psi.

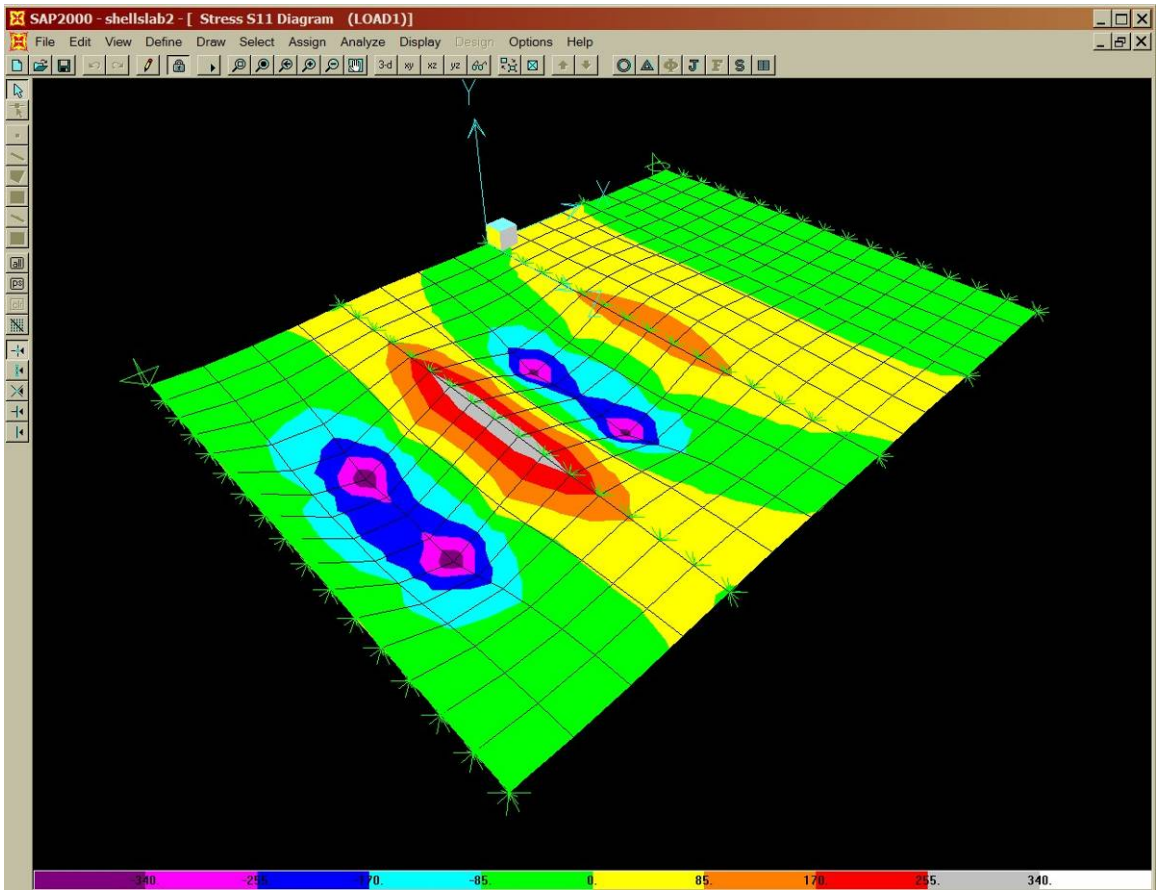

Figure 4.3 – Stress contour (in psi) for top surface X-direction stresses (transverse bridge direction)

Figure 4.4 is the longitudinal (Z-dir) stress contour on the bottom surface of the deck slab for the loading described above, viewed from beneath. The slab is shown in its deformed shape. The maximum longitudinal tensile stresses occur directly beneath the wheel loads and have a magnitude of approximately 310 psi.

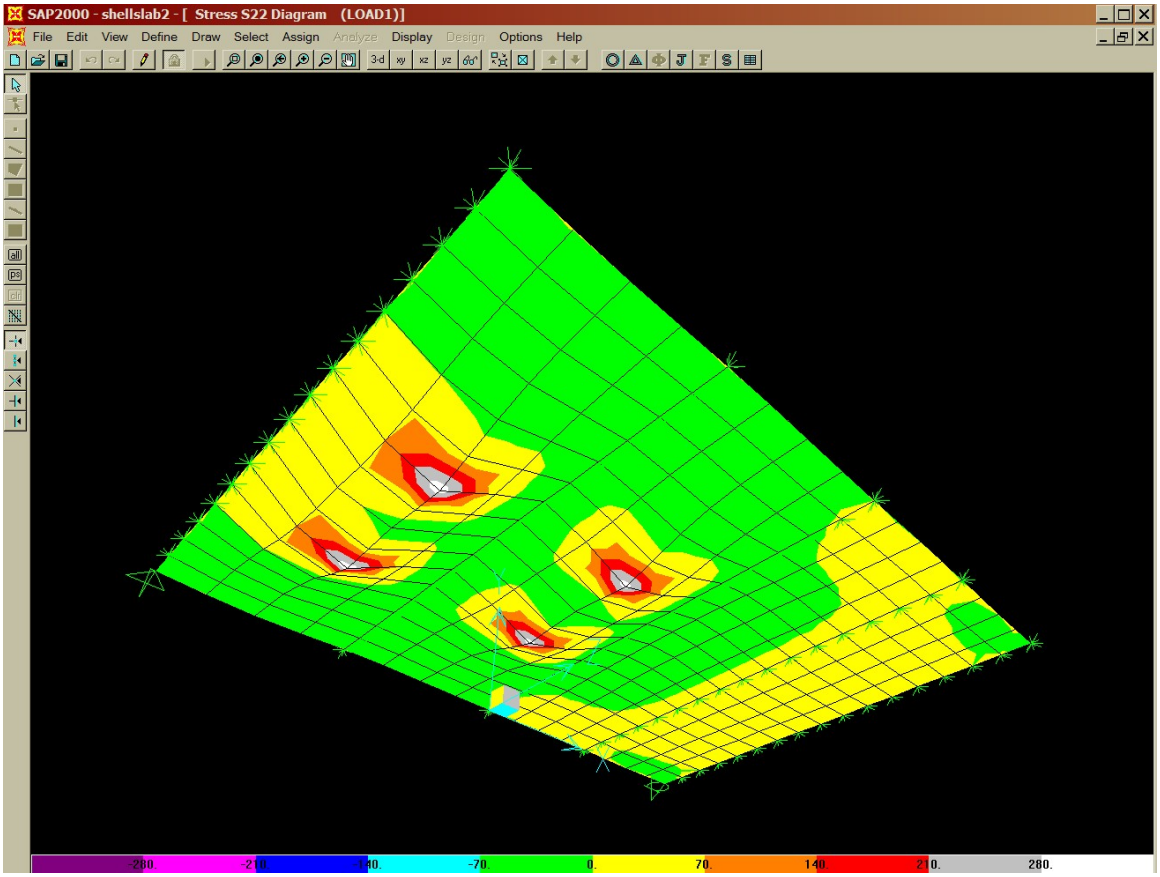

Figure 4.4 – Stress contour (in psi) for bottom surface Z-direction stresses (longitudinal bridge direction) viewed from beneath

The calculated tensile stresses can be compared to the modulus of rupture for the concrete, given in Equation (9-10) in ACI 318-08:

$$f_r = 7.5\lambda\sqrt{f_c'} \quad (in\ psi) \tag{4.1}$$

Where f'_c is the compressive strength of the concrete and λ is equal to 1.0 for normal weight concrete. Setting the f_r equal to the calculated stress, the compressive strength of the concrete can be solved for, which represents the strength at which cracking would occur for the given applied load. Repeating this for a number of axle loads (the calculated stress is found by scaling based on the axle load, since elastic behavior is assumed), a failure envelope is determined as shown in Figure 4.5.

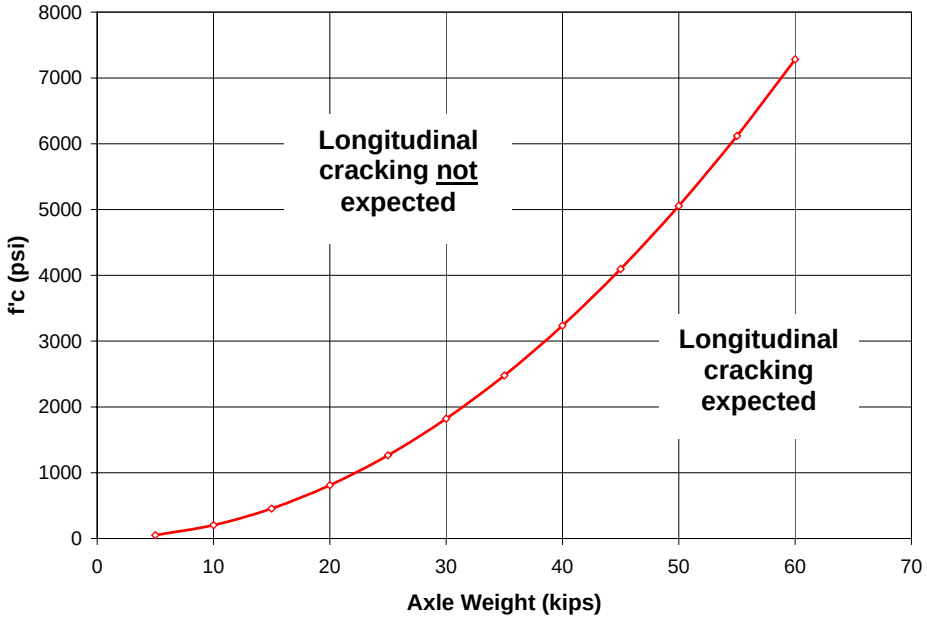

Figure 4.5 – Envelope for longitudinal cracking shown in terms of applied axle weight and concrete strength, f'_c, at time of load application for four span concrete slab with tandem axles (2 times axle weight) centered over first interior support

5. ANALYSIS OF POSSIBLE THERMAL-INDUCED TRANSVERSE CRACKING

Finite element analyses were performed to estimate the early-age thermal performance of the concrete slab and to assess whether thermal gradients generated during the curing process could have contributed to the transverse cracking observed in the concrete deck. The development of early-age heat evolution are considered in the analysis.

5.1 Analysis Description

5.1.1 Deck Selected for Analysis

Concrete placed during Stage 4 of the slab construction was considered for this analysis. The mix designs were similar for the concrete used in the other stages of construction. The design details were similar for all stages of construction. Stage 4 was unique in that it used the pour sequence specified in the design documents. Concrete was placed in the positive moment regions in the end spans first, followed by the positive moment region of the center span, and finishing with the negative moment regions over the two interior piers.

5.1.2 Finite Element Model

A two-dimensional finite element model was developed using ABAQUS version 6.8, a multi-purpose finite element code. Pre- and post-processing of the model was performed using FEMAP version 9.3 The length, time, mass, and energy units considered in this analysis are inches, hours, pounds, and Btu, respectively.

A transverse section of the deck was considered in the analysis. The width of the analysis contained three form flutes. The concrete, polystyrene flute filler material, and metal deck were all included in the model. Output is presented for one-half of one flute and adjacent pan, as the results were found to be symmetric about these vertical planes.

5.1.3 Analysis Procedure

During the transient heat transfer analysis, a non-linear heat generation versus time curve was used as input for the concrete material properties. Heat is generated by the concrete as it cures. A time period of 48 hours beginning with the initial placement of the concrete was considered in the analysis.

5.1.4 Finite Element Mesh

A schematic drawing of the model is presented in Figure 5.1. Each region of the model was meshed separately. The finite element mesh was generated using FEMAP and is shown in Figure 5.2.

ABAQUS element type “DC2D4” was used for the concrete and foam flute fillers. This element is a 4-noded linear heat transfer element, with one degree of freedom (temperature) per node. Two-noded linear heat transfer elements (element type “DC1D2”) were used for the metal deck material along the bottom surface of the model.

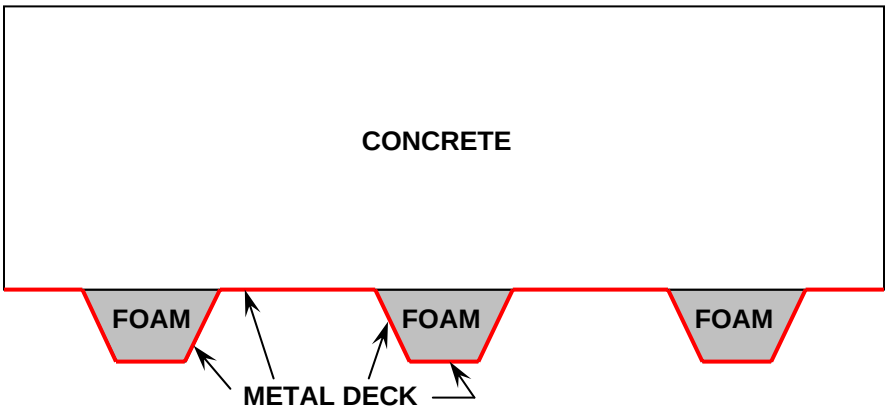

Figure 5.1 – Schematic drawing of the finite element model of the deck

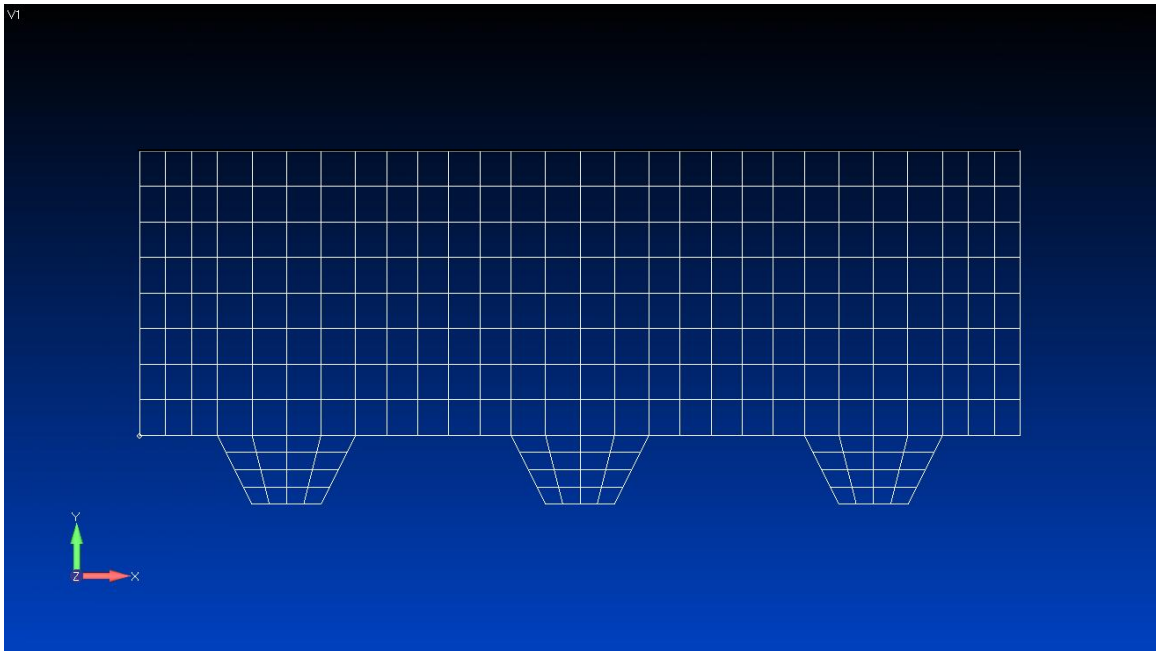

Figure 5.2 – Finite element mesh of deck

5.1.5 Thermal Boundary Conditions

Convective surface boundary conditions were applied along the top and underside of the concrete deck. These boundary conditions were specified with constant values, calculated at the time of concrete placement.

This surface accounts for the heat loss from the slab through convection with the outside air. Each side of the mesh (through the deck thickness) was considered as an adiabatic boundary.

5.2 Input Data

A number of key parameters were needed as input for the finite element analysis. These parameters were estimated based on published data from a variety of sources.

Additionally, parameters affecting the convective surface condition were obtained either from construction inspection reports or from historical data from weather stations near to the site. The assumptions used in developing these key input parameters are discussed in this section.

5.2.1 Thermal Conductivity

The thermal conductivity of the concrete was estimated using "ACI 122R-02 Guide to Thermal Properties of Concrete and Masonry Systems" prepared by ACI Committee 122. A value of k_c was estimated using Equation 2-3 in ACI 122:

$$k_c = 0.6 \cdot e^{0.02d} \tag{5.1}$$

where,

k_c = thermal conductivity, (Btu/hr-ft^2- (^{o}F/in))

d = dry density of concrete = 135 lb/ft^3

This equation yields a thermal conductivity, k_c of 8.93 Btu/hr-ft^2-(^{o}F/in) or 0.062 Btu/hr-in-^{o}F. This value was used for the concrete deck in the analysis.

For the polystyrene flute fillers, a thermal conductivity of 0.0015 Btu/hr-in-^{o}F was used.

5.2.2 Specific Heat

Each component of the concrete has a characteristic specific heat. Typical values are presented in ACI 207. A specific heat of 0.221 Btu/lb- ^{o}F was used for concrete in the analysis. The specific heat of the foam flute filler was assumed to be 0.3 Btu/lb- ^{o}F.

5.2.3 Adiabatic Temperature Rise/Heat Generation

As noted previously, heat is generated by the slab as it cures. This heat generation is non-linear with time. In lieu of test data for the mix used, heat generation was estimated using data developed by Committee 207 of the American Concrete Institute. Specifically, Figure 4.1 of ACI 207.2 R-9 presents a graph of adiabatic temperature rise versus time for mixes with various types of cement. This data presented in the figure is based on a mix that has 376 lb/cu yd of cement. ACI 207 suggests that the temperature rise for mixes with other cement contents can be obtained by linear scaling of the given rises in proportion to the actual cement content. The mix used for Stage 4 of the Church Road Bridge is a Type I cement with 650 lb/cu yd of cement. However, it was noted in the petrography report that the cement particles were fine more like a Type III cement. For a given cement composition, increased fineness will result in an increase in the rate of heat generation. However, the total energy released during the curing process is the same. To assess the effect of varying rate of heat generation on the temperature distribution in the concrete in the days following initial placement, four heat generation curves were considered.

The adiabatic temperature rise for Type I cement given in ACI 207.2 were scaled up by 650/376 = 1.73. Rates of twice and half this standard Type I rate were also used for analysis. To make a comparison between Type I and Type III cement, the standard Type III curve was also considered, again adjusted by a factor of 1.73 to account for the actual quantity of cement used. The four plots of adiabatic temperature rise versus time considered for these analyses are presented in Figure 5.3.

This adiabatic temperature rise is converted into heat flux as a function of time using the following formula:

$$Q_i = \frac{\Delta T_i \cdot \gamma}{\Delta t_i} C_p \tag{5.2}$$

where,

Q_i = heat flux due to internal heat generation at time i, (Btu/in^3-hr)

C_p = specific heat of the concrete = 0.221 Btu/lb-^{o}F

ΔT_i = change in temperature at time i, ^{o}F

Δt_i = change in time at time i, (hr)

γ = density of concrete = 0.0781 lb/in^3

The original curves were scaled from Figure 4.1 of ACI 207.2. A polynomial curve was fit to these scaled data yielding an explicit expression for adiabatic heat rise, T, as a function of time, or T(t). The heat flux, Q, is then found by taking the first derivative of T with respect to time, and is given by the following expression:

$$Q(t) = \frac{dT(t)}{dt} \gamma \cdot C_p \tag{5.3}$$

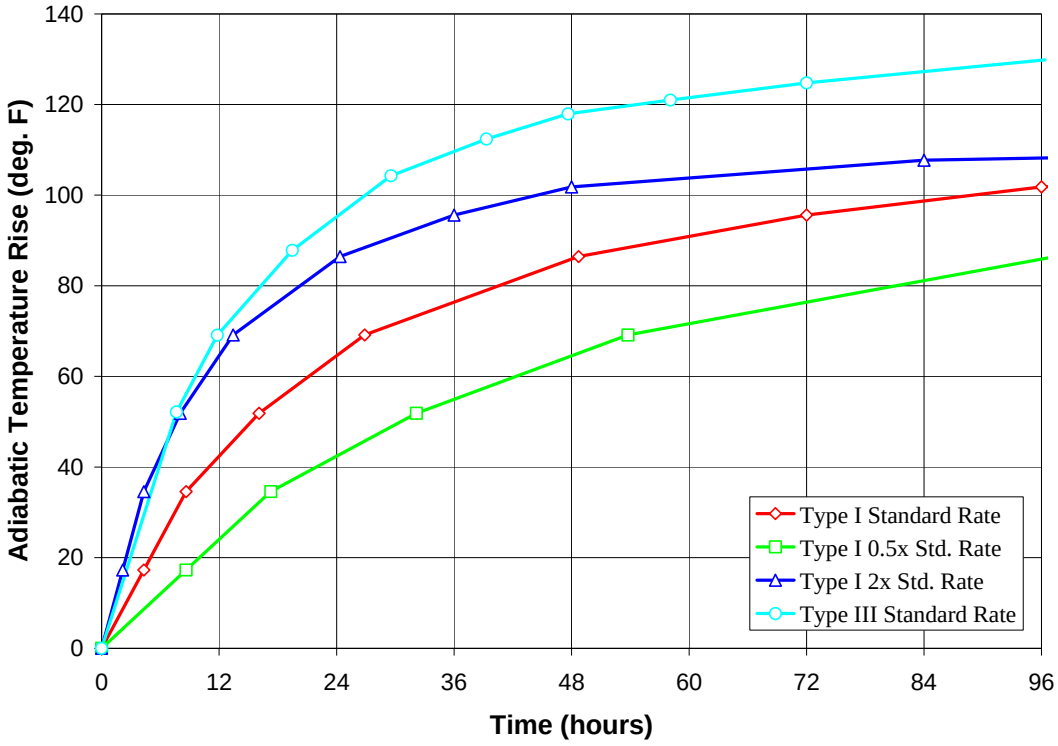

Figure 5.3– Assumed adiabatic temperature rise due to internal heat generation for Type I cement (standard rate, 2 times standard rate, and 0.5 times standard rate) and Type III cement used for thermal analysis - (Type I and Type III standard rates are for concrete with 650 lb/cy, after Figure 4.1 of ACI207.2 R-9)

A plot of heat flux due to heat generation versus time as used for this analysis is presented in Figure 5.4. The total energy input for the three Type I curves is the same. Therefore, the total adiabatic temperature rise is the same. The three curves of Figure 5.3 for Type I cement all approach the same final adiabatic temperature when extended out several weeks after initial placement. Because of a higher ratio of tricalcium silicate to dicalcium silicate, Type III cement yields a higher total adiabatic temperature rise than Type I for the same cement content.

The area under the three Type I curves of Figure 5.4 should be the same since by definition this area represents the total energy released during curing. Due to the fact that the plot only displays data through 48 hours (the early-age behavior is of interest), these areas are not the same since the entire heat generation history is not presented in the plot. The areas under the three Type I curves are the same when extended out several weeks.

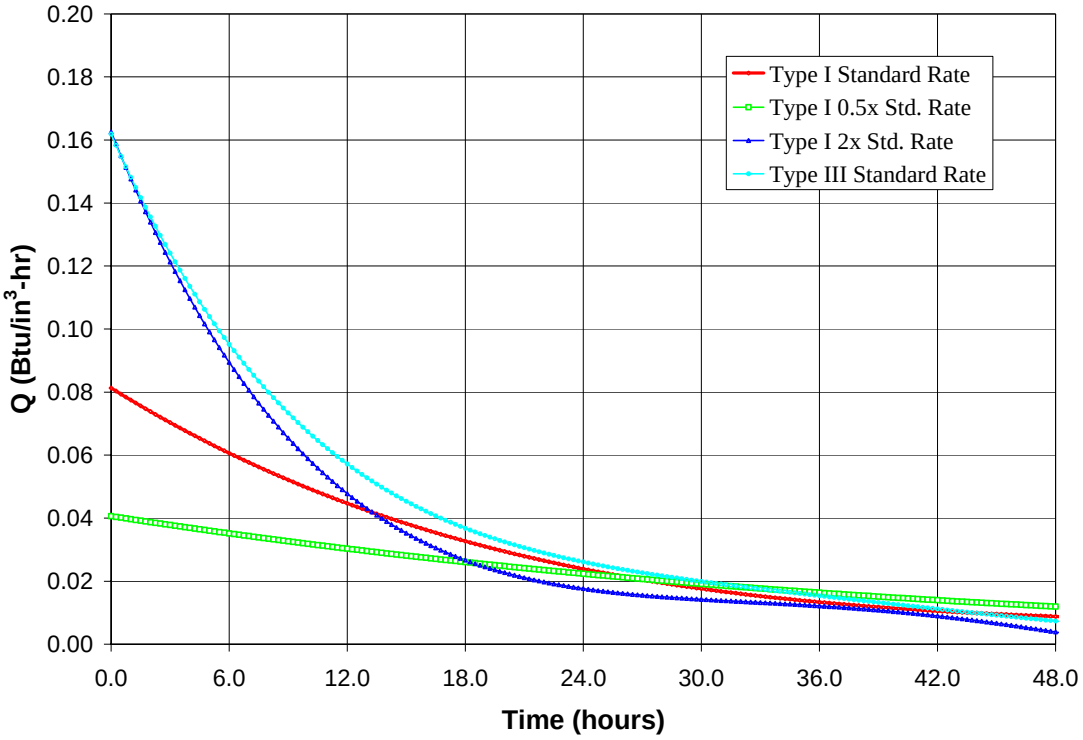

Figure 5.4 – Heat flux, Q, versus time corresponding to adiabatic temperature rises shown in Figure 5.3, for Type I cement (standard rate, 2 times standard rate, and 0.5 times standard rate) and Type III cement, all with 650 lb cement/cy concrete

5.2.4 Convection Surface Properties

A convection surface was specified along the entire top edge of the finite element model. This is specified in ABAQUS using the "FILM" command. The film represents a heat inflow/outflow from the model caused through convection of the outside air. Two parameters are necessary, both of which can vary with time. The first is the air temperature (or the "sink" temperature). The second is the convection coefficient, h. This parameter is a function of wind speed. The U.S. Army Corps of Engineers provides estimates of this coefficient in "Nonlinear, Incremental Structural Analysis of Massive Concrete Structures, ETL 110-2-365." For surfaces exposed to air (such as the top surface of the concrete deck) the coefficient is given by the following:

$$h = 0.1132V^{0.8} \qquad (5.4)$$

for V > 10.9 mph

$$h = 0.165 + 0.0513V \qquad (5.5)$$

for V < 10.9 mph

where:

h = film coefficient, (Btu/day-in^2- ºF)

V = wind speed (mph)

A convective boundary surface was also applied to the concrete surface on metal stay-in-place (SIP) forms. For this case, a modified film coefficient, h', was specified as:

$$h' = \frac{1}{\left(\frac{b}{k}\right)_{SIPform} + \left(\frac{1}{h}\right)} \tag{5.6}$$

where b is the thickness of the SIP form, and k is the conductivity of the metal deck.

These convective surface properties were calculated based on the average temperature and wind speed at the time of concrete placement, equal to 50 degrees F, and 2 mph, respectively. The properties of the convective surfaces were held constant for the duration of each analysis.

5.2.5 Initial Conditions

For each model, an initial temperature of all nodes of 70 degrees F was assumed. This was similar to the concrete temperature at placement for this bridge according to the concrete delivery tickets.

5.3 Summary of Models

Table 5.1 below is a summary of the analyses performed. As shown, Model 1A, Model 1B, and Model 1C considered polystyrene flute filler material with the three rates of heat generation for Type I cement. Model 1D considered Type III cement with standard heat generation rate. Model 2A, Model 2B, and Model 2C considered concrete-filled flutes with the three rates of heat generation for Type I cement. Model 2D considered Type III cement with standard heat generation rate.

Name	Flute Filler Material	Heat Generation
model_1A	Polystyrene	Type I – Standard rate
model_1B	Polystyrene	Type I – ½ times standard rate
model_1C	Polystyrene	Type I – 2 times standard rate
model_1D	Polystyrene	Type III – Standard rate
model_2A	Concrete	Type I – Standard rate
model_2B	Concrete	Type I – ½ times standard rate
model_2C	Concrete	Type I – 2 times standard rate
model_2D	Concrete	Type III – Standard rate

Table 5.1 – Summary of finite element models

5.4 Results

Figures 5.5 through 5.12 present temperature contour results for each of the 10 analyses performed. The contours are plotted at different times in each analysis and in all cases represents the time at the peak temperature in the slab. All 10 figures are plotted to the same temperature range (50 to 95 degrees F) to facilitate comparisons between figures, though in some cases the peak temperatures did not approach the 95 degree F value.

Figures 5.13 through 5.20 show the temperature time-history plots for each of the 10 analyses performed. The figures show the temperatures at 5 key locations in the cross-section of the slab. All 10 figures are plotted to the same temperature range to facilitate comparisons between figures.

Figures 5.5 through 5.12 show, as expected, that the higher temperatures exist near the center of the slab, and relatively cooler temperatures exist near both the top and bottom surfaces of the slab. These temperature gradients through the slab thickness will give rise to tension stresses at the top and bottom slab surfaces, because the center region at a higher temperature will expand relative to the cooler top and bottom surfaces. This will place the center of the slab in compression and the top and bottom surfaces in tension.

The analyses show that the insulating value provided by the foam-filled flutes in the stay-in-place form does modify the temperature distribution locally near the flute. Temperatures further away from the flute are largely unaffected. This can be seen for example by comparing the temperature time-history of node 247 in Figures 5.13 and 5.14. Figure 5.13 shows the result for Model 1A which includes the foam filled flutes. The peak temperature in that case is higher than in Model 2A (Figure 5.14) which is for the concrete filled flute. The temperature time-history at Node 735 near the center of the slab is similar for the two analysis cases.

The analyses also show that modifying the rates of heat release (simulating different finenesses in the Type I cement) increase the peak temperatures in the slab and also the relative temperature differences between different regions in the slab. A more rapid rate of heat release leads to both higher peak temperature and also a higher relative temperature difference between regions.

Figures 5.21 is a plot of the temperature differential between the center of the slab and the bottom surface of the slab for the Type I cement at the standard rate, the Type I cement at twice the standard rate, and the Type III cement (all for foam-filled flutes). Similarly, Figure 5.22 is a plot of the temperature differential between the center of the slab and the top surface of the slab for the Type I cement at the standard rate, the Type I cement at twice the standard rate, and the Type III cement. This figure shows that increasing the fineness of the cement (Model 1C as compared to Model 1A), or changing to a Type III cement (Model 1D as compared to Model 1A), will increase the temperature differential between the slab center and the top and bottom surfaces.

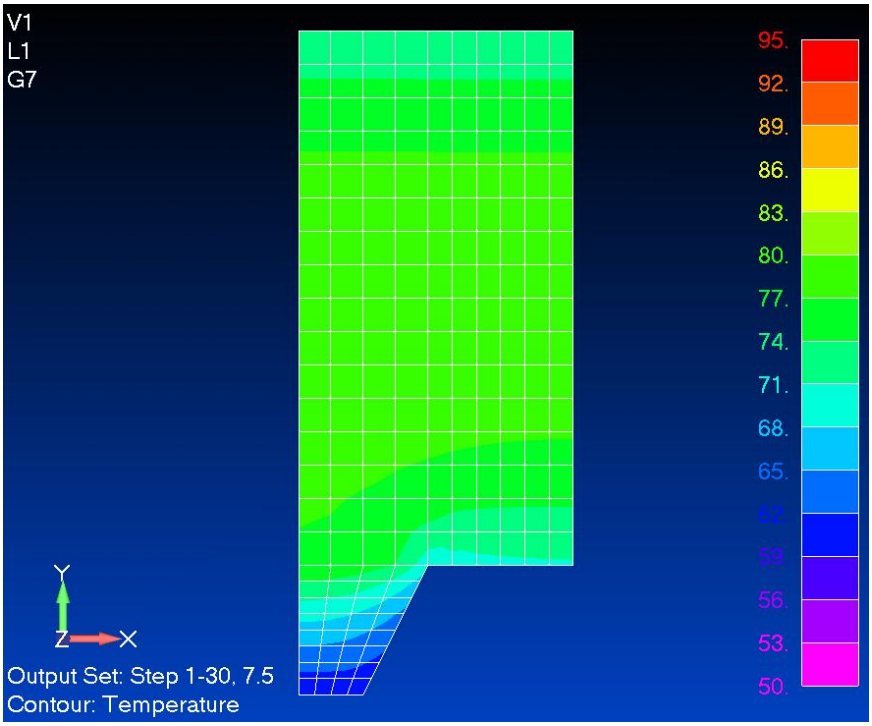

Figure 5.5 – Model 1A (Foam filled flutes, Type I cement, standard heat generation rate) – temperature contour at 7.5 hours from placement (maximum temperature)

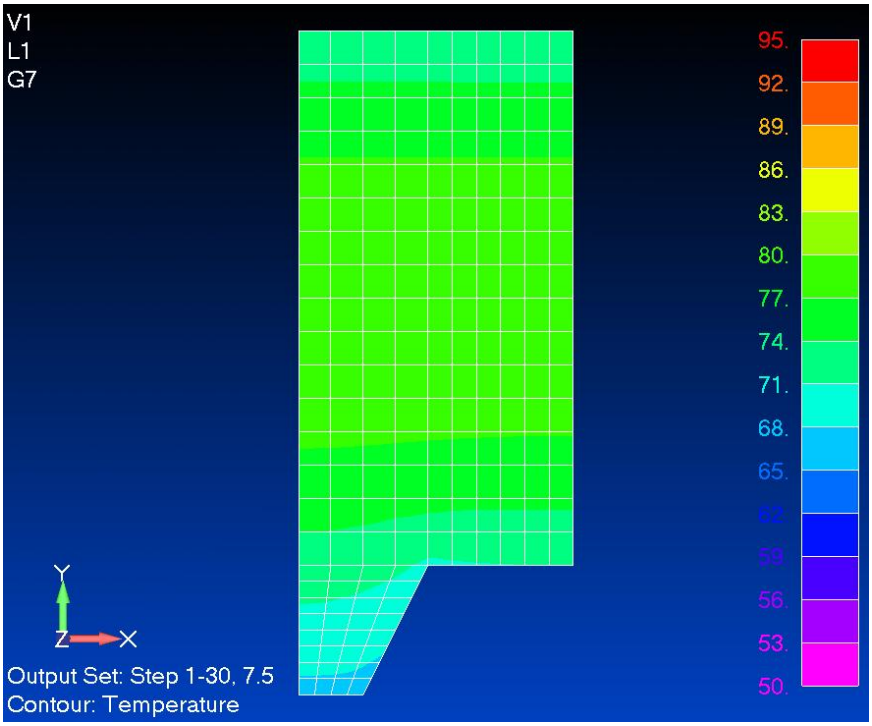

Figure 5.6 – Model 2A (Concrete filled flutes, Type I cement, standard heat generation rate) – temperature contour at 7.5 hours from placement (maximum temperature)

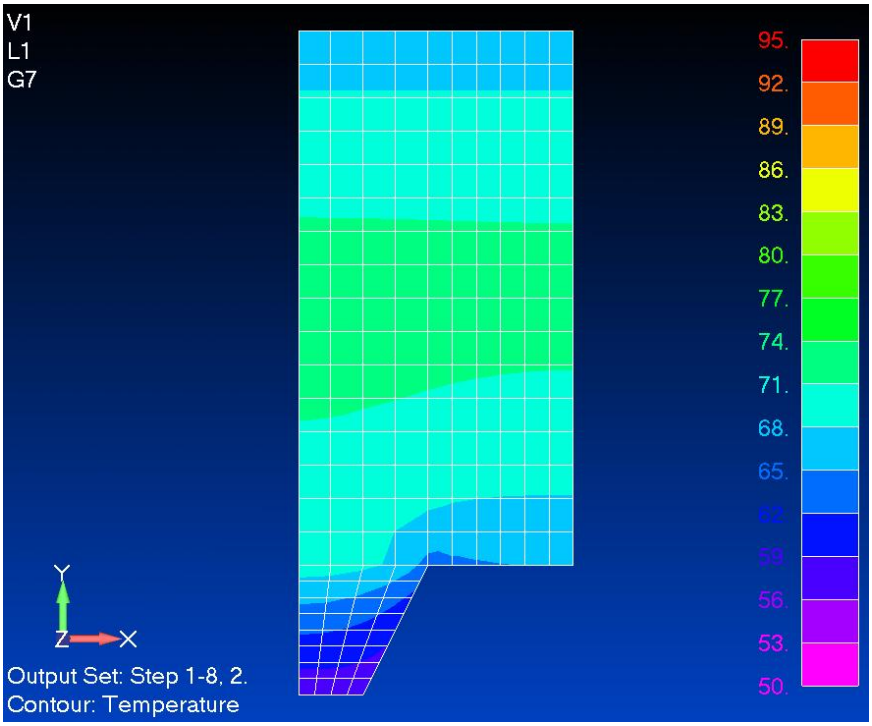

Figure 5.7 – Model 1B (Foam filled flutes, Type I cement, 0.5 times standard heat generation rate) – temperature contour at 2 hours from placement (maximum temperature)

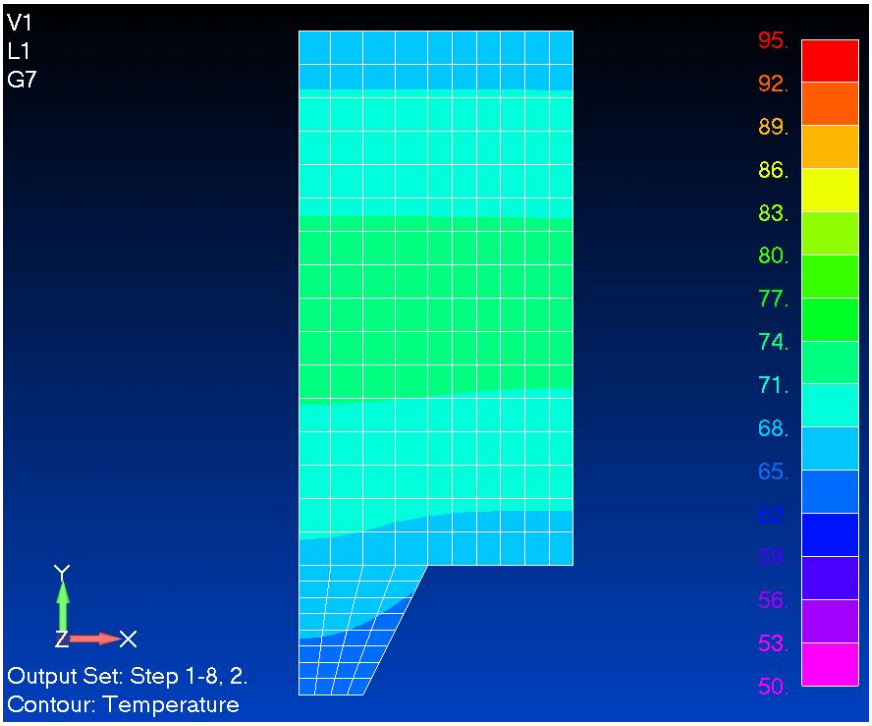

Figure 5.8 – Model 2B (Concrete filled flutes, Type I cement, 0.5 times standard heat generation rate) – temperature contour at 2 hours from placement (maximum temperature)

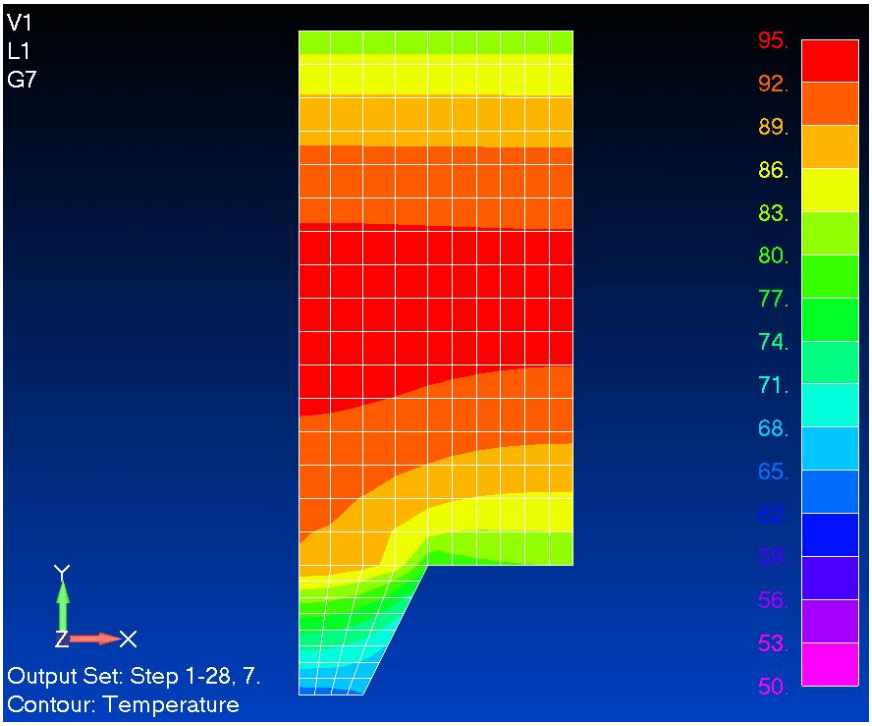

Figure 5.9 – Model 1C (Foam filled flutes, Type I cement, 2 times standard heat generation rate) – temperature contour at 7 hours from placement (maximum temperature)

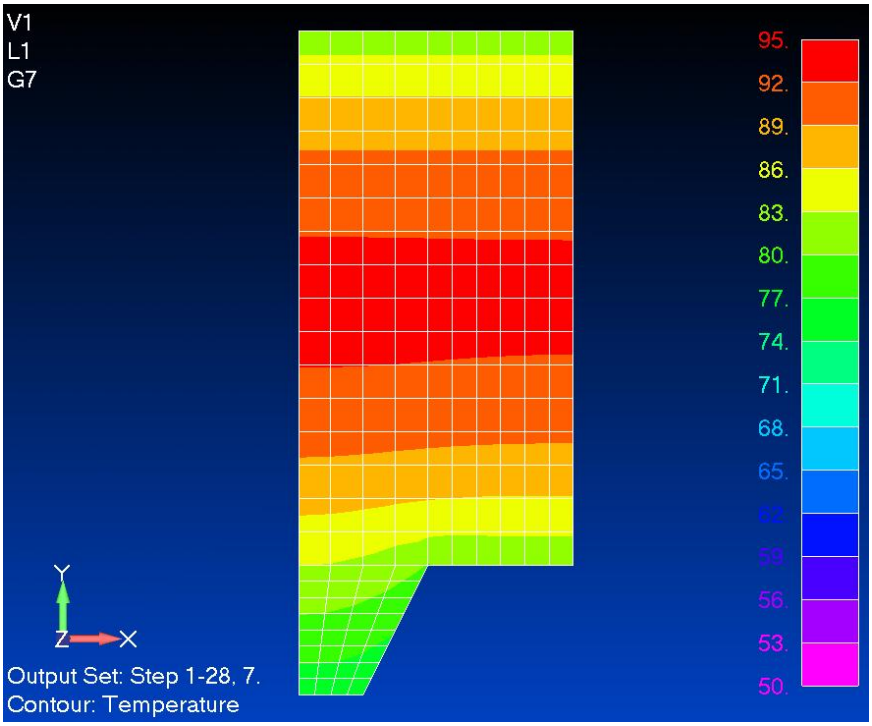

Figure 5.10 – Model 2C (Concrete filled flutes, Type I cement, 2 times standard heat generation rate) – temperature contour at 7 hours from placement (maximum temperature)

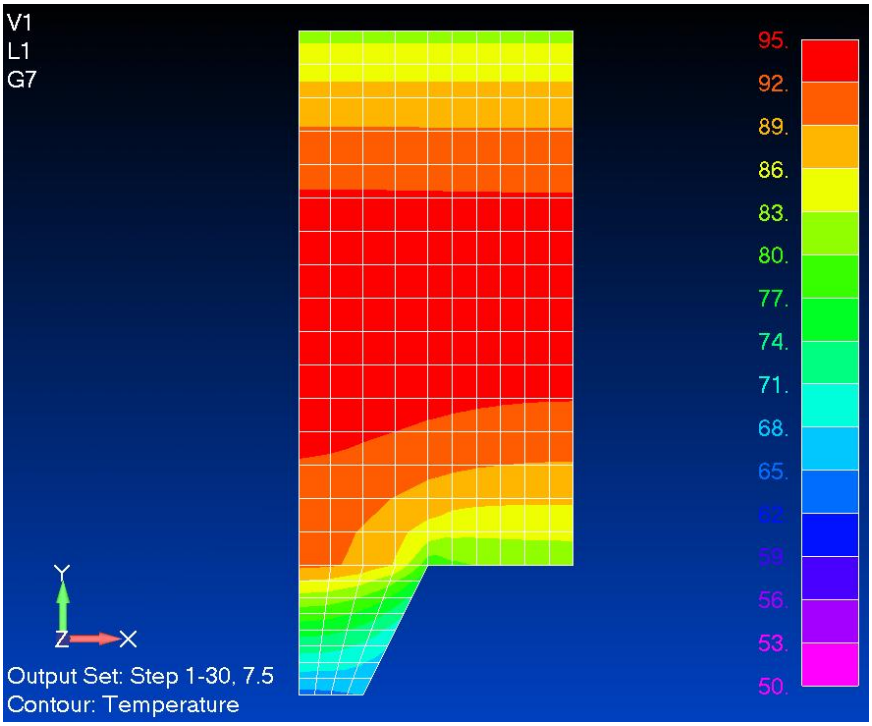

Figure 5.11 – Model 1D (Foam filled flutes, Type III cement, standard heat generation rate) – temperature contour at 7.5 hours from placement (maximum temperature)

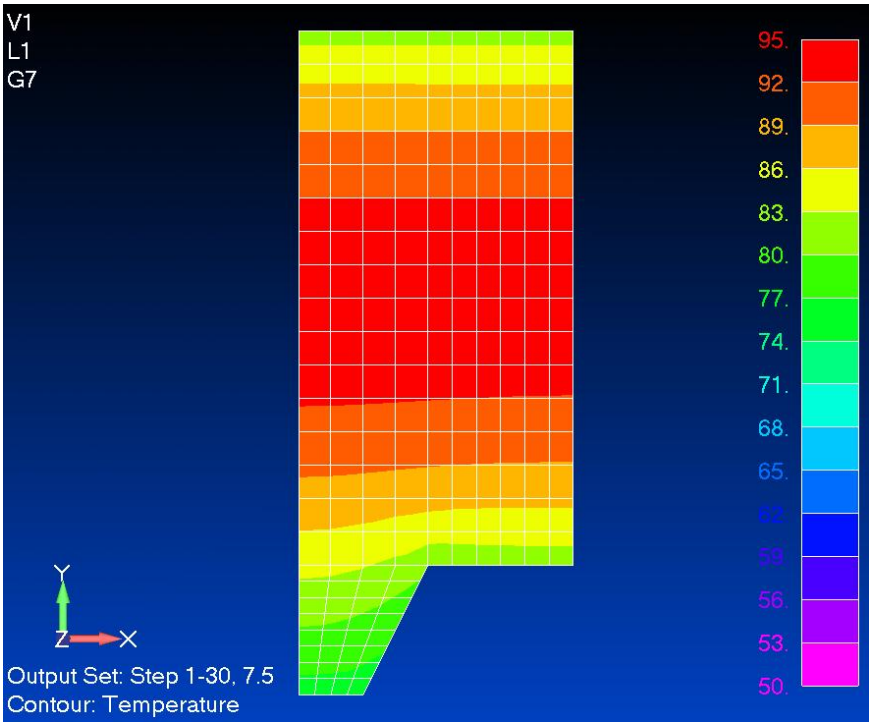

Figure 5.12 – Model 2D (Concrete filled flutes, Type III cement, standard heat generation rate) – temperature contour at 7.5 hours from placement (maximum temperature)

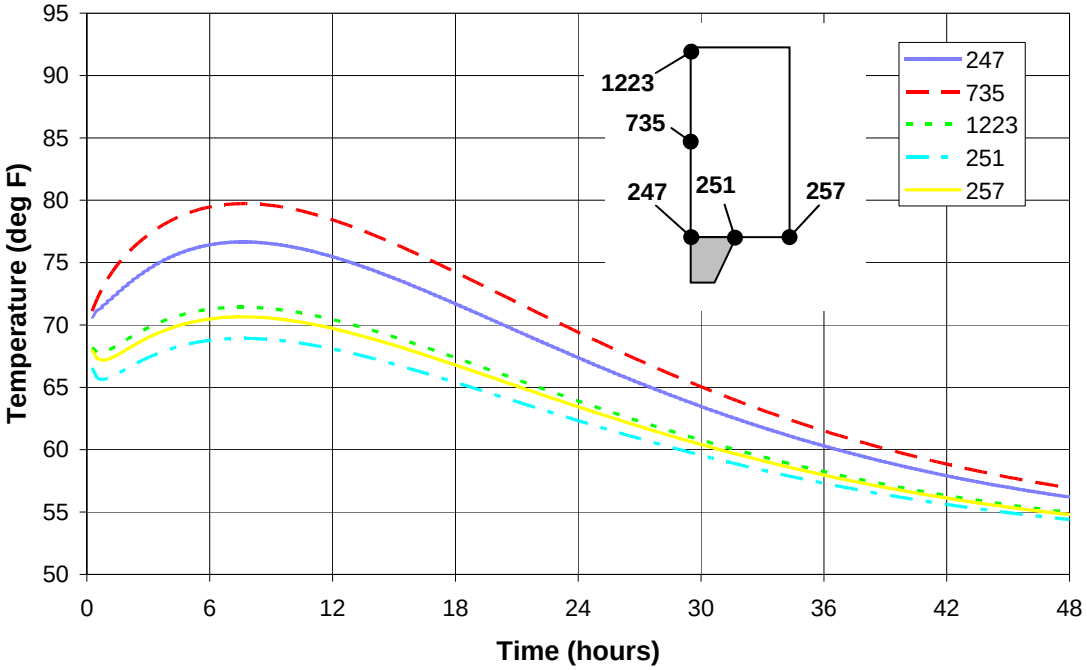

Figure 5.13 – Model 1A (Foam filled flutes, Type I cement, standard heat generation rate) – temperature time-history plot at key locations

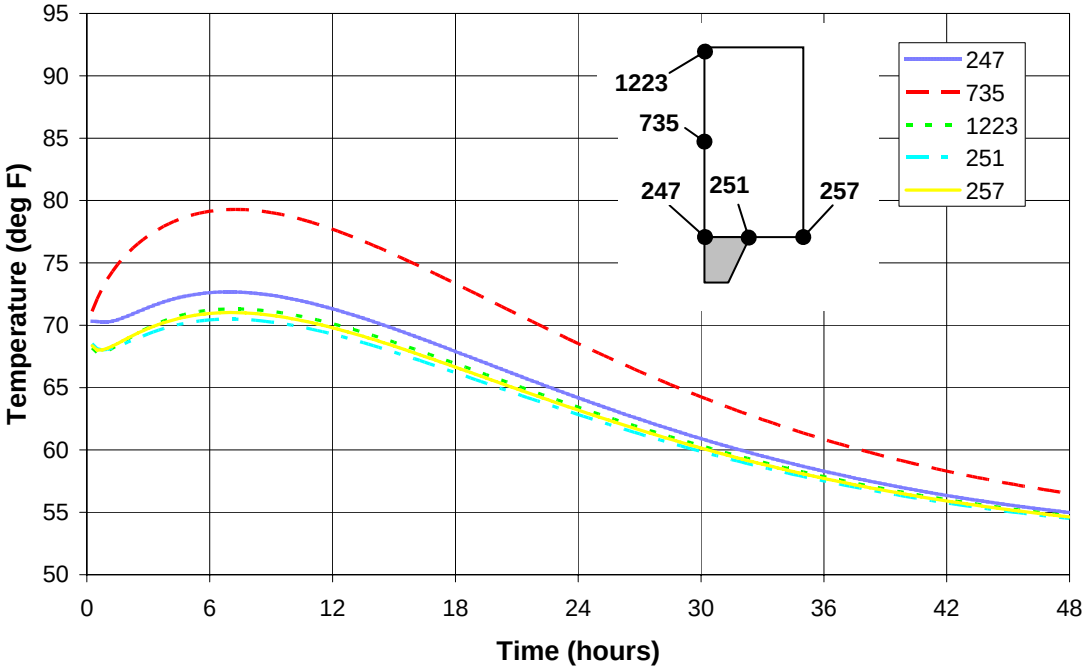

Figure 5.14 – Model 2A (Concrete filled flutes, Type I cement, standard heat generation rate) – temperature time-history plot at key locations

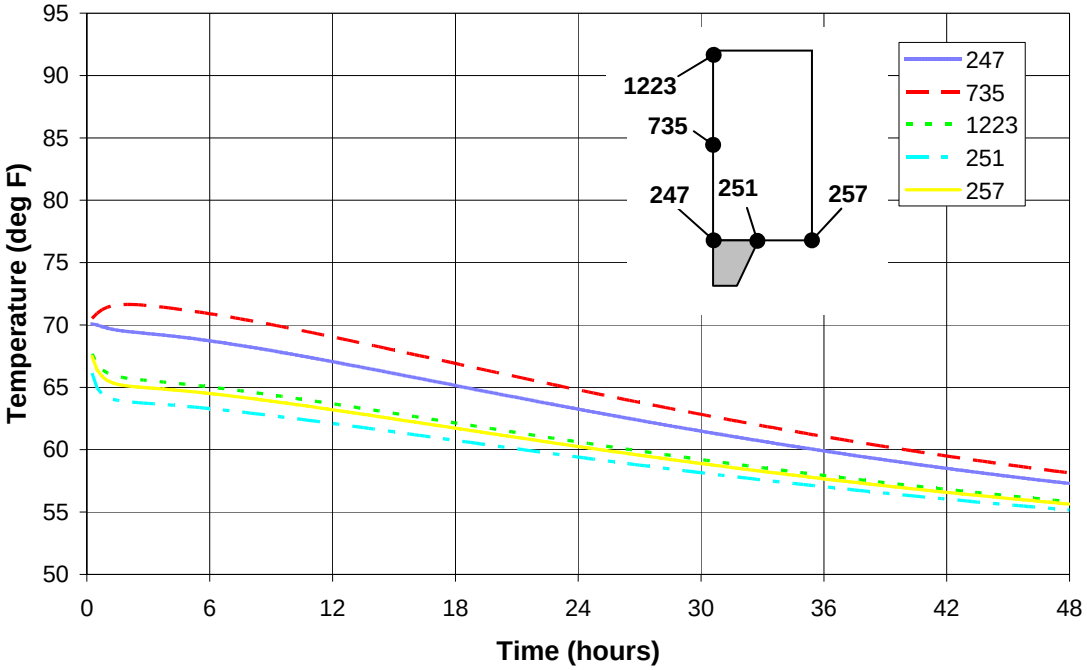

Figure 5.15 – Model 1B (Foam filled flutes, Type I cement, 0.5 times standard heat generation rate) – temperature time-history plot at key locations

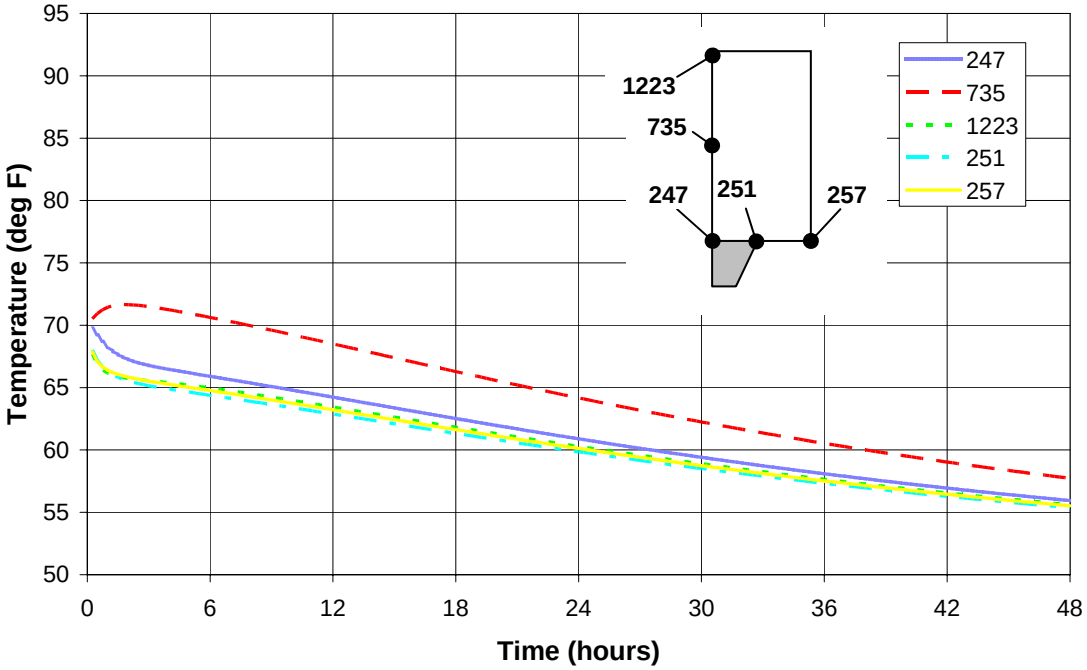

Figure 5.16 – Model 2B (Concrete filled flutes, Type I cement, 0.5 times standard heat generation rate) – temperature time-history plot at key locations

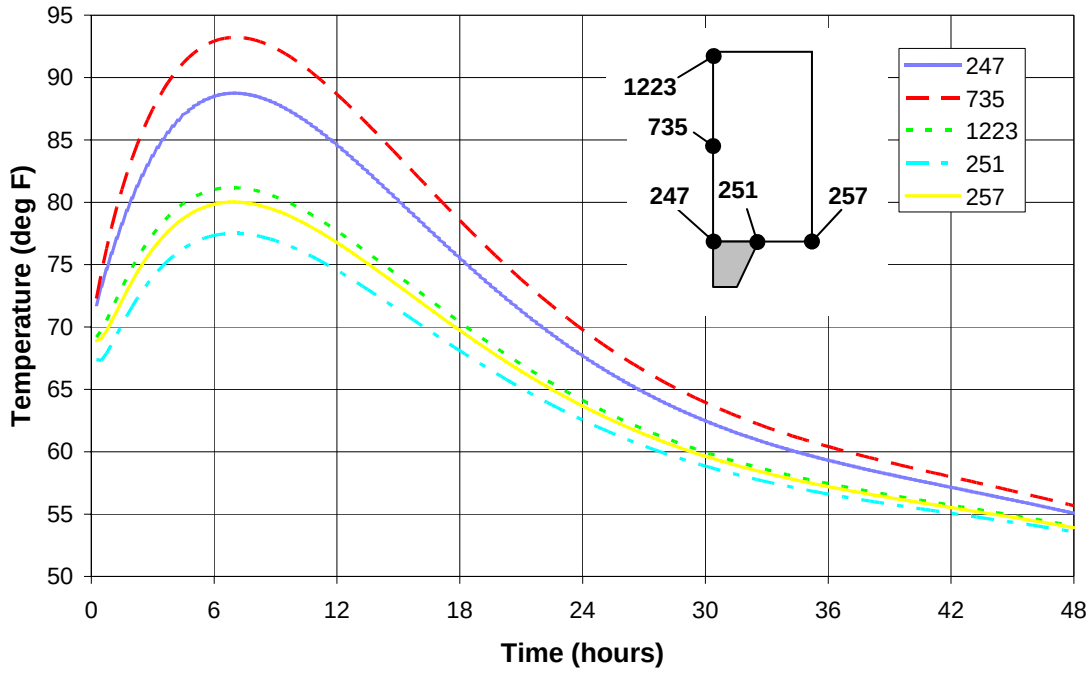

Figure 5.17 – Model 1C (Foam filled flutes, Type I cement, 2 times standard heat generation rate) – temperature time-history plot at key locations

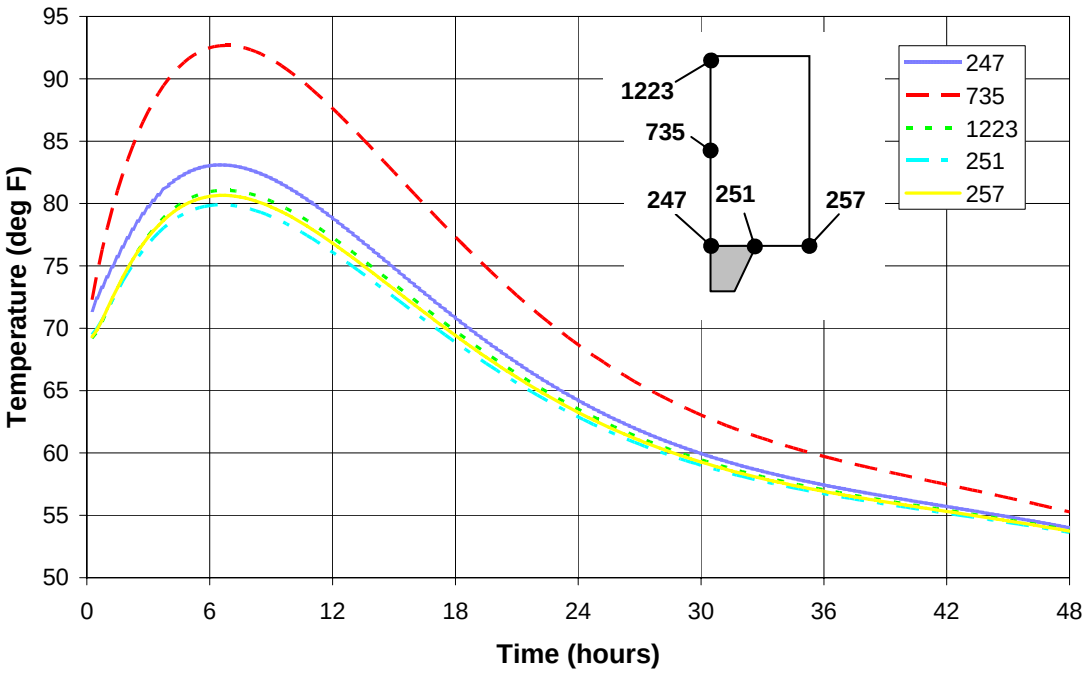

Figure 5.18 – Model 2C (Concrete filled flutes, Type I cement, 2 times standard heat generation rate) – temperature time-history plot at key locations

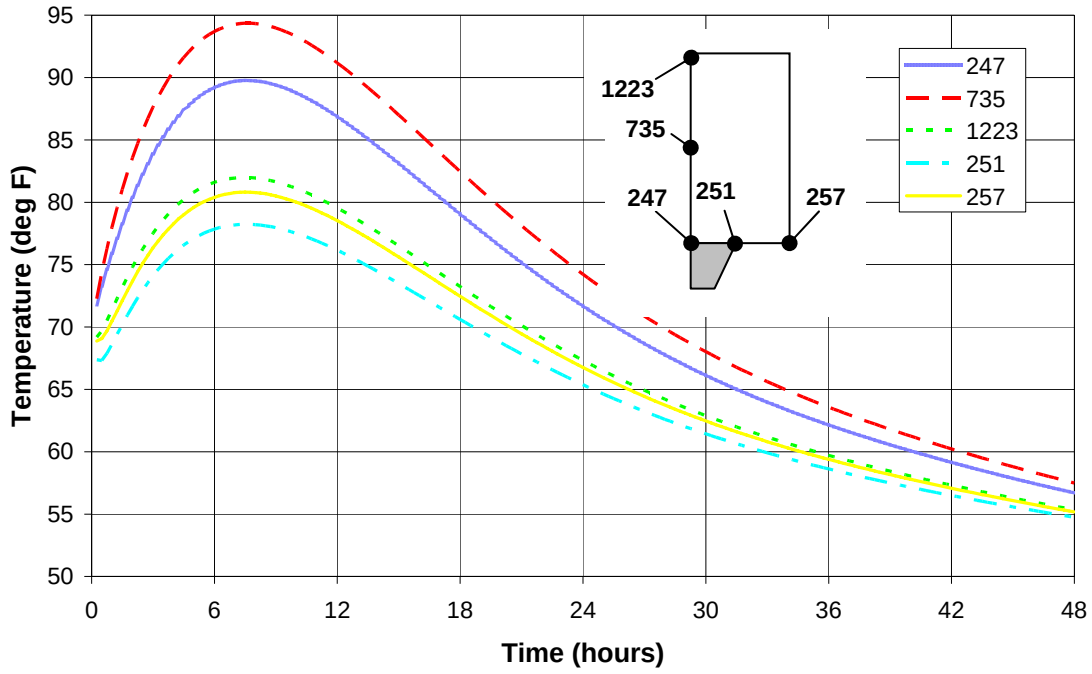

Figure 5.19 – Model 1D (Foam filled flutes, Type III cement, standard heat generation rate) – temperature time-history plot at key locations

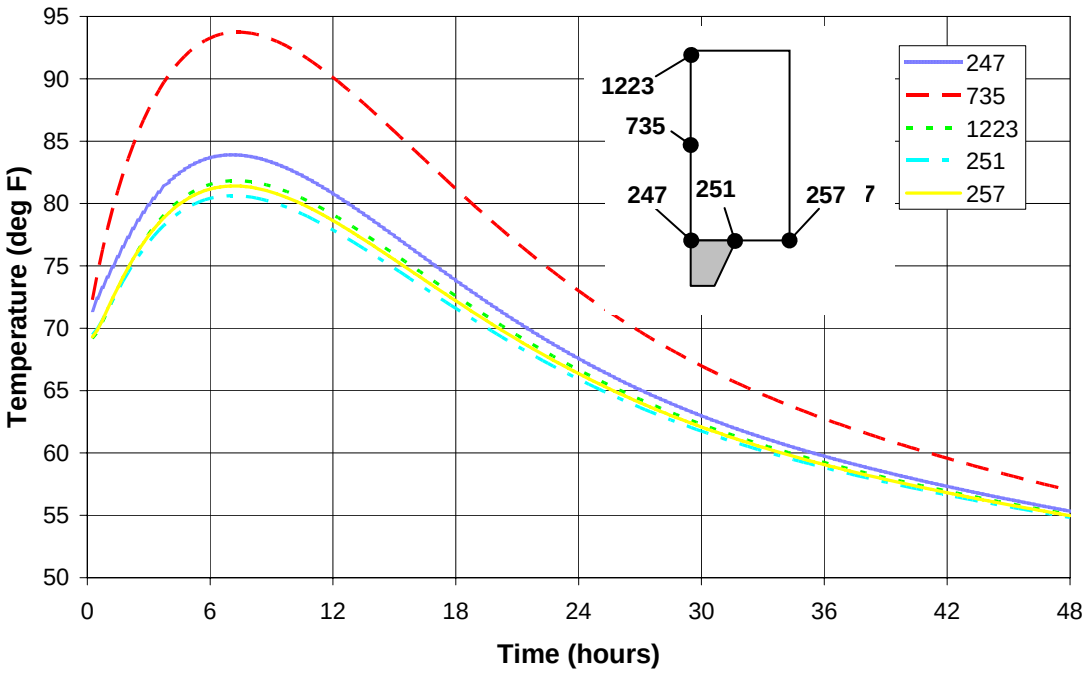

Figure 5.20 – Model 2D (Concrete filled flutes, Type III cement, standard heat generation rate) – temperature time-history plot at key locations

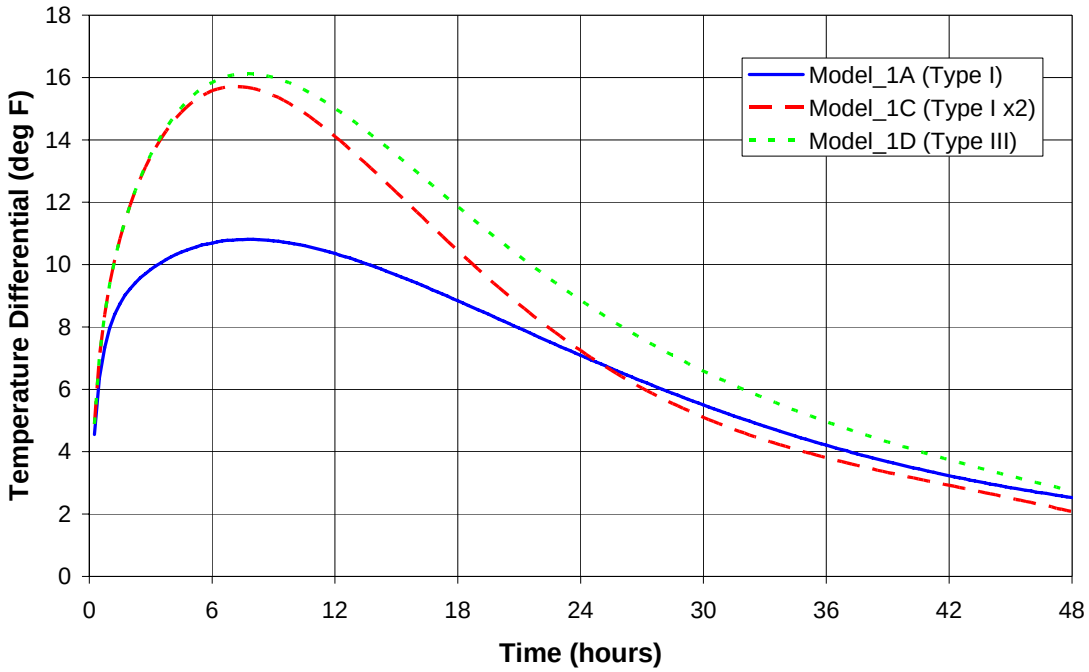

Figure 5.21 – Comparison of temperature differential between center of deck (node #735) and bottom surface of deck at the edge of the flute (node #251) for Type I and Type III cements with standard heat generation rates, and Type I with 2x heat generation rate

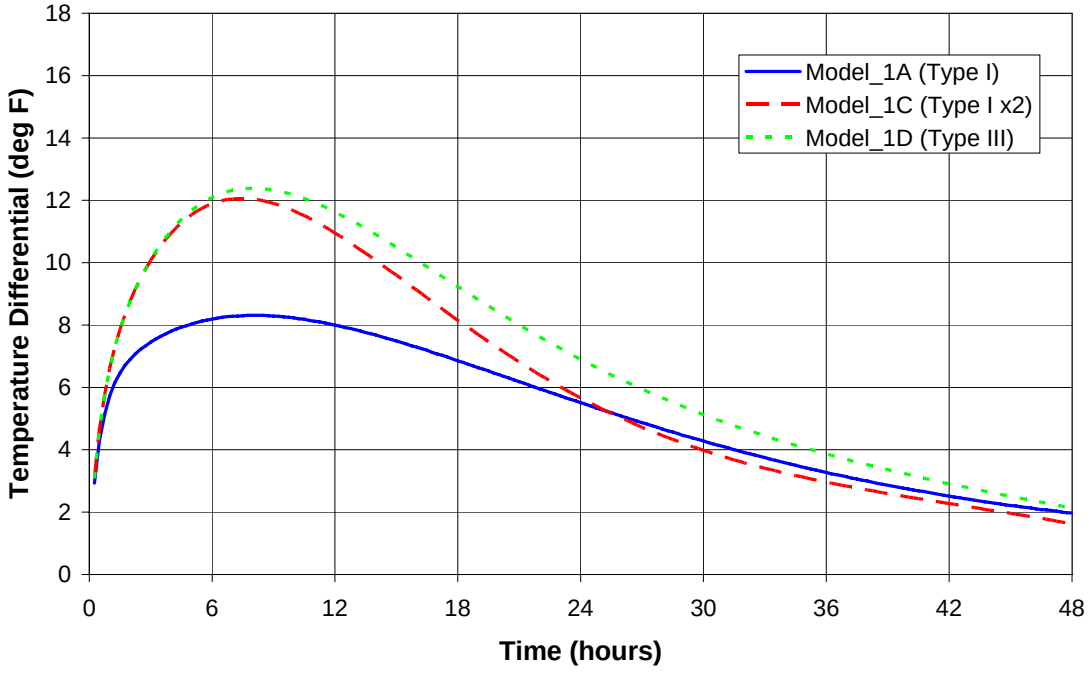

Figure 5.22 – Comparison of temperature differential between center of deck (node #735) and top surface of deck (node #1223) for Type I and Type III cements with standard heat generation rates, and Type I with 2x heat generation rate

6. DISCUSSION

6.1 Crack Surveys

As noted earlier, in general the transverse cracking appears to more extensive than the longitudinal cracking. This is true in both the positive and negative moment regions in which the cracks were recorded. In addition, a comparison of the positive and negative moment regions indicates that the transverse cracking is more extensive in the negative moment region as compared with the positive moment region. The cause for increased transverse cracking in the negative moment region is not immediately clear. It is understood that the slab may act in tension in the longitudinal direction in the negative moment regions, but it is not clear that load acted in a manner to cause this tension at the early age at which the transverse cracks formed.

6.2 Digital Image Correlation Testing

The limited digital image correlation testing that was performed indicates that the cracks are not opening and closing under the action of loads applied to the deck. Even the most severe case tested, a longitudinal crack over a girder with the wheel loads straddling did not cause appreciable opening of the crack.

6.3 Petrographic Analyses

Section 3 presented the results of petrographic analyses of three concrete cores extracted from the bridge deck. The petrographic analyses provided several key pieces of information which guided subsequent details of the investigation.

First, the analysis revealed that there were no inherent problems with the material properties of the concrete itself.

Second, the analysis provided information about the relative ages at which the transverse and longitudinal cracks formed. The transverse cracks in Cores #1 and #2 circumscribe aggregate particles and occurred very early in the life of the concrete (e.g. when the concrete was plastic, semi-plastic, or shortly thereafter), so the transverse cracking in the bridge deck was caused by effects early in the life of the concrete. The longitudinal crack in Core #3 transects numerous aggregate particles in contrast to the cracks that essentially circumscribe aggregate particles in the other two cores and, thus, occurred after there was significant aggregate-paste bond strength. Thus the longitudinal cracking in the bridge deck occurred later than the transverse cracking in the life of the concrete. The relative ages of cracking prompted the analyses to investigate the possibility of load-induced longitudinal cracking, and the possibility of thermal-induced transverse cracking.

Third, the cement to make the concrete was found to have particles exhibiting high fineness more like a Type III cement which may have resulted in a faster heat generation rate. The thermal analyses presented in Section 5 examined the influence of the cement fineness which influences the early rate of hydration and thus the rate of heat generation, and also the cement composition (relative proportions of tricalcium silicate and dicalcium silicate) which influences the total amount of heat generated.

6.4 Load-Induced Longitudinal Cracking

Section 4 presented an analysis of possible load-induced longitudinal cracking of the structure. Those analyses were prompted by the petrographic analysis of cores which indicated that the longitudinal cracking occurred at a later age in the life of the concrete.

The analyses were used to generate a plot to illustrate what axle weight could be expected to cause longitudinal cracking due to transverse flexural stresses for a range of concrete compression strengths (and hence concrete ages or maturities). Information is not available on the axle weights of construction vehicles that may have acted on the concrete deck during construction, so it is impossible to conclude with certainty that whether or not the longitudinal cracking is due to early loading during construction. However, Figure 4.5 does show that approximately 2/3 of the axle weight used in the digital image correlation testing would be expected to cause longitudinal cracking when the concrete compression strength is about 3000 psi. At a compression strength of about 3000 psi, the some fracture may be expected through the aggregate. Thus a heavy construction vehicle, if permitted on the structure at an early age, could have caused or contributed to the observed longitudinal cracking.

It is noted that transverse flexural stresses could have acted in combination with other stresses likely present in the structure. For example, load-induced transverse flexural stresses may act together with shrinkage stresses if curing operations were terminated while heavy construction loads were applied. This would essentially lower the axle weight needed to cause cracking. Further, surface temperature stresses resulting from any remaining temperature differential from hydration may also have acted with load-induced and shrinkage-induced stresses.

Finally, the presence of mild steel reinforcing bars and possibly other hardware cast in to the concrete deck may have created stress concentrations that contributed to the cracking. While such details are also present in similar bridge decks that did not exhibit the observed degree of cracking, the details nonetheless could lower the nominal stress at which the cracking occurs.

6.5 Thermal-Induced Transverse Cracking

Section 5 presented the results of an analysis of the temperature distribution in the concrete slab. Analysis variables examined the rate of heat generation as influenced by cement fineness, as well as the total amount of heat generated as influenced by cement composition. The results clearly showed that thermal gradients are anticipated in the slab, and that the anticipated thermal gradients will cause tension in both the top and bottom surfaces of the slab. The results also show that an increase in the rate of heat generation (caused by an increase in cement fineness), or an increase in the total amount of heat generated (caused by an increase in the proportion of tricalcium silicate relative to dicalcium silicate) will increase the temperature difference between the center of the slab and the slab surfaces. The greater temperature difference can be expected to cause an increase in surface tension stresses.

The temperature analysis results are for the stated convection values at the surfaces as described earlier. As noted earlier, wet curing procedures were used to promote concrete strength gain and prevent concrete shrinkage at early ages. The

introduction of curing water at the top of the slab is expected to lead to a further reduction in the top surface temperature as compared to the cases considered, though this effect is difficult to model without better information about the water temperature, the rate at which it was applied to the slab, as well as other information. Nonetheless the analyses show that thermal gradients were likely present, and it is possible that these gradients contributed to the observed transverse cracking at early-ages.

Again, as may have been the case for the longitudinal cracking, the presence of mild steel reinforcing bars and possibly other hardware cast in to the concrete deck may have created stress concentrations that contributed to the transverse cracking. While such details are also present in similar bridge decks that did not exhibit the observed degree of transverse cracking, the presence of the details nonetheless could lower the nominal stress at which the cracking occurs. In this particular structure, the presence of the details along with a thermal gradient not found in other structures may have contributed to the cracking observed in this structure.

Finally, it is noted that the staged construction sequence may have played a role in the observed transverse cracking. Traffic from active lanes may have imposed deformation or imparted vibration on the early-age concrete. These effects acting together with the thermal-induced stresses may have caused the early-age cracking observed in this structure.

7. REMEDIATION RECOMMENDATIONS

7.1 Introduction

Engineers from Michael Baker Jr., Inc. (BAKER) studied the available options for repair of the cracked concrete decks. They performed a review of publications on past repair projects, surveys of a number of state departments of the transportation, as well as manufacturer data. Their report summarizing this work and their findings is presented in Appendix B.

Their review of previous deck cracking studies revealed that concrete deck cracking is common throughout the United States. Of the forty transportation agencies who responded to a nationwide survey, 85 percent indicated that transverse cracking has occurred on their bridges. It was found that transverse cracking was the predominant mode of cracking.

BAKER evaluated a number of remediation options. These options are as follows:

1. Do nothing
2. Apply deck/crack sealer
3. Install asphalt overlay with membrane waterproofing
4. Install concrete overlay
5. Replace deck

The advantages and disadvantages of each method were evaluated. Recommendations for the remediation of the cracking are made.

7.2 Option 1 – Do Nothing

BAKER does not recommend the "do nothing" option. They point out however that the opportunity exists to evaluate the effectiveness of various crack sealer products by treating one lane and not treating an adjacent lane. The performance of the treated and untreated deck surfaces could then be evaluated after three years.

7.3 Option 2 – Apply Deck/Crack Sealer

Deck sealers are either solvent- or water-based chemicals that are applied to the surface of the deck and act as an impermeable layer. They can either be applied to the entire deck surface as a flood coat (deck sealer) or to individual cracks (crack sealer).

A review of the literature showed that the best performance can be achieved with high molecular weight methacrylate (HMWM). This is a three-component system. It requires extra care during mixing since a violent reaction can occur if prepared improperly. An alternative to HMWM with similar performance is methyl methacrylate (MMA). This is a two-part system without the potential for volatility. Other sealing options which exhibit good performance include epoxy, modified polyurethane (MPU), and urethane.

BAKER recommends applying a methyl methacrylate resin deck sealer to seal the existing cracks in the deck. They note that a good sealer should significantly increase the life of the existing concrete deck and structure.

Two commercially available products are provided in the report that have been approved for use by Minnesota Department of Transportation (MNDOT). The first is Degadeck Crack Sealer Plus manufactured by BASF. The second is SikaPronto 19 manufactured by Sika. Product literature is contained in the report in Appendix B. The report also contains the crack sealer standard specification used by MNDOT.

7.4 Option 3 – Install Asphalt Overlay with Membrane Waterproofing

This option comprises the application of a hot-mix asphalt concrete overlay and membrane (HMAM). The membrane serves as a barrier to the concrete deck below. This method had won favor throughout the country before 1970. However, by 1977, only 11% of respondents to a survey indicated that HMAM is one of the first three preferred options for deck repair.

BAKER noted the following disadvantages of the HMAM option:

1. Deck cracks may propagate through the asphalt
2. The membrane waterproofing can be unreliable
3. 3 in. asphalt overlay with a waterproof membrane will be more costly than application of deck crack sealer
4. The Department would not be able to evaluate new crack sealer products
5. Additional dead load would be added to the structure

For these reasons, BAKER does not recommend the use of HMAM for repair of these bridges.

7.5 Option 4 – Install Concrete Overlay

To goal of an overlay is to provide a protective barrier to the existing concrete below. Available overlay materials include latex-modified concrete (LMC), low-slump dense concrete (LSDC), micro-silica concrete (MSC), or polymer concrete (epoxy). Generally good performance has been reported however a number of problems have been observed including debonding of the overly from the deck and shrinkage cracking of the overlay. Additionally, care must be taken when determining the appropriate time to install an overlay on a deck.

Although a concrete overlay may extend the life of the existing deck more than the deck sealer option, BAKER does not recommend a concrete overlay repair for the following reasons:

1. Deck cracks may propagate through the overlay
2. The cost of a latex concrete overlay would be much greater than the application of a deck sealer
3. The concrete overlay would hide the progression of cracking
4. The Department would not be able to evaluate new crack sealer products
5. Additional dead load would be added to the structure

7.6 Option 5 – Replace Deck

BAKER does not recommend replacing the existing deck for the following reasons:

1. Deck replacement should only be considered when the existing deck shows major signs of distress
2. Unless the concrete mix design is changed or the cause of the deck cracking is conclusively determined, the new deck could exhibit similar cracking
3. Deck replacement is too costly

7.7 Summary

BAKER reviewed the advantages and disadvantages of five options for the remediation of cracking on the SR309 bridge over Church Road. BAKER recommends that a methyl methacrylate (MMA) deck sealer be used to repair the cracking on the bridge deck. Two commercially available products are suggested. The complete report by BAKER is presented in Appendix B.

8. CONCLUSIONS AND RECOMMENDATIONS

8.1 Conclusions

The following conclusions are made from the results of this investigation:

1. The observed cracking is not caused by any inherent material property defect in the concrete mixture. The concrete appears to have been batched, placed and cured properly. The cement used to make the concrete did exhibit a high fineness more like a Type III cement.
2. The observed transverse cracking likely occurred early in the life of the concrete, when the concrete was plastic, semi-plastic, or shortly thereafter. This is based upon the observation that the transverse cracking circumscribes aggregate particles and thus occurred when the concrete had very little strength.
3. The observed transverse cracking in the structure is most likely due to thermal gradients in the slab early in the life of the concrete caused by heat generated by hydration of the cement and slag in the concrete. An increase in the rate of heat generation caused by an increase in cement fineness as reported in the petrography analysis will increase the thermal gradient present in the slab.
4. The observed longitudinal cracking occurred later in the life of the concrete when the concrete had gained some appreciable strength. This is based on the observation that the longitudinal cracking transects aggregate particles and thus occurred when the concrete had some appreciable strength, and relatively greater strength than when the transverse cracking formed.
5. The observed longitudinal cracking may be due in part to early-age construction loading, but more likely includes significant contributions of other effects including drying shrinkage and possibly stress concentrations due to the mild steel reinforcing and / or other stress concentrations in the deck.

8.2 Recommendations

The following recommendations are made from the results of this investigation:

1. To prevent similar cracking in future similar concrete deck placements (whether replacement decks or new decks), consideration should be given to factors that influence the temperature distribution in the deck and a thermal management plan should be implemented. This thermal management plan should consider all factors that influence the temperature distribution in the deck at early ages. Implementation of the thermal management plan may include the need for additional specifications that govern the construction of the decks.
2. To gain further insight in to current practice, the following recommendations are made:
    a. Concrete decks currently under construction should be instrumented with thermocouples to measure the temperature distribution in the slabs at early ages.

b. The constituent materials used in the actual concrete mixtures used for these same decks should be further quantified to understand the properties of the cement that influence heat generation.

c. Careful inspection of these same decks for cracking should be performed to better identify when cracking occurs should it occur. This, combined with thermocouple data as described above, may provide additional insight into the early-age cracking phenomenon.

3. An experimental program should be undertaken to study in a controlled manner the issue of thermal cracking in concrete bridge decks at early ages. Such a program would provide information that may be gained from monitoring actual bridge decks under construction as described in 2 above, but would be done in a controlled manner that would allow a systematic variation in key parameters to provide detailed insight into the cracking phenomenon and thus would inform the development of any thermal management plan and changes in specifications for the construction of new or replacement concrete bridge decks.

4. BAKER reviewed the advantages and disadvantages of five options for the remediation of cracking on the SR309 bridge over Church Road. BAKER recommends that a methyl methacrylate (MMA) deck sealer be used to repair the cracking on the bridge deck. Two commercially available products are suggested. The complete report by BAKER is presented in Appendix B.

9. REFERENCES

1. PennDOT District 6-0, Construction Unit "*SR0309 over Church Road, Montgomery County, Structure #S-22967, ECMS #16476, Preliminary Report: Deck Cracking*", dated June 15, 2007.
2. American Concrete Institute, "Guide to Thermal Properties of Concrete and Masonry Systems, ACI 122R-02", 2002.
3. American Concrete Institute, "Report on Thermal and Volume Change Effects on Cracking of Mass Concrete, ACI 207.2R-07", 2007.
4. American Concrete Institute, "Building Code Requirements for Structural Concrete and Commentary, ACI 318-08", 2008.
5. United States Army Corps of Engineers, "Engineering and Design, Thermal Studies of Mass Concrete Structures, Technical Letter No. 1110-2-542", dated May 30, 1997.
6. United States Army Corps of Engineers, "Nonlinear, Incremental Structural Analysis of Massive Concrete Structures, Technical Letter No. 110-2-365", dated August 31, 1994.

APPENDIX A

Petrography Report by the Erlin Company

TEC **THE ERLIN COMPANY**

TELEPHONE: **(724) 539-1800**
FAX: **(724) 539-7305**

5578 ROUTE 981
LATROBE, PA 15650

PETROGRAPHIC EXAMINATIONS OF THREE CONCRETE CORES

FOR

LEHIGH UNIVERSITY
(Bridge PA SR309 – Church Road)

January 9, 2009

TEC **THE ERLIN COMPANY**

TELEPHONE: **(724) 539-1800**
FAX: **(724) 539-7305**

5578 ROUTE 981
LATROBE, PA 15650

January 9, 2009
TEC 1108162

PETROGRAPHIC EXAMINATIONS
OF THREE CONCRETE CORES

FOR

LEHIGH UNIVERSITY
(Bridge PA SR309 – Church Road)

*** * * * * * ***

SUMMARY AND DISCUSSION

Concrete Composition – The cores are air-entrained and made using: (a) crushed argillite coarse aggregate; (b) natural siliceous sand fine aggregate**;** (c) estimated equivalent $6^{1}/_{2}$ to 7 bags of cementitious materials per cubic yard of which a significant amount (e.g. 30 percent) is ground granulated blast-furnace slag; and (d) estimated 0.40 water-cement ratios that is slightly less in the bottom portions of the cores. The components and their proportions conform to the reported mix-design.

Portland cement hydration is normal and advanced and cement particle sizes are indicative of cements having high finenesses (e.g. Type III). Hydration of the slag is normal and advanced. Air contents are estimated from 7 to $7^{1}/_{2}$ percent. Carbonation is from less than $^{1}/_{64}$ inch to $^{1}/_{16}$ inch – very shallow and characteristic of low-water-cementitious materials ratios.

Chlorides – Chloride contents in the core interiors nominally are from 0.023 to 0.033 percent by concrete mass. In surface regions, the chloride contents are from 0.068 to 0.105 percent by concrete mass. The data indicate chloride-deicing salts have been applied to, and intruded into, surface regions of the cores. There is no evidence chlorides have caused concrete deterioration.

To nominal depths of one-half to three-quarter inch, paste flanking cracks has been "bleached" by atmospheric intrusion that turns the deep blue-green paste color to warm-tone brown, a typical and normal phenomenon for slag-containing pastes, and without adverse ramifications.

Steel – Reinforcing bars are green epoxy-coated. Tie-wires are yellow epoxy-coated. Mesh is uncoated. Reinforcing bars are positioned in the upper and lower portions of the cores. Mesh is located at nominal 4, 6, and 8-inch depths. None of the steel is corroded.

Cracks –A major vertical crack in Cores 1 and 2 tightens with depth and extends to the bottom of each core. For practical purposes, the cracks circumscribe aggregate particles and occurred very early in the life of the concrete (e.g. when the concrete was plastic semi-plastic, or shortly thereafter). Dirt has infiltrated the cracks to depths of $4^1/_2$ inches in Core 1 and 6 inches in Core 2. The cracks circumscribe green epoxy-coated reinforcing bars. In Core 1 on interface surfaces of the upper and lower bars and flanking mortar are very fine, discontinuous, matted deposits of secondary ettringite sometimes containing intergrown calcium hydroxide and calcium chloroaluminate (Friedel's salt). These deposits are not present in the bar-mortar interface surfaces of Cores 2 and 3.

The ettringite/calcium hydroxide deposits at the bar-mortar interface indicate a fine separation was present at that location into which the secondary deposits formed. The separation can be associated with the vertical crack or indicate slight movement of the bar(s) (such as due to vibrations incidental to construction) when the concrete was semi-plastic. The calcium chloroaluminate deposits reflect later interactions of chlorides from deicing chemicals that intruded along the crack to the reinforcing bar-crack interface.

In Core 1 a fine crack (perpendicular to the main crack) intersects the main crack, transects aggregate particles, and extends to the level of the top No. 5 bar ($2^{7}/_{8}$ inches). In Core 2 two fine cracks (perpendicular to the main crack) intersect the main crack and terminates at depths of $^{3}/_{8}$ inch. These cracks in both cores are judged due to normal drying shrinkage.

A major vertical crack in Core 3 tightens with depth and terminates $2^{1}/_{2}$ inches from the bottom of the core, and is lined with dirt to a depth of 3 inches. The crack transects numerous aggregate particles in contrast to the cracks that essentially circumscribe aggregate particles in the other two cores and, thus, occurred after there was significant aggregate-paste bond strength.

Alkali-Silica Aggregate Reactions – Alkali-silica gel is present on surfaces of fractured surfaces of coarse aggregate particles transected by vertical cracks. The argillite coarse aggregate contains fine crystals of strained quartz (SiO_2). Strained quartz in the argillite coarse aggregate is alkali-silica reactive and judged the component responsible for the alkali-silica gel. The only gel observed is associated with transected argillite coarse aggregate particles along the vertical cracks in Cores 1 and 2, and in an associated air void in Core 2. Argillite particles are devoid of features indicative of deleterious alkali-silica reactions such as: darkened peripheral rims; internal cracks; peripheral cracks just inside particle perimeters; peripheral cracks along outside surfaces; and radial cracks.

The major vertical cracks in Cores 1 and 2 are sufficiently young to indicate they may have been caused by plastic shrinkage or concrete movement such as from vibrations incidental to the construction. The major crack in Core 3 is of much later vintage and occurred after significant strength had been attained – it thus may have been caused by structurally induced stresses.

Although alkali-silica aggregate reactions are demonstrated by alkali-silica gel, the gel is observed at two localized locations along major vertical cracks in two of the three cores. Features typically associated with deleterious alkali-silica aggregate reactions are not

present. On that basis, it does not appear that at the present service life of the concrete, alkali-silica aggregate reactivity is responsible for the cracks.

* * * * * * *

INTRODUCTION

Reported herein are the results of petrographic examinations and chloride analyses of three concrete cores submitted by Ian C. Hodgson/Stephen Pessiki, Lehigh University. The cores are reported to be from the southbound shoulder and right lane of the PA SR309 Bridge over Church Road in Flourtown, PA, where cracks were present before final reopening of the bridge in October 2006.

Requested are petrographic examinations to evaluate the concrete and cracks so the cause of the cracks can be identified.

Accordingly, the: (1) cores were examined using methods of ASTM C856, "Petrographic Examination of Hardened Concrete"; (2) chloride contents were determined using methods of ASTM 1152, "Acid-Soluble Chloride in Mortar and Concrete"; and (3) depths of carbonation were determined using a phenolphthalein indicator supplemented by petrographic microscopy.

The Mix #1 mix-design required per cubic yard: Type I portland cement, 455 lbs.; ground granulated blast-furnace slag, 195 lbs.; water, 31.1 gallons (259 lbs.); #57 coarse aggregate, 1474 lbs.; #8 aggregate, 372 lbs.; fine aggregate, 1130 lbs.; and air entraining, retarding, and high range water-reducing admixtures. The water-cementitious materials ratio is 0.40, the air-content range is 4.5 to 7.5 percent, and the unit weight is 143.9-lbs./ ft.^{3}. Reported 28-day cylinder strengths of jobsite concrete cylinders are 5017, 5164, and 5727 psi – the reported average 28-day mix-design compressive strength is 7178 psi.

The concrete thus has an equivalent 6.9 bags of portland cement per cubic yard of which 30 percent is ground granulated blast-furnace slag.

STUDIES

Cores – Received for the work were three cores identified as Nos. 1, 2, and 3. Core 1 was taken over the intersection of transverse and longitudinal cracks; Core 2 was taken over a transverse crack; and Core 3 was taken over a longitudinal crack. The cores have $3^3/_4$-inch diameters and respective lengths of $8^3/_4$, $8^3/_8$, $8^1/_2$, inches. Top core ends are tined surfaces with impressions spaced variably but usually $1^3/_4$ to 2 inches apart; bottom core ends are formed surfaces.

Sections of green epoxy-coated No. 5 bars are present in the upper and lower part of Cores 1 and 2 (Figures 1, 2, 4, 5) and the upper half of Core 3 (Figures 3, 6). Associated with bars in Cores 1 and 2 are yellow epoxy-coated tie-wires (Figures 4, 4B, 5, 5B). Sections of $^7/_{32}$- and $^3/_{16}$-inch diameter mesh are present in Core 1 (Figures 4, 4A, 4B). The steel and location information are summarized in Table 1.

Each core was saw-cut to provide cross-sections for petrographic examinations. One-half inch-thick sections from the top and middle of each core were saw-cut for chloride analyses. Concrete remaining was broken-up and used for more detailed petrographic examinations and depth of carbonation analyses.

Petrographic Examinations

Aggregates – Coarse aggregate is crushed, fine-grained, deep brown with a black overtone and occasionally dark olive, finely bedded, fissile argillite having a 1-inch nominal maximum size. Particles are blocky in the finer sizes to elongated in the intermediate and finer sizes (Figures 4, 5, 6). An occasional particle is white to light grey. The argillite contains potassic clay intergrown with fine, authigenic strained quartz and minor amounts of calcite ($CaCO_3$) (Figure 7). A few particles are internally cracked randomly and/or along bedding planes. On fracture surfaces of aggregate particles transected by a vertical crack in Cores 1 and 2, and lining an adjacent air void, is alkali-silica gel (Figures 8, 9).

Fine aggregate is natural sand that contains major amounts of clear to translucent grey, translucent pale orange and pale yellow, single- and multi-crystal quartz, plus trace amounts of coarse aggregate tailings.

The aggregates are relatively well graded and well distributed (Figures 4, 5, 6).

Pastes – Pastes of the cores are similar. They are dark blue-green, dense, firm, and fracture surfaces have semi-conchoidal textures. There is an apparent very slight darker to lighter color tone from bottom to top of the cores. In surface regions, to nominal depths of $^{1}/_{2}$ to $^{3}/_{4}$ inch, pastes have a warmtone brown color, a result of "atmospheric bleaching" of the slag component (Figures 4, 4A, 5, 5A, 6, 6A). That phenomenon occurs sporadically below those regions so pastes have a mottled appearance (Figures 4A, 5A, 6A), and also along cracks (Figures 4, 4A, 4B, 5, 5A, 5B, 6, 6A, 6B).

Relict portland cement particles are abundant; hydration of the cement is normal and advanced; the calcium hydroxide ($Ca(OH)_2$) component of cement hydration occurs as very fine platy units; and particle sizes are indicative of a finely ground portland cement (e.g. Type III). Distributed throughout the pastes is ground granulated blast-furnace slag having the fineness of portland cement, and which is extensively hydrated (an occasional "core" of residual slag surrounded by hydrated slag is present, Figure 10). Trace amounts of quartz and mica representing fine-fines from the fine aggregate are distributed throughout the pastes.

Features of the pastes are indicative of cementitious materials contents equivalent to $6^{1}/_{2}$ to 7 bags of portland cement per cubic yard of which a significant amount (e.g. 30 percent) is ground granulated blast-furnace slag. Estimated overall water-cementitious materials ratios are 0.40 – in bottom areas it is estimated 0.38 to 0.39 due to bleeding. The data are summarized in Table 1.

Carbonation – Freshly fractured surfaces were tested. Respective depths of carbonation for Cores 1, 2, and 3 are $<^{1}/_{64}$, $^{1}/_{8}$, and $<^{1}/_{64}$ inch. The data are given in Table 1.

Air – Air in each core occurs as multitudes of small, spherical voids characteristic of entrained-air voids, and a relatively few coarse spherical and non-spherical voids characteristic of entrapped air – the cores are air-entrained. Estimated respective air contents of Cores 1, 2, and 3 are 7, 7, and 7 to $7^1/_2$ percent. The data are in Table 1.

Secondary Compounds – Lining or partially filling most air voids is secondary white, acicular ettringite ($3CaO{\cdot}Al_2O_3{\cdot}3CaSO_4{\cdot}32H_2O$) (Figure 11). Sometimes intergrown with the ettringite are hexagonal platelets of calcium hydroxide ($Ca(OH)_2$).

At interface surfaces of epoxy-coated reinforcing bars and flanking paste is a discontinuous film of ettringite. Occasionally associated with the ettringite is calcium chloroaluminate (Friedel's salt)/calcium hydroxide (Figure 12). That feature indicates a fine, peripheral space existed at that interface in which the secondary compounds formed.

On a vertical crack surface in the upper part of Core 1 is a film of shiny, white, potassic alkali-silica gel (Figure 13). On the surface of a coarse aggregate particle intersected by a crack at about mid-point of Core 2 are clear and white deposits of alkali-silica gel (Figure 13). Lining an air void adjacent to the aggregate particle in Core 2 are two generations of alkali silica gel (Figure 9).

Cracks

Core 1 – A vertical crack (surface width at narrowest location, 0.004 inches) on the surface travels between tine markings, extends from top to bottom of the core, circumscribes aggregate particles (except for two) and tightens with depth. At a depth of two inches it clips the end of a coarse aggregate particle, and at a depth of 5 inches transects a thin, elongated aggregate particle**.** The crack is lined with infiltrated dirt to depths of $4^1/_2$ inches, and in localized areas on the crack surface are secondary acicular, white ettringite deposits and a shiny, white, film of alkali-silica-gel (Figure 13).

A fine crack (perpendicular to the main crack) intersects the main crack, transects aggregate particles, and terminates at the level of the top No. 5 bar ($2^7/_8$ inches).

Core 2 – A vertical crack (surface width at narrowest location, 0.003 inches) parallel to tine markings extends from top to bottom of the core, except for two aggregate particles circumscribes aggregate particles, and tightens with depth. At a depth of two inches it intersects an elongated coarse aggregate particle and, at a depth of $5^{3}/_{8}$ inches, clips the side of a coarse aggregate particle**.** The crack is lined with infiltrated dirt to depths of 6 inches.

A fine crack (perpendicular to the main crack) intersects the main crack and terminates at a depth of $^{3}/_{8}$ inches.

Core 3 – A vertical crack (surface width at narrowest location, 0.005 inches) perpendicular to tine markings tightens with depth and terminates $2^{1}/_{2}$ inches from the bottom of the core. It intersects coarse aggregate particles at depths of $^{1}/_{2}$, $1^{7}/_{8}$, $2^{1}/_{16}$, $4^{3}/_{4}$, and $5^{5}/_{8}$ inches. The crack is lined with infiltrated dirt to depths of 3 inches.

Chloride Analysis

One-half-inch thick sections from the top and interior of each core were analyzed. The data are in Table 2.

The Erlin Company

Bernard Erlin, Petrographer
Project Manager

Samples will be discarded after thirty days unless other disposition is requested in writing.

Table 1 – Core lengths, crack widths, bar size and cover, mesh depth and cover, and some petrographic data for the cores.

Core	Length [1] (in.)	Crack Width (in.)	Steel Type	Nominal Depth of Cover (in.)	Carbonation Depth (in.)	Estimated		
						Air (%)	Equivalent Portland Cement (bg/yd^3)	Overall *w/cm*
1	$8^3/_4$	0.004	No. 5T [2] No. 5L [2] Mesh ($^7/_{32}$) No. 5L [2] Mesh ($^3/_{16}$) No. 5T [2] [3] Mesh ($^3/_{16}$)	$2^7/_8$ $3^1/_2$ $4^1/_8$ 6 6 $6^3/_4$ $8^1/_4$	$< {}^1/_{64}$	7	$6^1/_2$-7	0.40 [4]
2	$8^3/_8$	0.003	No. 5T [2] No. 5L [2] [3] No. 5T [2] [3]	$2^3/_8$ $5^3/_4$ $6^1/_2$	$^1/_8$	7	$6^1/_2$-7	0.40 [4]
3	$8^1/_2$	0.005	No. 5T [2] No. 5L [2] No. 5T [2] Socket from hexagonal nut	Socket, $2^1/_4$ $2^7/_8$ Socket $6^1/_2$ Bottom	$< {}^1/_{64}$	7-$7^1/_2$	$6^1/_2$-7	0.40 [4]

[1] Each core has a $3^3/_4$-inch diameter.
[2] Green epoxy-coated. T= transverse bar; L = longitudinal bar.
[3] Associated tie-wires have $^1/_{16}$-inch diameters and are yellow epoxy-coated.
[4] Slightly lower in bottom portions of the cores.

Table 2 – Acid-soluble chloride contents for the cores (ASTM C1152).

Depth (in.)	Chloride, % by Mass		
	Core 1	Core 2	Core 3
$0 - {}^{1}/_{2}$	0.105	0.068	0.099
$4^{1}/_{2} - 5$	0.033	--	--
$4^{3}/_{4} - 5^{1}/_{4}$	--	0.023	--
$3^{1}/_{4} - 3^{3}/_{4}$	--	--	0.030

Side A Side B Side C

Top Bottom

Figure 1 – Views of Core 1 as received. Scale in inches.


Side A


Side B


Side C

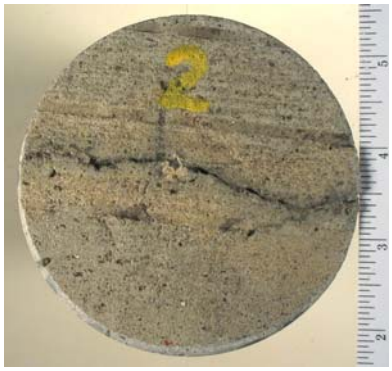
Top

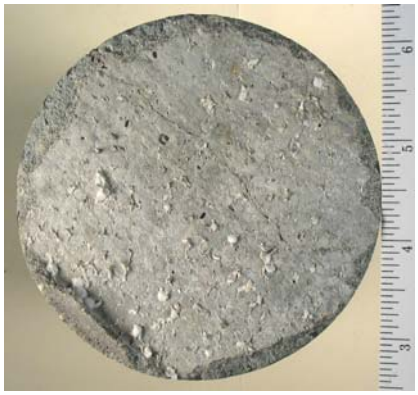
Bottom

Figure 2 – Views of Core 2 as received. Scale in inches.

Side A

Side B

Side C

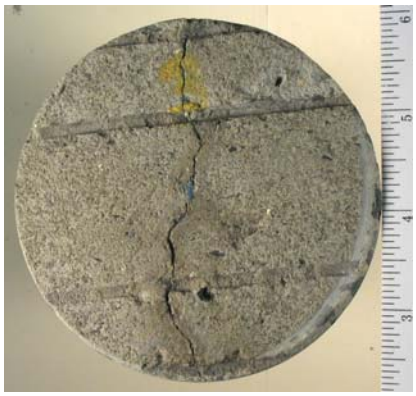

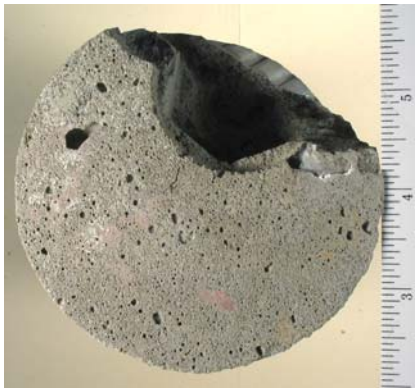

Figure 3 – Views of Core 3 as received. Scale in inches.

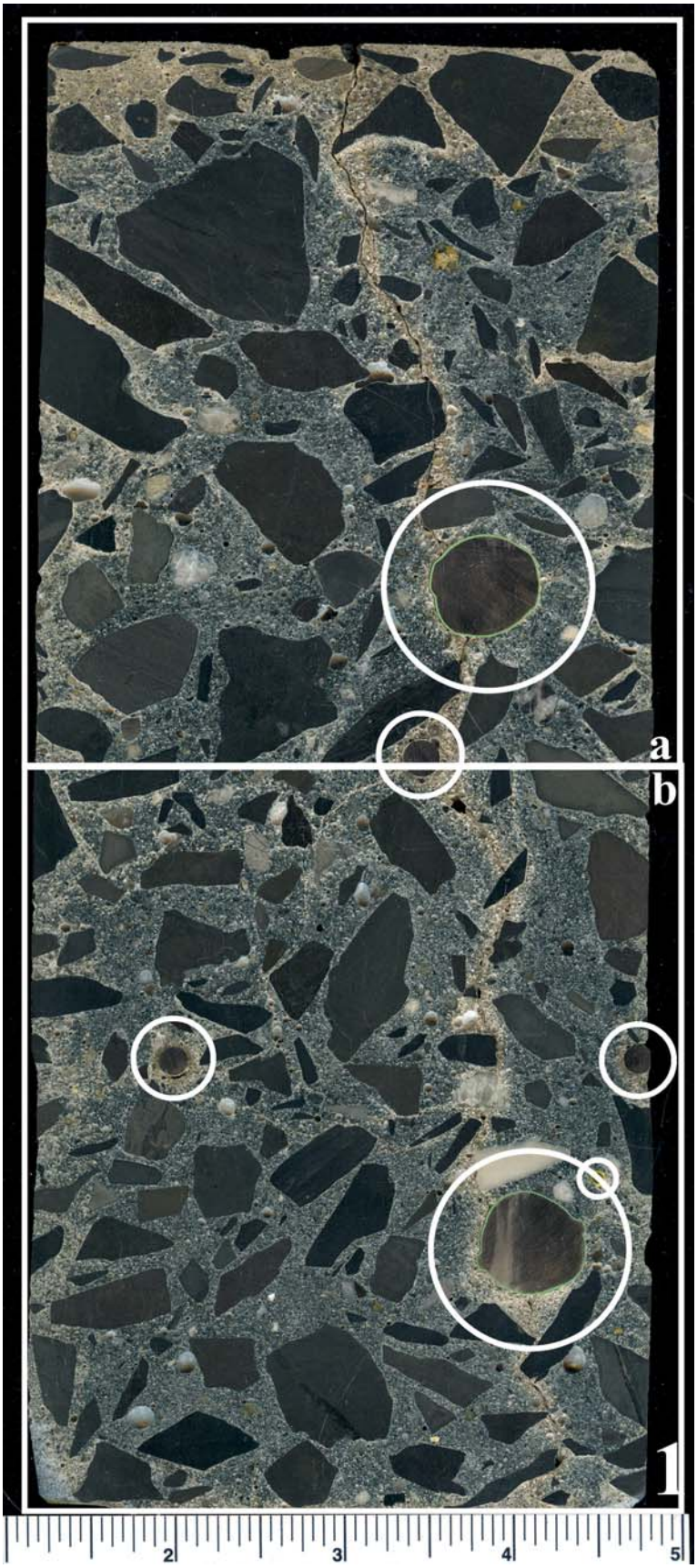

Figure 4 – Cross-section of Core 1 showing: (a) aggregate grading and distribution; (b) dark blue-green coloration typical of pastes containing ground granulated blast-furnace slag; (c) "bleaching" of the paste due to atmospheric intrusion in the surface region and along cracks; (d) a vertical crack that extends from top to bottom of the core (defined by "bleaching" along the crack path); (e) green epoxy-coated No. 5 reinforcing bars (large circles); (f) yellow epoxy-coated tie-wire (small circle); and (g) mesh sections (intermediate-sized circles). Boxed Areas "a" and "b" are shown in Figures 4A and 4B. Scale in inches.

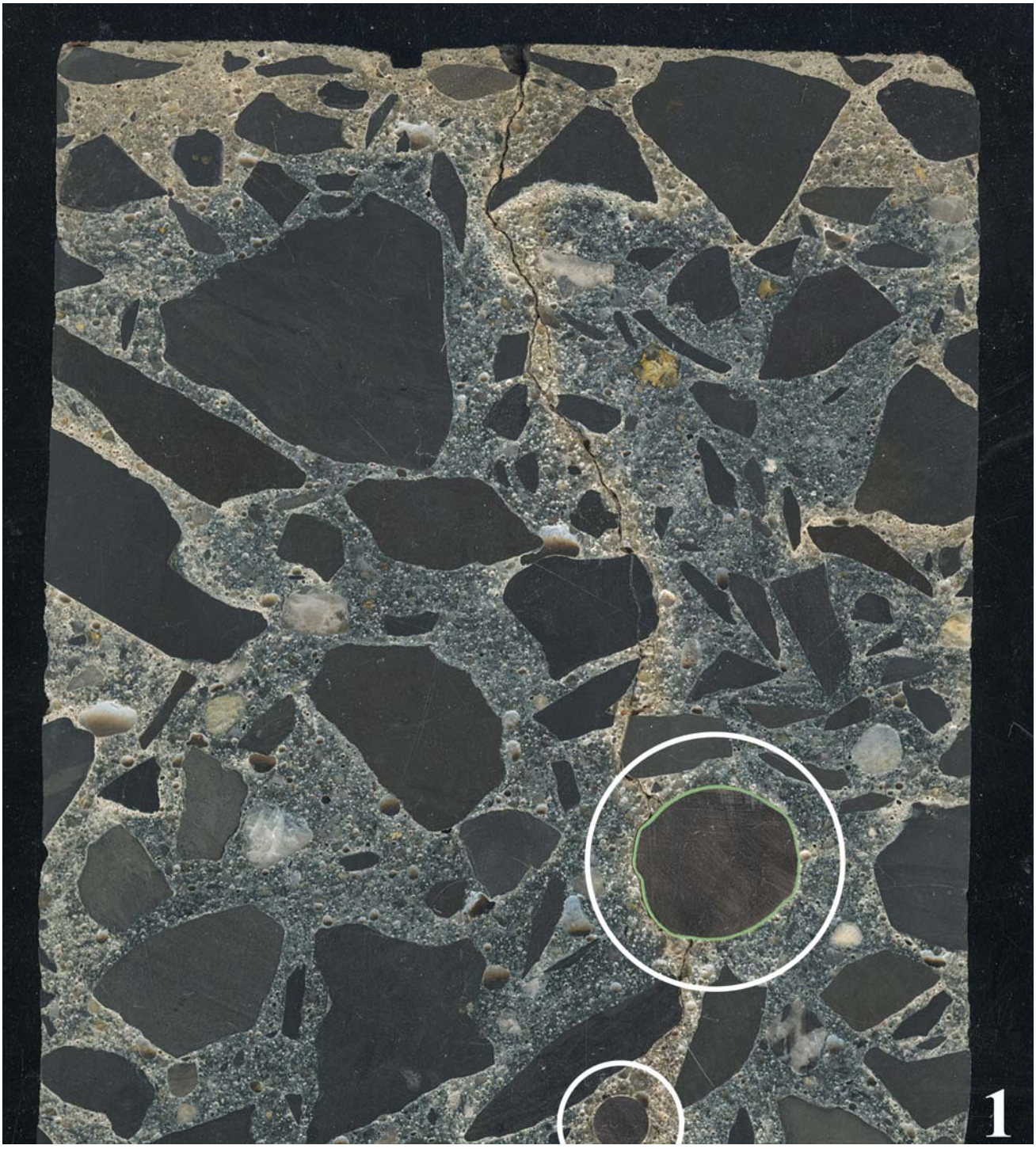

Figure 4A – Boxed Area "a" in Figure 4. A reinforcing bar (large circle) is green epoxy-coated. A mesh section is circled. The vertical crack circumscribes most aggregate particles.

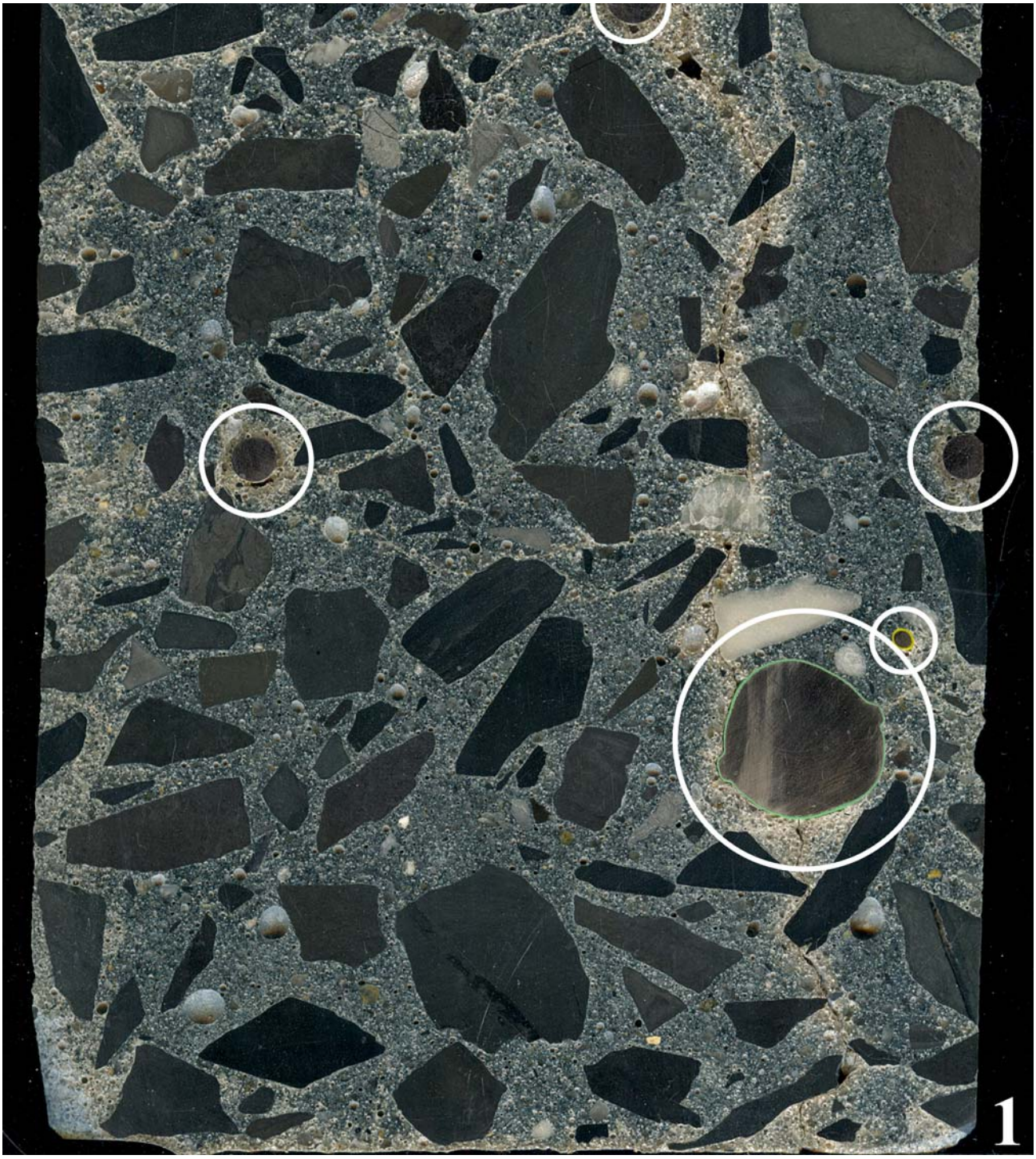

Figure 4B – Boxed Area "b" in Figure 4. The reinforcing bar (large circle) is green-epoxy-coated. A tie-wire (small circle) is yellow-epoxy-coated. Mesh sections are within the intermediate-sized circles. The vertical crack circumscribes most aggregate particles and extends to the core bottom.

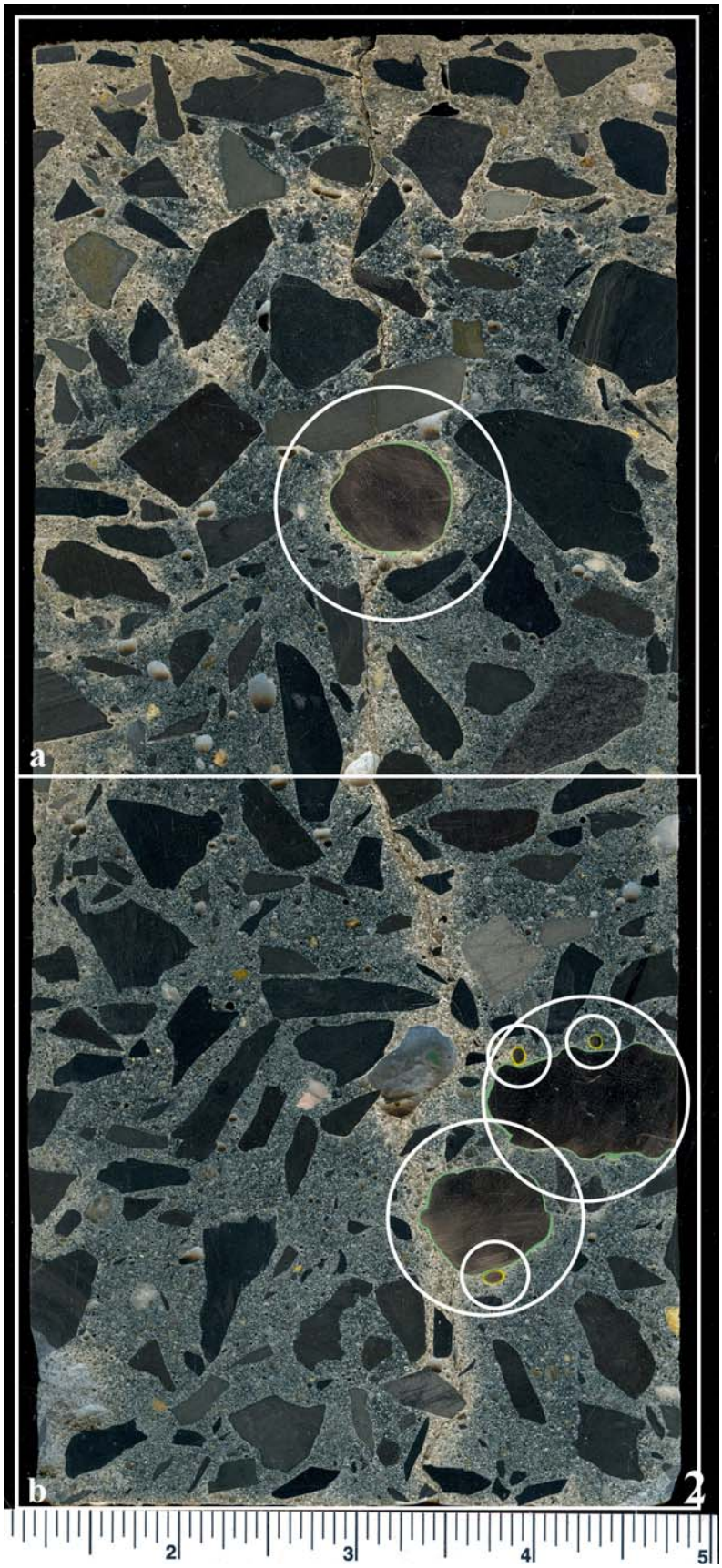

Figure 5 – Cross-section of Core 2 showing: (a) aggregate grading and distribution; (b) dark blue-green coloration typical of pastes containing ground granulated blast-furnace slag; (c) "bleaching" of the paste due to atmospheric intrusion in the surface region and along cracks; (d) a vertical crack that extends from top to bottom of the core (defined by "bleaching along the crack path); (e) three green epoxy-coated No. 5 bars (large circles); and (f) yellow epoxy-coated tie-wires (small circles). Boxed Areas "a" and "b" are shown in Figures 5A and 5B. Scale in inches.

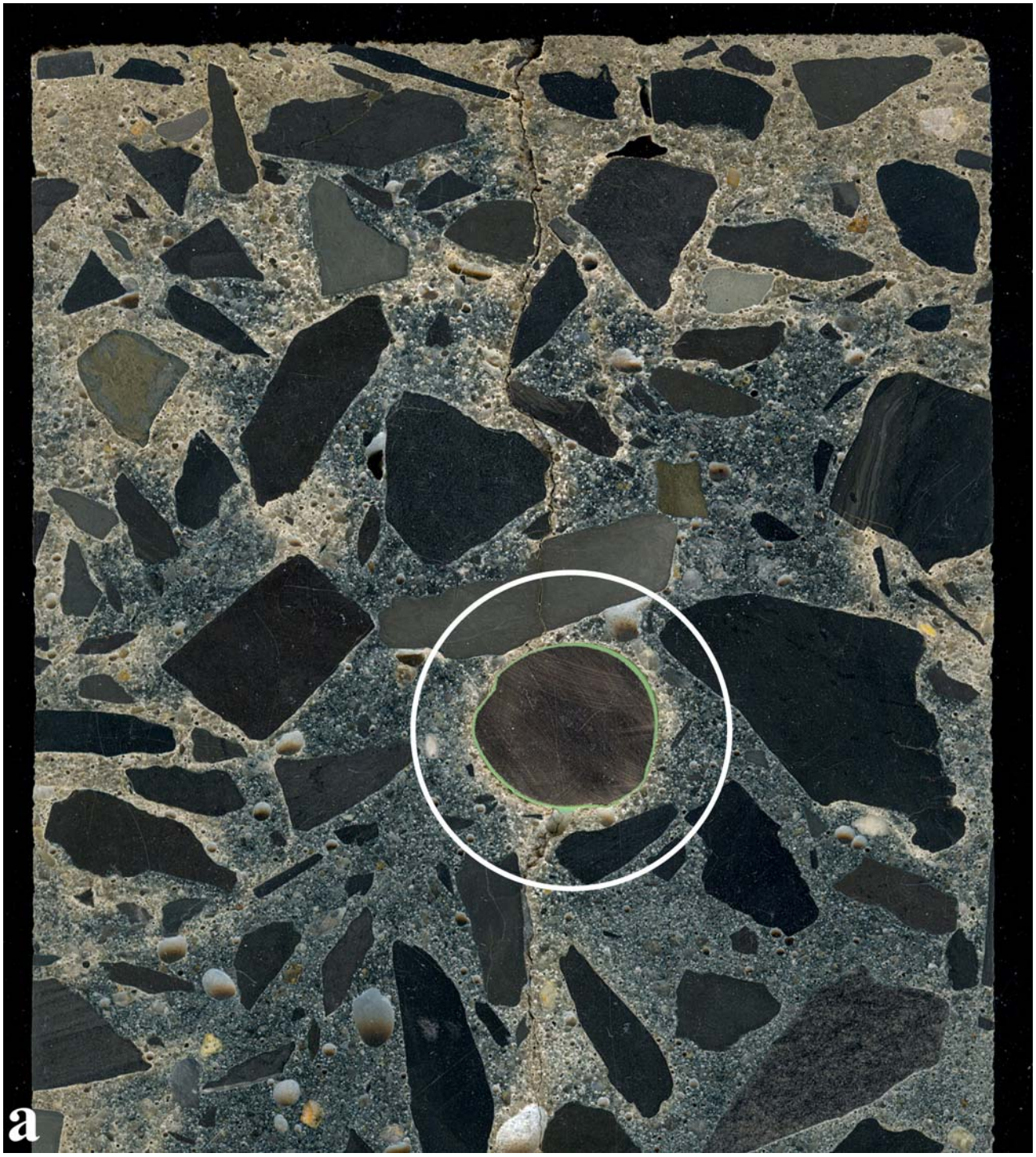

Figure 5A – Boxed Area "a" in Figure 5. The reinforcing bar (circled) is green epoxy-coated. The vertical crack circumscribes most aggregate particles.

Figure 5B (Core 2) – Boxed Area "b" in Figure 5. No. 5 bars (large circle and ellipse)are green epoxy-coated, and tie-wires (small circles) are yellow epoxy-coated. Within the red circle is a large entrapped air void. The vertical crack circumscribes most aggregate particles and extends to the core bottom.

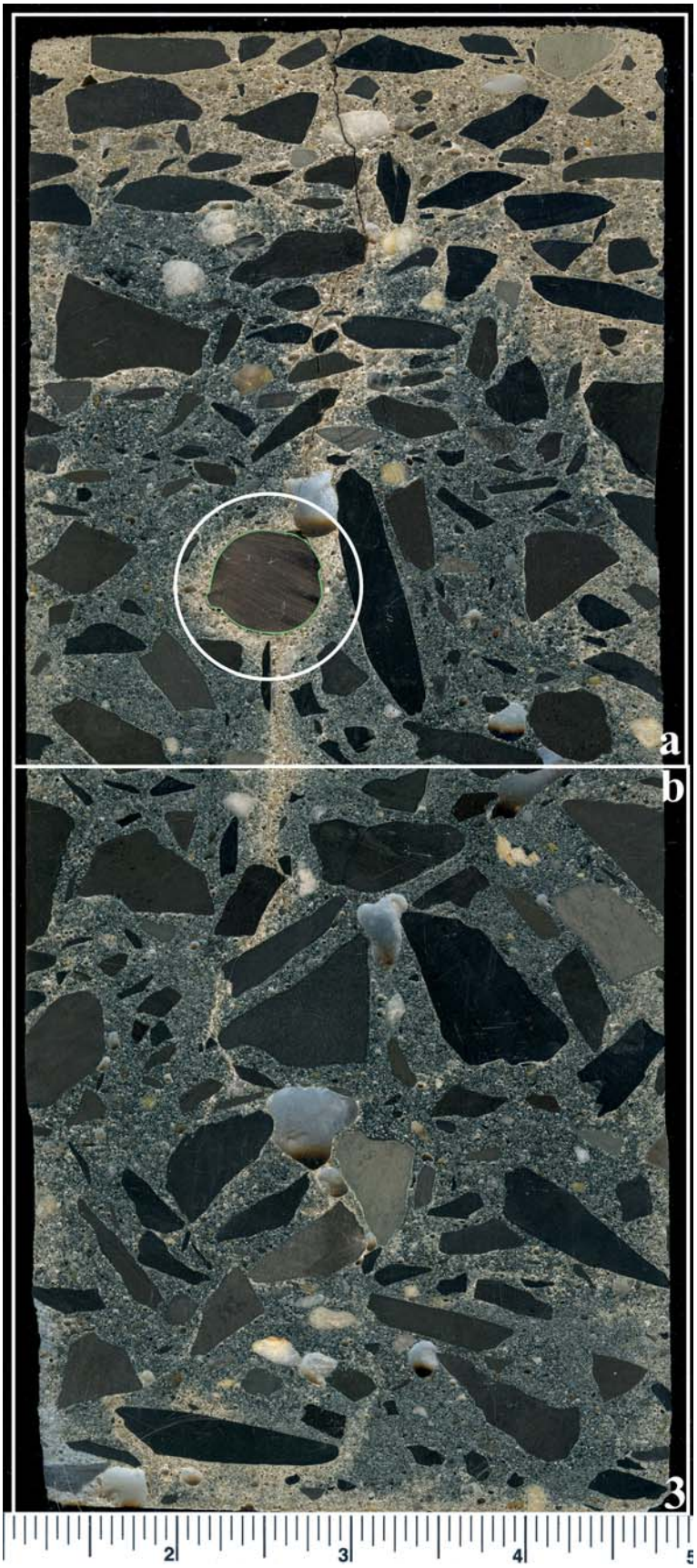

Figure 6 – Cross-section of Core 3 showing: (a) aggregate grading and distribution; (b) dark blue-green coloration typical of pastes containing ground granulated blast-furnace slag; (c) "bleaching" of the paste due to atmospheric intrusion in the surface region and along a crack; (d) a vertical crack that extends from top to $2^{1}/_{2}$ inches from the core bottom (defined by "bleaching along the crack path); and (e) an epoxy-coated No. 5 reinforcing bar (circled). Boxed Areas "a" and "b" are shown in Figures 6A and 6B. Scale in inches.

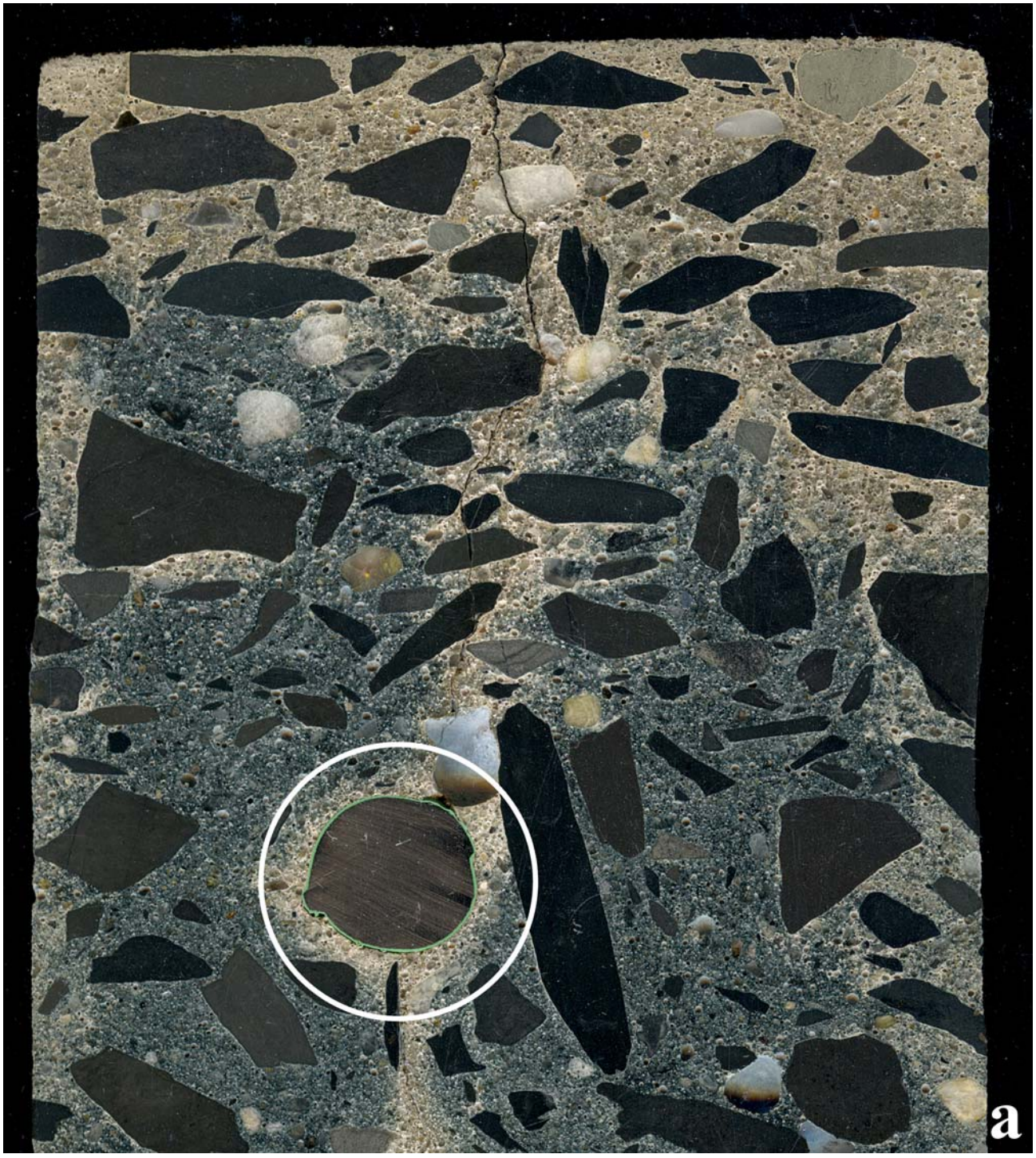

Figure 6A – Boxed Area "a" in Figure 6. The reinforcing bar (circled) is green-epoxy-coated. The vertical crack transects several aggregate particles and mainly circumscribes aggregate particles.

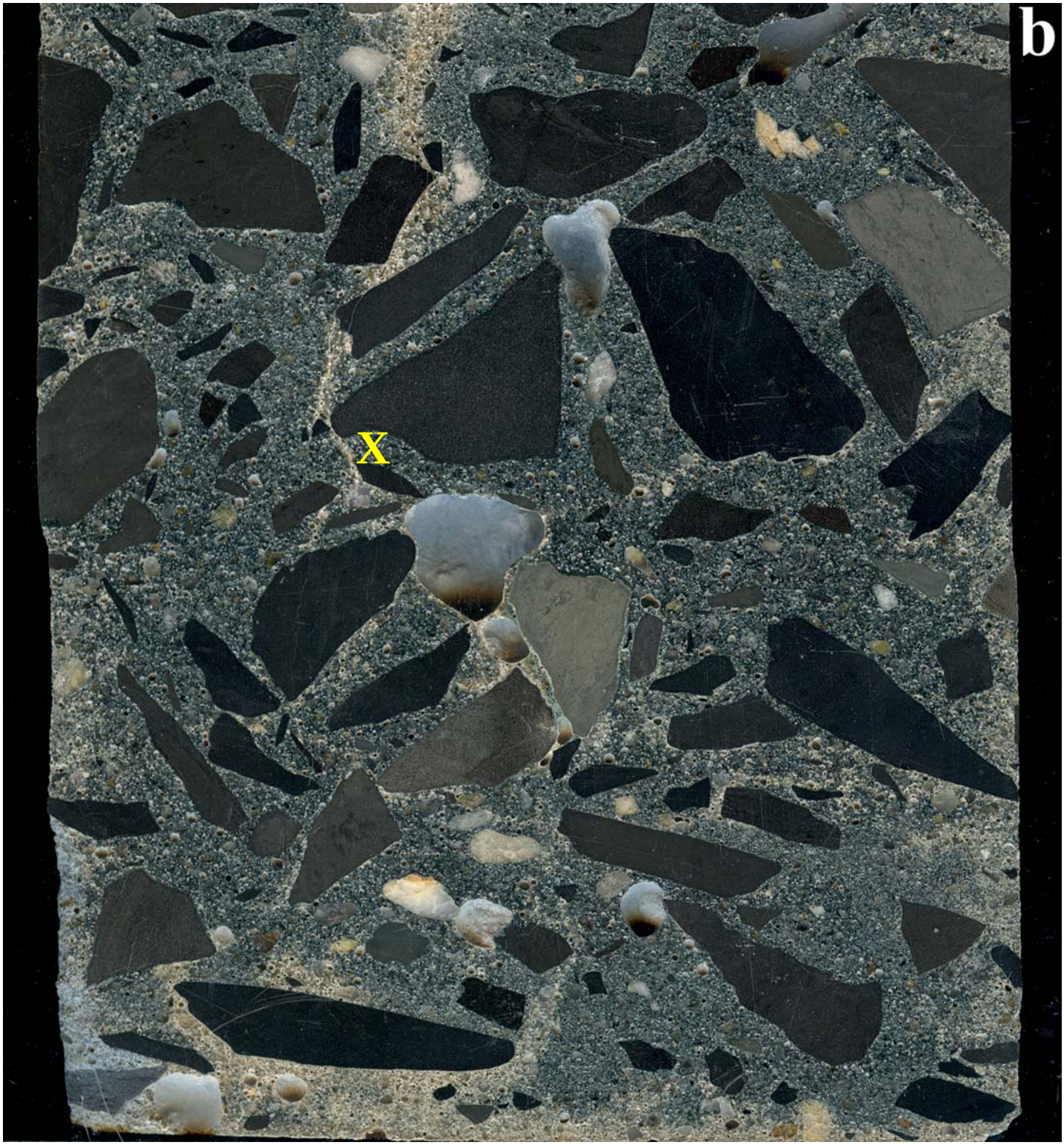

Figure 6B – Boxed Area "b" in Figure 6. The vertical crack transects many aggregate particles and terminates $2^{1}/_{2}$ inches from the core bottom (denoted by the X).

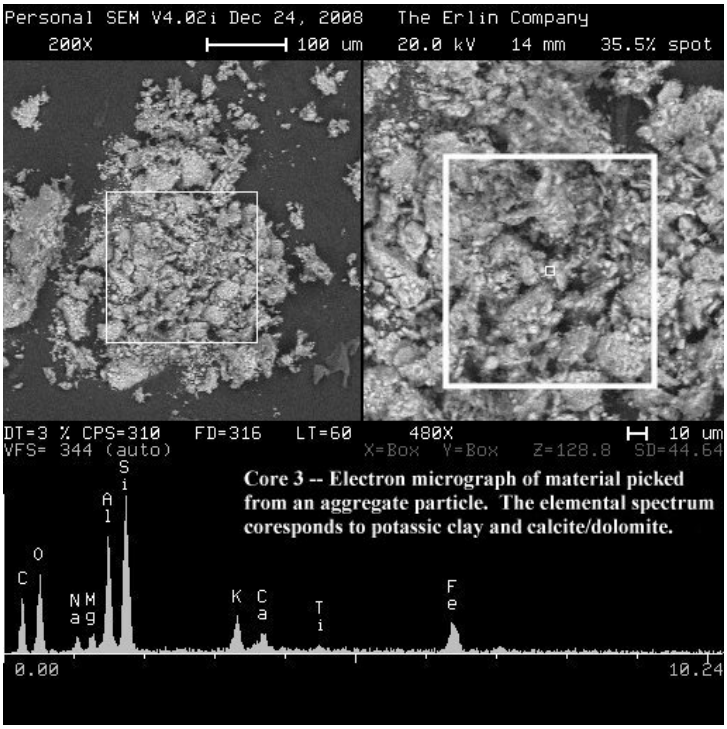

Figure 7a (Core 3) – The right micrograph is the box area in the left micrograph. The elemental spectrum is of the large boxed area in the right micrograph and corresponds to potassic clay and calcite/dolomite.

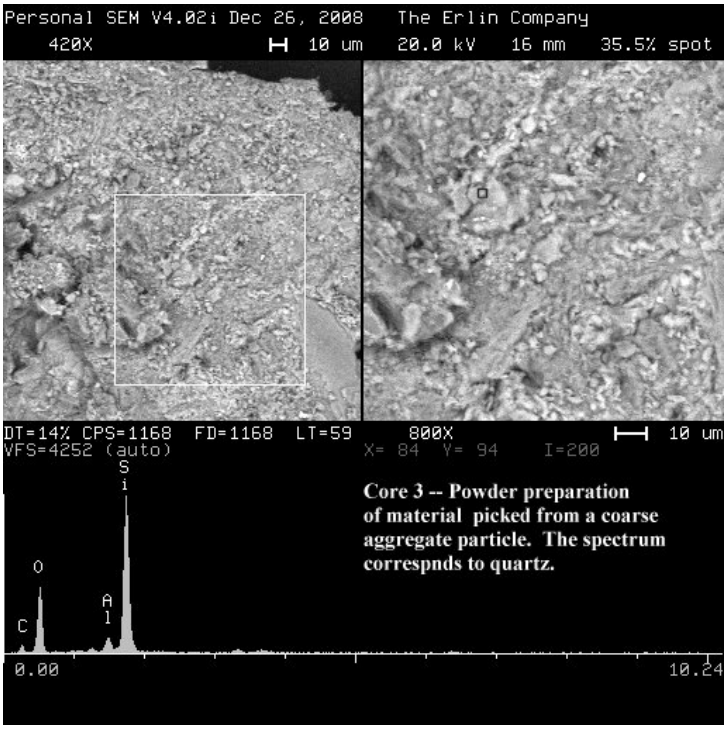

Figure 7b (Core 3) – The right micrograph is the box area in the left micrograph. The elemental spectrum is of the small-boxed area above and left of center in the right micrograph and corresponds to quartz.

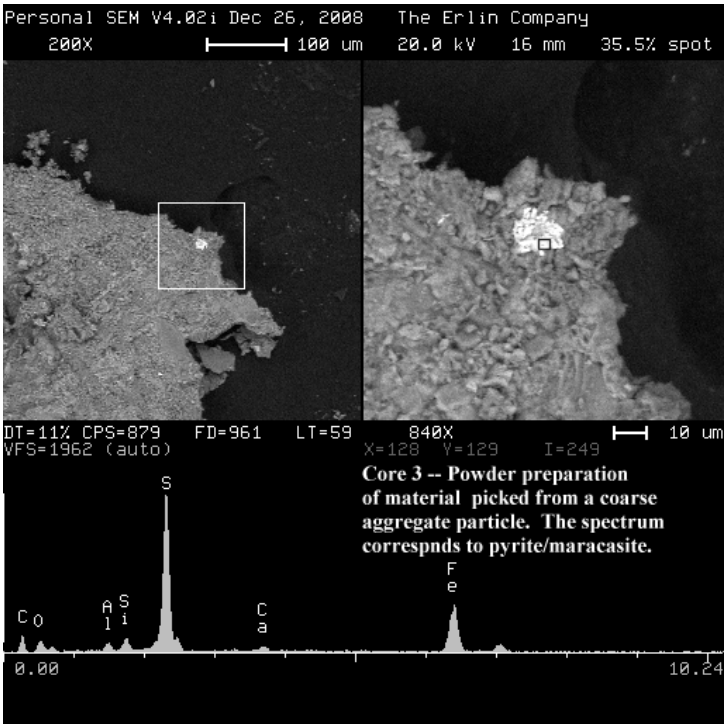

Figure 7c (Core 3) – The right micrograph is the box area in the left micrograph. The elemental spectrum is of the small-boxed area in the bright material above center in the right micrograph and corresponds to pyrite/marcasite.

Figure 7 (Core 3) – Electron micrographs of material picked from coarse aggregate particles. In each Figure the right micrographs are the boxed area in the left micrograph. The elemental spectra are of the large (Figure 7a) or small (Figures 7b, 7c) boxed areas in the right micrographs. Figure 7a spectrum corresponds to potassic clay and calcite/dolomite; Figure 7b spectrum corresponds to quartz (SiO_2); and Figure 7c spectrum corresponds to pyrite/marcasite (FeS).

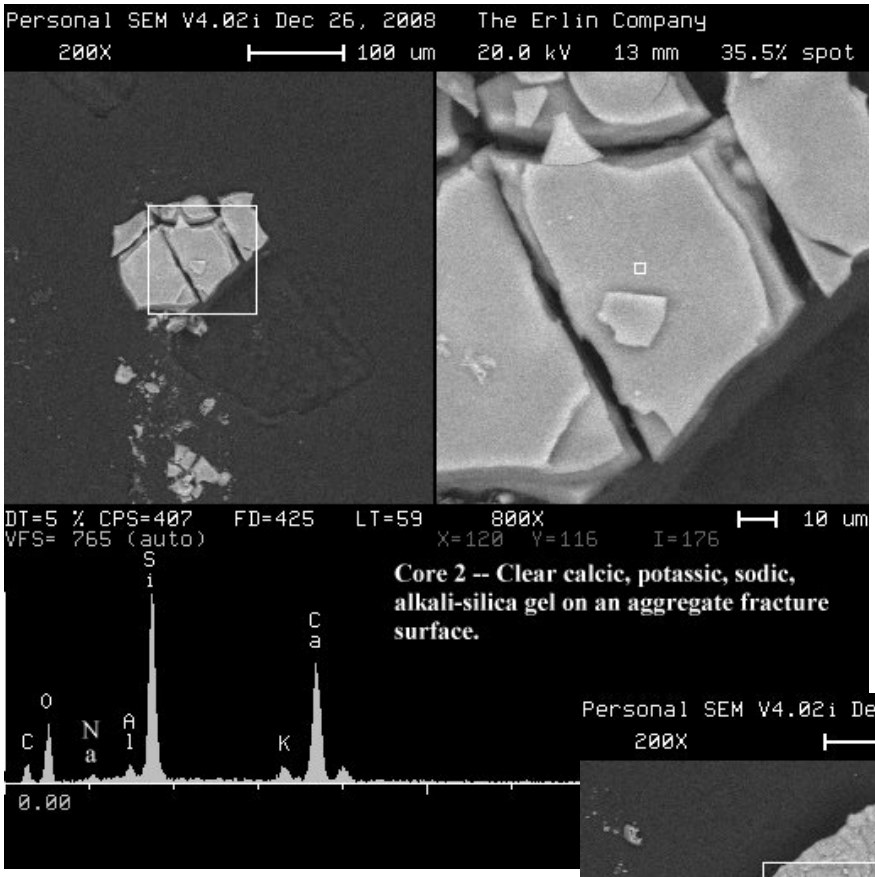

Figure 8a – Clear calcic, potassic, sodic, alkali-silica gel from an aggregate fracture surface. The elemental spectrum is of the small-boxed area at center in the right micrograph. Contiguous white gel is shown in Figure 8b.

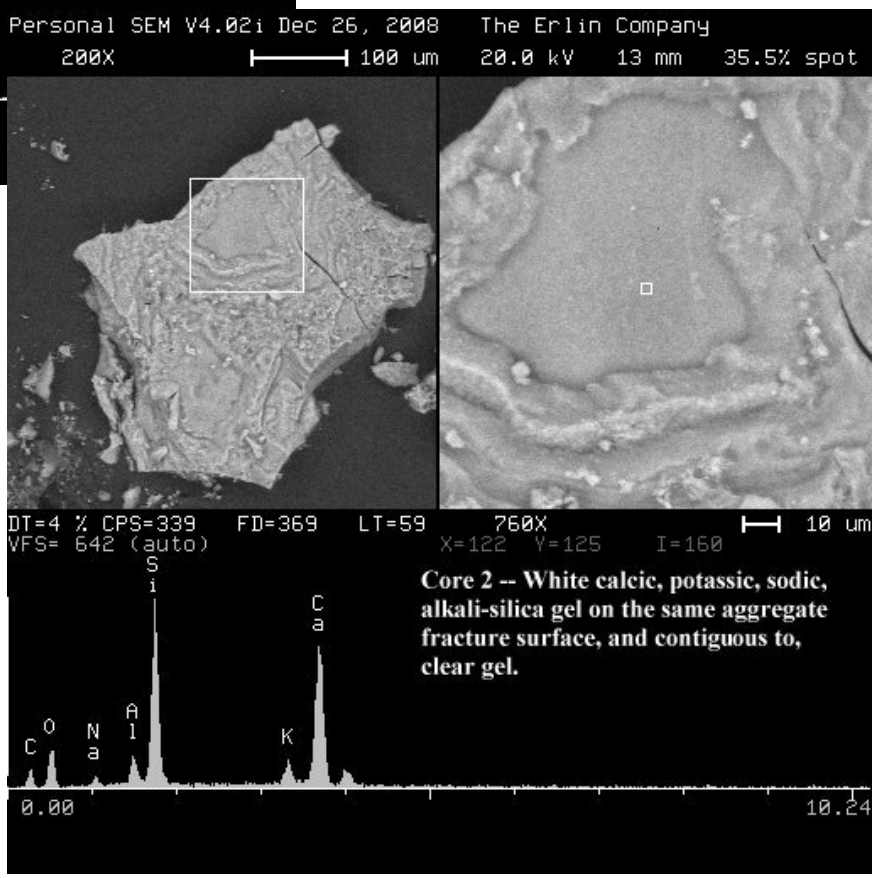

Figure 8b – White calcic, potassic, sodic, alkali-silica contiguous to the clear gel shown in Figure 8a. The elemental spectrum is of the small-boxed area at center in the right micrograph.

Figure 8 (Core 2) – Electron micrographs of clear (Figure 8a) and white (Figure 8b) calcic (Ca)-potassic (K)-sodic (Na) alkali-silica gel on the fracture surface of an aggregate particle. The right micrographs are the boxed areas in the left micrographs. The elemental spectra are of the small-boxed areas at about center in the right micrographs.

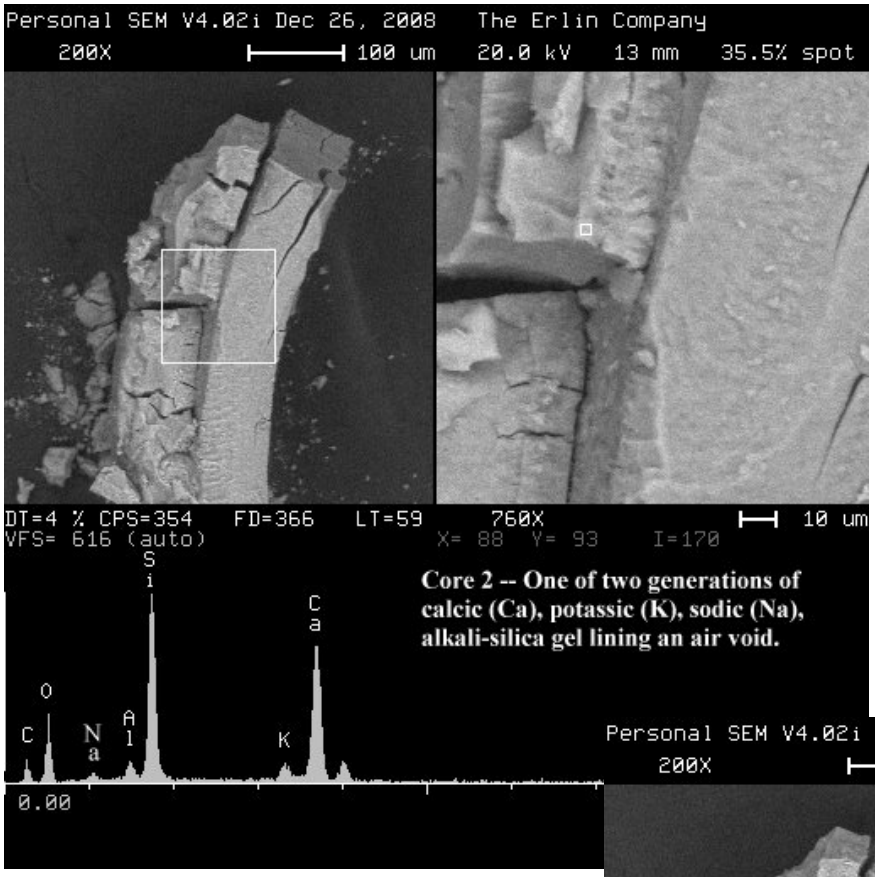

Figure 9a – Base generation of white calcic, potassic, sodic, alkali-silica gel lining an air void. The elemental spectrum is of the small-boxed area left and above center in the right micrograph. The gel is overlain by a second generation of gel (Figure 9b).

Figure 9b – Second generation of white calcic, potassic, sodic, alkali-silica gel lining an air void. The elemental spectrum is of the small-boxed area right of center in the right micrograph.

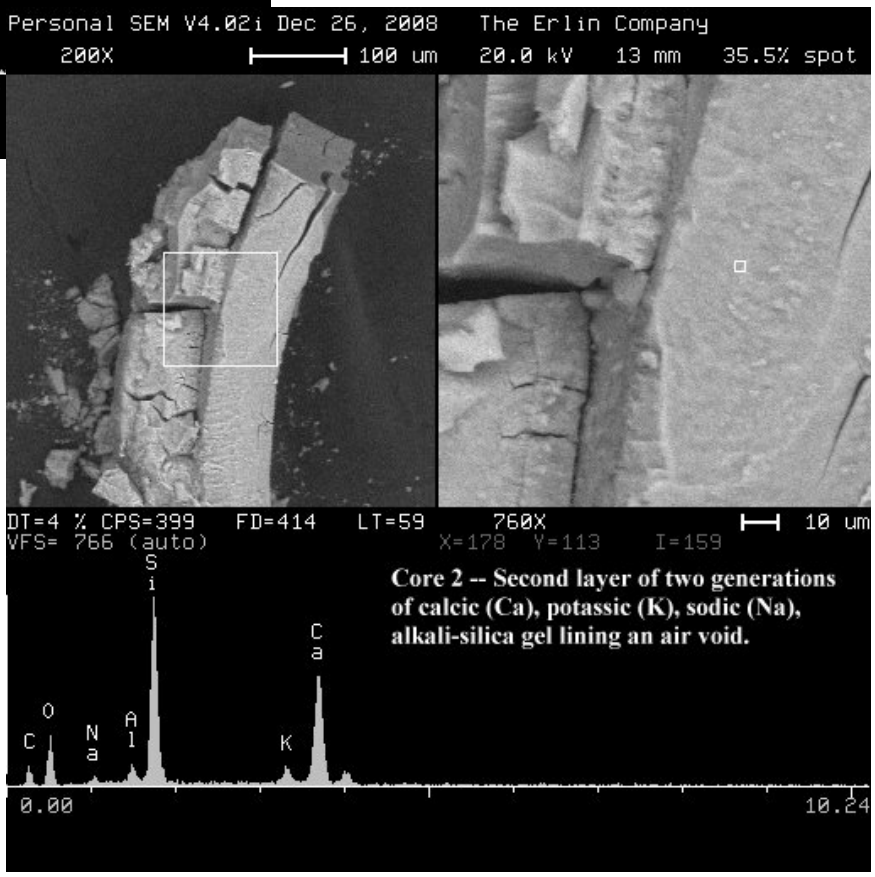

Figure 9 (Core 2) – Electron micrographs of two generations of white, calcic (Ca)-potassic (K)-sodic (Na) alkali-silica gel lining an air void. The right micrograph is the box area in the left micrograph. The elemental spectrum is of the small-boxed area at about center in the right micrograph.

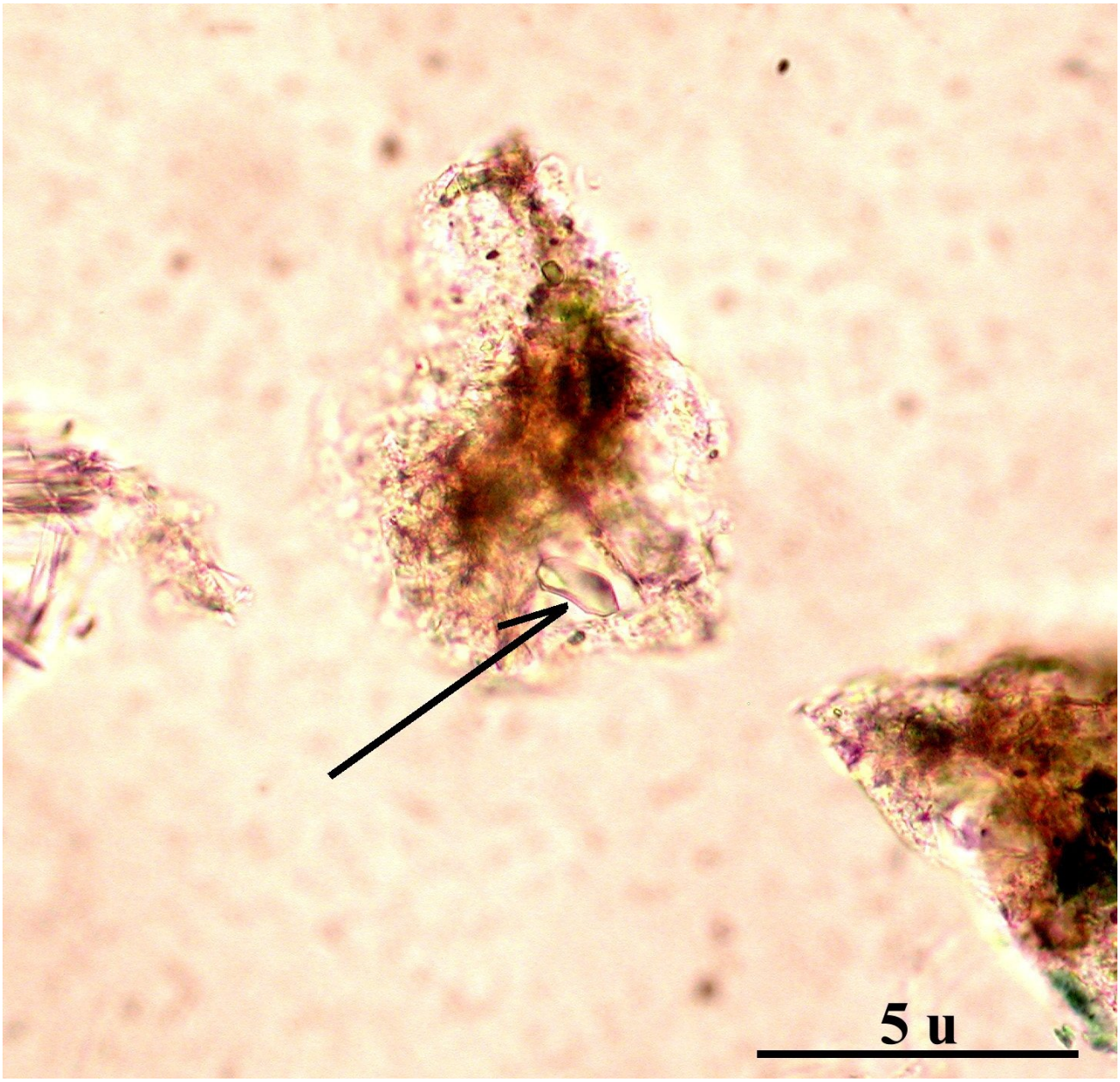

Figure 10 (Core 1) – Powder preparation observed using a petrographic microscope and plane-polarized light. The arrow points to a "core" of unhydrated ground granulated blast-furnace slag surrounded by a rim of hydrated slag. Scale in microns.

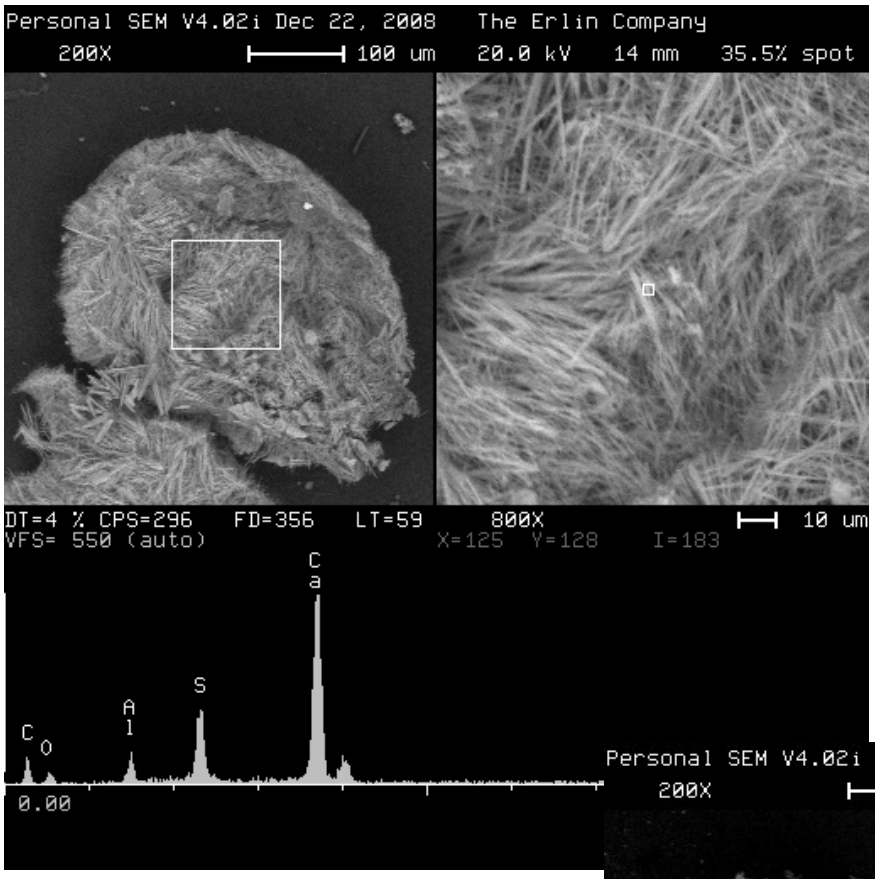

Figure 11a – Acicular ettringite picked from an ettringite-filled void.

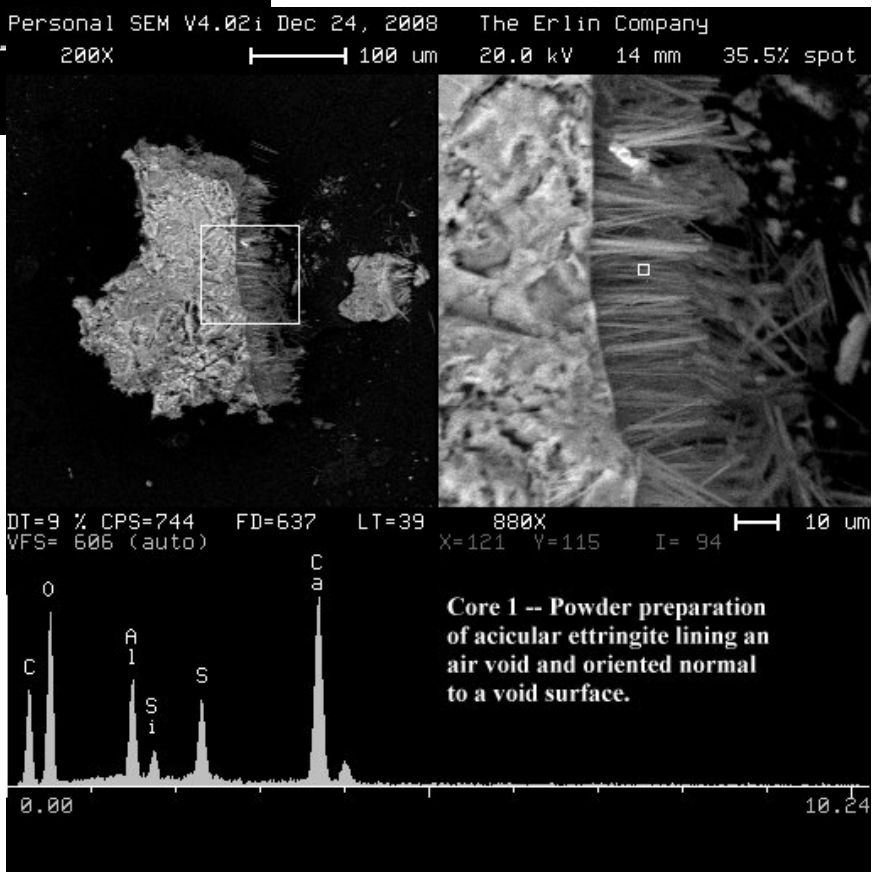

Figure 11b – Acicular ettringite lining an air-void and oriented normal to the void wall.

Figure 11 (Core 1) – Electron micrographs of acicular ettringite. In Figure 11a the specimen is from an air void filled with ettringite. In Figure 11b ettringite lines an air void. In each figure, the right micrograph is the box area in the left micrograph. The elemental spectra are of the small-boxed areas at about center in the right micrographs. The spectra correspond to ettringite.

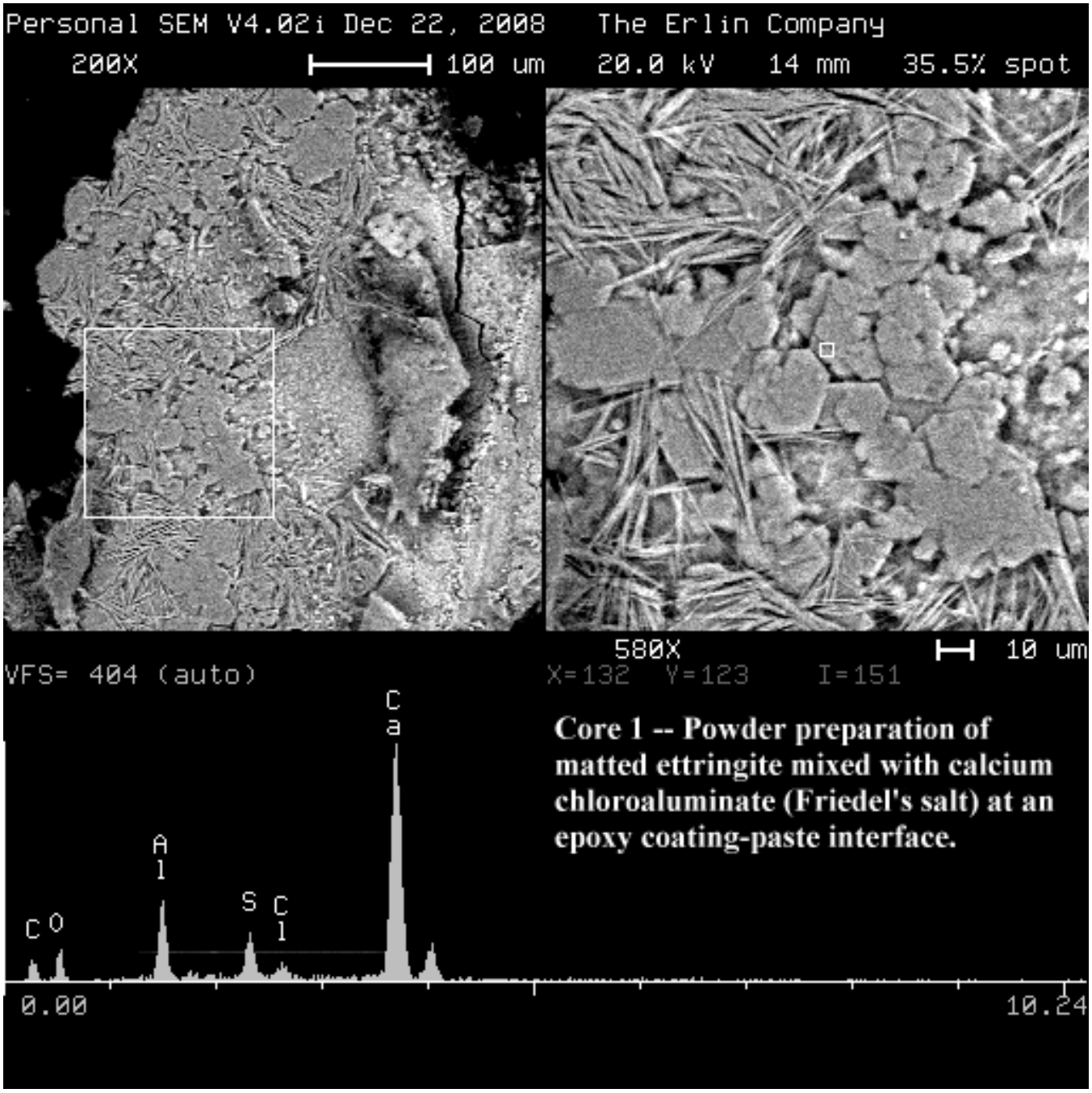

Figure 12 (Core 1) – Electron micrograph of secondary products in the interface surface of a green epoxy-coated reinforcing bar and flanking mortar. The right micrograph is the box area in the left micrograph. The elementary spectrum is of the small-boxed area at about center in the right micrograph. The spectrum corresponds to a mixture of ettringite (possibly mono sulfoaluminate) and calcium chloroaluminate (Friedel's salt).

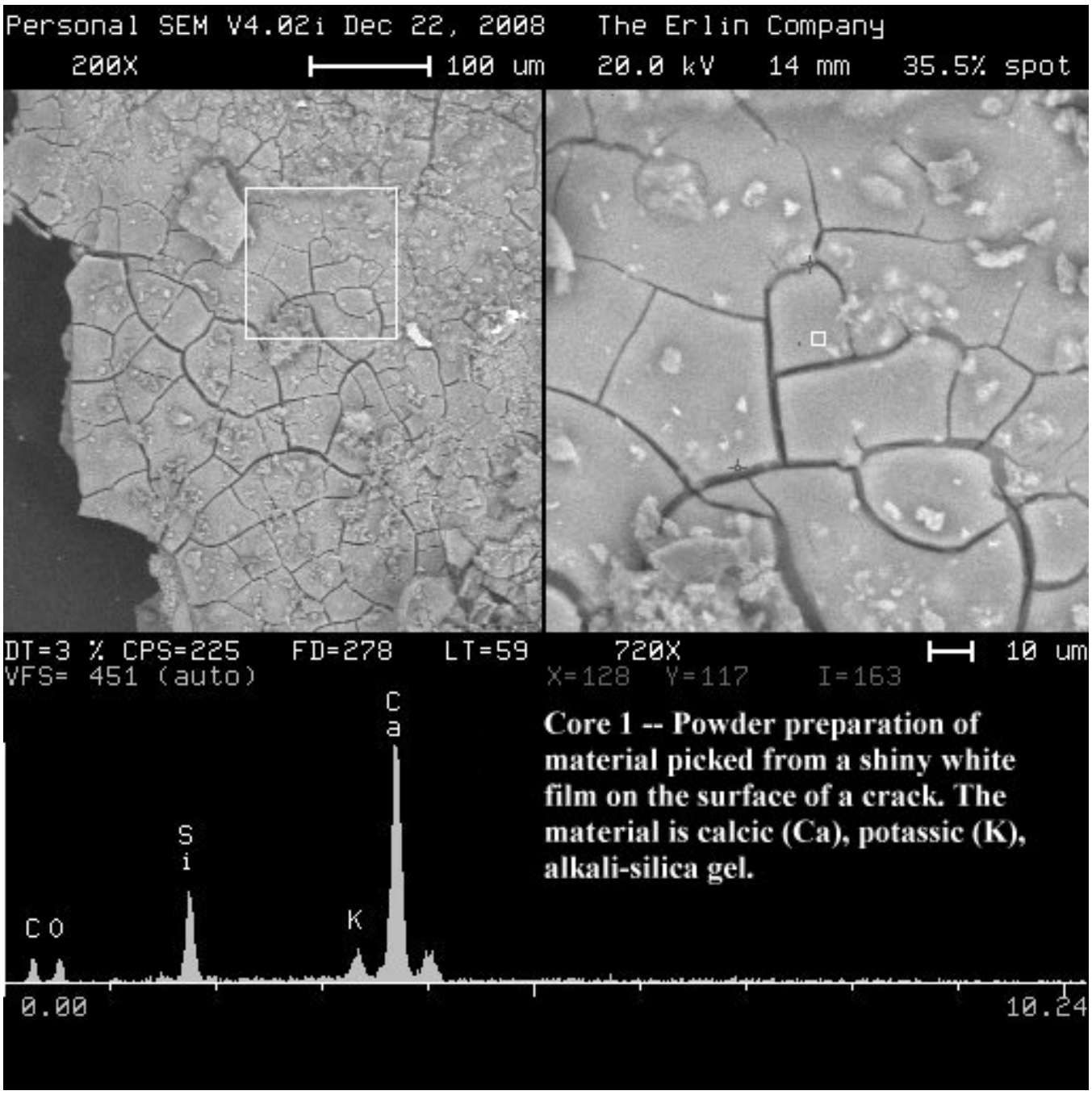

Figure 13 (Core 1) – Electron micrograph of calcic-potassic alkali-silica gel from a crack surface. The right micrograph is the box area in the left micrograph. The elemental spectrum is of the small-boxed area at about center in the right micrograph. The spectrum corresponds to calcic (Ca)-potassic (K), alkali-silica gel.

APPENDIX B

Deck Cracking Remediation Recommendations
by Michael Baker Jr., Inc.

Concrete Deck Cracking Report
SR 309 over Church Road
Remediation Recommendations

August 27, 2009

By
Richard J. Flango
Michael Baker Jr., Inc.

OBJECTIVE

Objective

At the Department's request, the following remediation options were investigated:

- Do Nothing
- Apply Deck/Crack Sealer
- Install Asphalt Overlay With Membrane Waterproofing
- Install Concrete Overlay
- Replace Deck

Based on findings in Lehigh's report, it can be concluded that early age deck cracking occurred. Therefore, deck cracks pose no immediate threat to public safety. A brief review of previous research regarding deck cracking and performance of deck sealers is provided. Advantages and disadvantages of each remediation options are listed along with recommendations.

Previous Research

The occurrence of deck cracking has been widely documented and researched by several state agencies. Despite the large number of studies, concrete deck cracking is still a problem faced by many state agencies. Below are some key highlights of some of the findings.

- Rahim and Jansen (2006) conducted a nationwide survey to learn the current state-of-practice in sealing bridge decks. Forty transportation agencies responded to the survey. Eighty-five percent responded of having transverse cracks.

Crack Types Experienced by Different DOTs			
Type of Cracks	**Caltrans**	**# of DOTs[1]**	**Percent,[2]**
Transverse	x	34	85
Random	x	26	65
Other[3]	x	6	15

1 Other than Caltrans
2 Some DOTs reported experiencing more than one crack type
3 Include longitudinal and diagonal

Sealant Types Used by Different DOTs			
Type of Sealant	**Caltrans**	**# of DOTs[1]**	**Percent,[2] %**
HMWM	x	17	42.5
Epoxy		21	52.5
Polyester		3	7.5
Other[3]		15	37.5

1 Other than Caltrans
2 Some DOTs reported using more than one sealer
3 Include Urethanes, Silanes, Siloxanes, Linseed Oils and Bituminous membrane.

Surface Preparation Technique			
Surface Preparation	**Caltrans**	**# of DOTs[1]**	**Percent,[2] %**
Power Broom		6	15.0
Forced Air		11	65.0
Pressurized Water		2	12.0
Other[3]	x (sand blasting)	5	12.5

1 Other than Caltrans
2 Some DOTs reported employing more than one technique
3 Include sand blasting, shot blasting, and follow manufacturer instruction

Crack Width Criteria for Using HMWM			
Width Criterion	**Caltrans**	**# of DOTs[1]**	**Percent,[2] %**
<1.6 mm (<0.0625 in)	x	12	70.0
1.6-3.2 mm (0.0625-0.125in)	x	6	35.0
Other[3]		1	6.0

1 Other than Caltrans
2 Some DOTs reported adopting more than one criterion
3 Follow manufacturer's instruction

- The overall trend in deck cracking (crack density equal to crack length per area of bridge deck) has increased from 1984 to 1993 (Darwin, Browning, and Lindquist, 2004).

- Colorado DOT reported that eight-two percent of their bridges had some form of deck cracking (Yunping Xi et al., 2003). These bridges were constructed from 1993 to 2002.

- Plastic shrinkage occurs mainly due to a rapid loss of water from the concrete surface before it has time to set. Chemical shrinkage results from chemical reactions within the cement paste and includes hydration shrinkage. Drying shrinkage is caused by the reduction in volume due to water loss during the drying process (Gilbert, 2001).

- A cooperative study by the Portland Cement Association and ten state transportation agencies concluded the predominant mode of deck cracking was in the transverse direction, perpendicular to traffic (Carden and Ramey, 1999).

- According to another survey, more than 100,000 bridge decks in the U.S. have exhibited some form of early transverse cracking (Krauss and Rogalla, 1996).

- A combination of shrinkage and thermal stresses cause most of the transverse deck cracks (Krauss and Rogalla, 1996).

- Ineffective curing was the most common reason suggested by transportation agencies for excessive transverse deck cracking (Krauss and Rogalla, 1996).

- Corrosion of reinforcing steel in bridge decks is primarily associated with the diffusion of chlorides into the concrete. Chloride ingress into the concrete is the result of chloride bearing deicing salts. Chlorides deposited on the deck surface will diffuse through the porous concrete and, in time, cause corrosion of the steel reinforcement.

- Studies have shown that chloride levels between 1.0 to 1.4 lbs/cy accelerate corrosion of steel deck reinforcement (DM-4 2007). However, bridge decks have continued to perform well with 6 to 9 lbs/cy.

- There is no single chloride concentration that is appropriate for use as the threshold concentration. Threshold values can vary widely between bridge decks as well as within a single bridge deck. Factors affecting the threshold concentrations include: cement composition, moisture content water to cement ratio, and temperature. These factors influence the chloride binding capacity of the cement paste, the capability to initiate corrosion of the steel, and the ability for localized corrosion (pitting) to form (Williamson 2007).

- Krauss and Rogalla, (1996) reported disagreement among researchers and transportation agencies regarding how wide a crack can be before affecting the deck performance.

- ACI 2001 defines crack severity as; fine for crack widths less than 0.04", medium for cracks between 0.04" and 0.08", and wide for cracks greater than 0.08" wide. According to ACI 224, a tolerable crack width for structures exposed to deicing chemicals is 0.007", six times smaller than a "fine" crack.

- A transportation agency survey by Soriano (2002) identified acceptable crack width ranges from 0.001" to 0.125".

- Crack widths of less than 0.01 inch have little effect on the overall corrosion of steel reinforcement (Houston et al., 1972; Ryell and Richardson, 1972). Although wider cracks can accelerate the onset of corrosion over several years, crack width alone has little effect on the rate of corrosion (Beeby 1978). Cracks that follow the length of a reinforcing bar are more serious than cracks crossing transversely because the length of exposure is greater.

- Penetration of water through cracks is the most important factor involved in nearly every form of concrete deterioration, including freezing and thawing damages, reinforcement corrosion, alkali-aggregate reactions, dissolution, sulfate attack, and carbonation (Cody, 1994).

- Any reduction in the amount of water and chloride intrusion into a bridge deck has the potential to slow corrosion and reduce freeze/thaw damage (Megger 1998).

“DO NOTHING” RECOMMENDATION

Based on the above information, BAKER does not recommend the “do nothing” option. However; if the Department would like to experiment to determine the effectiveness of deck sealers, one lane could be treated with a deck sealer and the other lane not treated. The crack and deck performance could then be evaluated after three years to assess the differences.

Crack Sealers

Deck sealers can either be solvent or water based liquids that are applied to the deck surface, creating a finite impermeable layer. This layer prevents chloride-laden water from penetrating the concrete deck. Only penetrating sealers, silanes and silxanne are recommended for deck surfaces. Deck sealers will allow water vapor to escape thus permitting the concrete to dry out. In general, no sealer can fully prevent any of the various potential forms of concrete deterioration (Cady 1994). However, good quality products can retard the attack of many types of concrete deterioration and can mitigate the effects of deterioration in progress.

For deck crack sealers, high molecular weight methacrylate (HMWM) is cited as demonstrating the best performance with respect to crack penetration, bridging, and sealing (McGettigan 1992; Weyers et al. 1993; Krauss and Rogalla, 1996). HMWM is a three-component system that requires extra precaution during mixing because a violent reaction may occur if the initiator and promoter are mixed improperly.

An alternative to HMWM system is reactive methyl methacrylate (MMA). This two-component crack sealer, without the volatility potential, possesses similar performance characteristics to HMWM. Other sealing materials that exhibit good performance are epoxy, modified polyurethane (MPU), and urethane crack sealers.

Most of these products have a pH above 7 and are considered alkaline in nature. Product hazards include skin irritation, dermatitis, and other allergic responses due to prolonged exposure. Safe handling requires eyeglasses with safety shields or goggles (McGettigan, 1990). An eyewash station should also be provided. Skin protection requires rubber or neoprene gloves, an apron, and full-length shirt and pants.

There are numerous variables pertaining to the application of these products that affect a crack sealer’s overall performance. Most of these variables can be accounted for during or prior to application. Variables that affect the product performance include temperature, moisture, age of crack, and cleanliness of crack (Johnson et. Al.).

The gel time of the crack sealer is greatly affected by the temperature of the sealer. If the sealer is applied to a deck that is too hot, the sealer will cure too fast and not have

enough time to effectively penetrate the deck. If the sealer is too cold, it will take too long to cure.

Due to cleaning methods and rainfall, bridge decks often have considerable moisture residing in the cracks. Because the moisture in cracks can cause problems with the depth of penetration and bond strength of the sealer, steps must be taken to understand and deal with the moisture problem.

Cleaning cracks is a very important process in bridge repair. Contaminants like dirt, dust, and carbonation can build up in cracks of both new and old bridges. If these contaminants are not removed from the crack prior to application of the sealer, the bond strength and depth of penetration will be greatly reduced. The bond strength is reduced because the contaminants line the surface of the crack. When the sealer hardens, it bonds to a combination of the contaminants and the crack wall. As a result, a complete bond with the crack wall is not achieved.

There are two common strategies for applying crack sealers to bridge decks:

- Flood Coat - A flood coat consists pouring a large batch of crack sealer mixture over the deck. The sealer is then moved and manipulated with brooms and squeegees to direct it into the cracks. This strategy is useful for decks having extensive cracking. Typical rate of application for a flood coat of HMWM sealer is between 90-150 ft2/gallon.

- Individual crack repair – This consists of sealing the individual cracks instead of the entire deck. This can be achieved by applying the sealer with handheld bottles or wheel carts. Each apparatus would have a tapered nozzle to direct the sealer into the crack. Because of the expense of sealing products, some states prefer this method, if there fewer well-defined cracks.

Minnesota DOT prepared a report (Johnson, Schultz, French, and Reneson, March 2009), regarding concrete deck crack sealant performance. The report included:

- A comprehensive literature review on the background, application, and performance of concrete deck sealants and crack sealers

- Summary of a survey conducted by MnDOT

- Assessment of selection criteria, materials, application practices, and performances

Some of the conclusions and recommendation from the Minnesota report are given below for information.

- "The information collected in the literature review and performance survey indicates that the performance of two of the crack sealer products standout. Epoxy crack sealers tend to have the highest bond strength as well as a good resistance to freeze-thaw effects. However, HMWM products are much less viscous which enables them to achieve a larger penetration depth."

- "The information collected in the literature review and performance survey indicates that the performance of two of the crack sealer products stand out. Epoxy crack sealers tend to have the highest bond strength as well as a good resistance to freeze-thaw effects. However, HMWM products are much less viscous which enables them to achieve a larger penetration depth. Because of this property, product selection may need to depend on project conditions. If very narrow cracks are present in the bridge deck, depth of penetration may be deemed more important than bond strength indicating that an HMWM product is the best choice. Crack sealers provide no benefit to a cracked bridge deck if they do not penetrate the cracks sufficiently. However if the bridge deck cracks are large, bond strength may become a more important criterion in the selection indicating that an epoxy crack sealer is the best choice. Additionally, HMWM products are typically applied in a flood coat and epoxy products are generally applied to individual cracks. This means the extent of cracking on the bridge deck may also be a factor in the decision. If there are numerous cracks throughout the bridge deck a flood coat may be more appropriate. If the number of cracks is minimal, application of a sealer to individual cracks is more cost effective. "

- "To better understand the selection and performance of crack sealers, more research is needed in several areas. First, most of the field research exclusively used HMWM sealers to repair cracks. Because of this limitation, it is difficult to determine how sealers such as epoxies (which were promising in laboratory tests) will perform in the field. Second, more research should also be conducted to determine which sealers stand up to the rigors of freeze-thaw testing, because sealers of the same generic family can have very different reactions when subjected to similar changes in temperature. Third, the lifespan of sealed cracks should be investigated further, as well as the age when a sealer should be reapplied to a previously sealed deck. The need for this line of research is the lack of information on the topic, much which has generated a lot of conflicting opinions. Fourth, the occurrence of re-cracking should be studied further because very little research effort has been dedicated to this issue. However, of the small amount of research found on this topic, re-cracking did not seem to be an issue. Lastly, field and laboratory studies should be closely coordinated to better understand how laboratory results can be extrapolated to field performance."

Crack Sealer Recommendation

BAKER's opinion is that the existing concrete cracks will reduce the life of the structure and increase maintenance costs. Freeze-thaw cycles of water in cracks will cause additional crack widening and infiltration of de-icing chemicals. BAKER recommends applying a protective system to seal the existing cracks. A good sealer should significantly increase the life of the existing concrete deck and structure.

BAKER has based this recommendation on the following factors:

- CalTrans and MnDOT have both performed extensive research into deck cracking and sealant performance. BAKER has reviewed specifications and approved products listed by Minnesota and recommends applying a methacrylate resin deck sealer in accordance with the standard specification and manufacturer's instructions. Minnesota's approved list of methacrylate deck sealers is given in the following table.

Methacrylate Resin Crack Sealers (25 cps or less)			
Manufacturer	**Manufacturer Website**	**Product Name**	**Approved Date**
BASF	www.buildingsystems.basf.com	Degadeck® Crack Sealer Plus *	4/2/2007
Sika	www.sikaconstruction.com	SikaPronto® 19 *	4/2/2007

- Product literature is provided for both of these products at the end of this report.
- The crack sealer standard specification, used by MnDOT, is provided at the end of this report.
- The Department can use their own maintenance personnel or hire a contractor to apply the crack sealer. For both cases, personnel need to be trained and follow the manufacturer's instructions.
- If sandblasting is used, caution should be taken to prevent the sandblasting operation from opening the cracks.

Asphalt Overlay with Membrane Waterproofing

A deck overlay may consist of a hot-mix asphalt concrete and membrane (HMAM). The membrane is a barrier placed on top of the concrete and then protected by asphalt that functions as the riding surface. *NCHRP Synthesis of Highway Practice 4* (1970) reported that the use of an impermeable interlayer membrane had won favor throughout the country. Maine, Massachusetts, New Hampshire, and Rhode Island were specifying an interlayer on all important bridges. California, Illinois, Michigan, Ohio, and Tennessee were specifying membranes on selected bridges.

In 1977, only 19% of the respondents to a survey indicated that membranes were the preferred protective system on new decks and only 11% selected membranes as one of the first three options for deck repair (Manning 1995).

Asphalt Overlay with Membrane Waterproofing Recommendation

BAKER does not recommend an asphalt overlay for the following reasons:

- Deck cracks may propagate through the asphalt.
- Membrane waterproofing can be unreliable.
- 3” Asphalt overlay with a waterproof membrane will be more costly than application of a deck crack sealer.
- Asphalt overlay could hide the progression of cracking.
- The Department would not be able to evaluate new crack sealer products.
- Additional dead load would be added to the structure.

Concrete Overlays

The purpose of an overlay is to create a protective barrier over a concrete deck. Overlays may consist of latex-modified concrete (LMC), low-slump dense concrete (LSDC), micro-silica concrete (MSC), or polymer concrete (epoxy). The overwhelming number of concrete overlays in 1979 consisted of low-slump, dense concrete; polymer-modified concrete; or internally sealed concrete (*NCHRP Synthesis of Highway Practice 57* 1979). Initially, overlays were no more than 32 mm (1.25 in.) thick (Bergren and Brown 1975); however, later a nominal thickness of 50 mm (2 in.) was specified.

Generally, good performance was reported (Bergren and Brown 1975; Tracy 1976; Manning and Owens 1977). Problems associated with concrete deck overlays include

debonding of the overlay from the deck, shrinkage cracking of the overlay, and determining the appropriate time to install an overlay on a deck.

Concrete Overlay Recommendation

Although a concrete overlay may extend the life of the deck longer than a deck sealer, BAKER does not recommend this option is due to the following reasons:

- Deck cracks may propagate through the concrete overlay.
- The cost of a latex concrete overlay would be much greater than the application of a crack sealer.
- Concrete overlay would hide the progression of cracking.
- Concrete overlay eliminates the benefits of evaluating new deck crack sealer products.
- Additional dead load would be placed on the structure.

Replace Deck

BAKER does not recommend replacing the existing deck due to the following reasons:

- It is BAKER's opinion a deck replacement should only be considered when the existing deck shows major signs of distress.
- Unless the concrete mix design is changed or the cause of the deck cracking is conclusively determined, the new deck could exhibit similar cracking.
- Deck replacement is too costly.

BASF

The Chemical Company

PRODUCT DATA

7 07 18 00 **Concrete Rehabilitation**

DEGADECK® CRACK SEALER PLUS

Reactive methacrylate resin for sealing cracks and concrete decks

Description

DEGADECK® Crack Sealer Plus is a very low viscosity, low surface tension, solvent free, rapid curing reactive methacrylate resin formulated to penetrate, repair and seal cracks in concrete substrates.

POWDER HARDENER is 50% dibenzoyl peroxide (BPO) in granulated powder form to initiate the cure of the DEGADECK® resin.

Yield

100 ft²/gallon (2.5 m²/L), depending on number and volume of cracks as well as porosity of concrete.

Powder Hardener:
See mixing charts for the appropriate products.

Packaging

DEGADECK® Crack Sealer Plus is sold by weight and packaged in 38 lb (17.3 kg) pails and 396 lb (180 kg) drums. This is equivalent to 4.7 gallons (17.8 L) and 49 gallons (185.5 L) respectively.

Powder Hardener:
2.5 lb bottle
50 lb box

Color

Clear liquid

Shelf Life

1 year when properly stored

Storage

Store in cool, clean, dry area. Keep out of direct sunlight. Maximum storage temperature is 86° F (30° C). Store in original and unopened container.

Features	Benefits
• Fast curing (1 hour)	On highway and bridge projects, allows fast return of traffic flow, contributing directly to worker and driver safety
• UV resistance	Exposure to sunlight does not affect product performance
• Weather and aging resistant	Provides long-lasting service life
• 2 component	User friendly; ease of installation; shelf life stable
• Compatible with other DEGADECK® methacrylate systems	Provides complete systems approach to concrete protection
• Protects against water and chloride ion ingress	Prevents premature deterioration
• Can be used at temperatures ranging from 14 to 104° F (-10 to 40° C)	Extended application season

Where to Use

APPLICATION

- Bridge decks
- Parking structures
- Civil engineering applications
- Penetrating flood coat sealer to prevent moisture and ion ingress into substrate

LOCATION

- Exterior
- Horizontal

SUBSTRATE

- Concrete

How to Apply

Surface Preparation

1. Inspect the concrete substrate before preparation. Note the location of surface cracks and the presence of contaminants. Concrete surfaces must be dry and free of dust, dirt, oil, wax, curing compounds, efflorescence, laitance, and all other bondbreaking materials.

2. Inspect the underside of the deck for signs of leakage due to full depth cracks.

3. Check weather forecast to ensure dry conditions. Wet substrates must be allowed to dry prior to beginning work.

4. Using a dust-free, mobile shotblaster or gritblaster, brush-blast the substrate to expose surface cracking.

5. Do not use wet preparation methods.

6. Perform a second inspection, noting newly-found surface cracks. Mark these for pre-treatment. Clean out cracks and the deck surface with oil-free compressed air.

Protection and Repair

Technical Data

Composition

DEGADECK® Crack Sealer Plus is a reactive methacrylate resin.

Compliances

- DEGADECK® Crack Sealer Plus is classified under DOT regulations as Resin Solution, UN 1866, Class 3, PG II.

Test Data

PROPERTY	RESULTS	TEST METHODS
Appearance	Liquid	
Specific gravity	0.97	ASTM D 4669
Viscosity, cP (mPa-sec), at 73° F (23° C)	5-15	ASTM D 2393
Flash point, ° F (° C)	48 (9)	ASTM D 3278
Tensile strength, psi (MPa)	8,100 (56.4)	ASTM D 638
Compressive, psi (MPa)	12,800 (88.2)	ASTM D 638
Flexural Strength, psi (MPa)	11,550 (79.6)	ASTM D 638
Elongation at break, %	5.5	ASTM D 638
Hardness, Shore D	> 80	ASTM D 2240
Water absorption, % / 24 hrs	0.60	ASTM D 570

Mixing

DEGADECK® Crack Sealer Plus must be mixed with the appropriate amount of Powder Hardener just prior to application. Air/substrate temperature determines the amount as follows:

DEGADECK CRACK SEALER (1 GALLON)

TEMPERATURE ° F (° C)	WEIGHT %	VOLUME OUNCES
41 (5)	5	11
50 (10)	4	8.5
59 (15)	3	6.5
68 (20)	2	4
86 (30)	1	2

* Please consult BASF Technical Services for applications outside this temperature range.

At temperatures below 40˚ F, the DEGADECK® Crack Sealer Plus requires the addition of a cold weather additive for proper curing. Below are the instructions for use.

- Add 12 vol. oz. DEGADECK® CW Additive to 1 gallon DEGADECK® Crack Sealer Plus. Mix approximately 1 minute.
- Add hardener powder (BPO) to above mixture per ratios below. Quantities are calculated per 1 gallon batch of a (above).

TEMPERATURE ° F	VOLUME OUNCES	CURING TIME (MIN)
40	4	35
32	6.5	40
23	11	60
14	11	90

CAUTION: DO NOT MIX HARDENER POWDER (BPO) INTO DEGADECK® CW ADDITIVE, ONLY ADD PREMIXED BATCH AS IN (a) ABOVE.

Using clean, dry plastic buckets, add Powder Hardener to DEGADECK® Crack Sealer Plus and mix until dissolved (approximately 1 minute). Mixed DEGADECK® Crack Sealer Plus must be applied immediately. Do not exceed 5-gallon (20 L) batch mixes.

Application

1. DEGADECK® Crack Sealer Plus is applied as a flood coat in a gravity-fed process by broom or roller.

2. The contents of the mixed batch should be immediately poured onto the substrate and worked into cracks by distributing with 1/2" to 3/4" (13 – 20 mm) nap solvent grade rollers or broom. Do not allow material to pond. Application rate is 100 ft^2/gal (2.5 m^2/L).

3. Do not allow the mixed batch to remain in the mixing vessel. It is advisable to randomly broadcast a 30 mesh (600 µm), dry aggregate into the wet, uncured resin at the rate of approximately 4 lb/100 ft^2 (200 g/m^2).

4. Working time for ® Crack Sealer Plus is between 10 and 15 minutes once it has been applied to the substrate. Full cure to specification will be between 45 minutes and 1 hour.

Pre-Treat Wide Cracks

Cracks over 1/8" (3 mm) should be treated individually prior to deck application. Full depth cracks may require alternative treatment to prevent runoff of resin. Fill wider cracks with dry, 30 mesh silica sand. Mix a small amount of ® Crack Sealer Plus, pour into cracks and distribute with a paint brush. Squeeze bottles can also be used.

Drying Time

Allow one hour for DEGADECK® Crack Sealer Plus to gain full mechanical properties. Check for dry-to-touch condition. End result should be a darker-colored, matte finish with a minimal surface film and some loose broadcast aggregate. Open to traffic.

Clean Up

Clean tools as needed with MMA, acetone, ethyl acetate or similar solvents.

For Best Performance

- Application temperature range of substrate is between 14 and 104° F (-10 and 40° C).
- DEGADECK® Crack Sealer Plus is NOT a high molecular weight methacrylate (HMWM).
- DO NOT use for vertical surface treatments.
- DEGADECK® Crack Sealer Plus is a sacrificial film that will wear out over time, however the cracks will continue to be protected.
- Periodically inspect the applied material and repair localized areas as needed. Consult a BASF representative for additional information.
- Make certain the most current versions of product data sheet and MSDS are being used; call Customer Service (1-800-433-9517) to verify the most current version.
- Proper application is the responsibility of the user. Field visits by BASF personnel are for the purpose of making technical recommendations only and not for supervising or providing quality control on the jobsite.

Health and Safety

DEGADECK® CRACK SEALER PLUS

Warning

DEGADECK® Crack Sealer Plus contains methyl methacrylate; acrylic polymer; and methacrylic acid ester.

Risks

FLAMMABLE LIQUID AND VAPOR. May cause skin and eye irritation. Ingestion may cause irritation. Inhalation of vapors may cause irritation and intoxication with headaches, dizziness and nausea. Repeated exposure may cause injury to the kidneys and liver. Repeated or prolonged overexposure may cause central nervous system damage. May cause dermatitis and allergic responses. Repeated or prolonged contact with skin may cause sensitization.

Precautions

KEEP AWAY FROM HEAT, FLAME AND SOURCES OF IGNITION. Heat, aging, or contamination may lead to violent rupture of sealed containers. Vapors are heavier than air. Keep container closed. Check periodically for warm or bulging containers. Use only with adequate ventilation. DO NOT get in eyes, on skin or on clothing. Wash thoroughly after handling. DO NOT breathe vapors. DO NOT take internally. Use impervious gloves, eye protection and if the TLV is exceeded or used in a poorly ventilated area, use NIOSH approved respiratory protection in accordance with applicable Federal, state and local regulations. Empty container may contain hazardous residues. All label warnings must be observed until container is commercially cleaned or reconditioned.

First Aid

FIRST AID MEASURES: In case of eye contact, flush thoroughly with water for at least 15 minutes. SEEK IMMEDIATE MEDICAL ATTENTION. In case of skin contact, wash affected areas with soap and water. If irritation persists, SEEK MEDICAL ATTENTION. Remove and wash contaminated clothing. If inhalation effects occur, remove to fresh air. If discomfort persists or any breathing difficulty occurs, or if swallowed, SEEK IMMEDIATE MEDICAL ATTENTION.

Refer to Material Safety Data Sheet (MSDS) for further information.

VOC Content

< 250 g/L or 2.09 lbs/gallon, less water and exempt solvents.

POWDER HARDENER

Danger - Organic Peroxide

Powder Hardener contains dibenzoyl peroxide; and dicyclohexyl phthalate.

Risks

May cause skin, eye and respiratory irritation. May cause dermatitis and allergic responses. Repeated or prolonged contact with skin may cause sensitization. May cause dermatitis and allergic responses. Ingestion may cause irritation.

Precautions

KEEP AWAY FROM HEAT, FLAME AND SOURCES OF IGNITION. Use only with adequate ventilation. Avoid contact with skin, eyes and clothing. Keep container closed when not in use. Wash thoroughly after handling. DO NOT take internally. Prevent inhalation of dust. Use impervious gloves, eye protection and if the TLV is exceeded or used in a poorly ventilated area, use NIOSH/MSHA approved respiratory protection in accordance with applicable Federal, state and local regulations. Empty container may contain hazardous residues. All label warnings must be observed until container is commercially cleaned or reconditioned.

First Aid

In case of eye contact, flush thoroughly with water for at least 15 minutes. In case of skin contact, wash affected areas with soap and water. If irritation persists, SEEK MEDICAL ATTENTION. Remove and wash contaminated clothing. If inhalation causes physical discomfort, remove to fresh air. If discomfort persists or any breathing difficulty occurs or if swallowed, SEEK IMMEDIATE MEDICAL ATTENTION.

Refer to Material Safety Data Sheet (MSDS) for further information.

VOC Content

0 g/L or 0 lbs/gallon, less water and exempt solvents when components are mixed and applied per manufacturer's instructions.

DEGADECK® CRACK SEALER PLUS CW

Warning

DEGADECK® Crack Sealer Plus CW contains n,n-Dimethyl-p-toluidine.

Risks

Toxic by inhalation, in contact with skin or by ingestion. May cause skin, eye and respiratory irritation. Prolonged exposure to vapors or repeated skin exposures may effect liver, nervous system and blood-forming system and may cause fatigue, loss of appetite, headache and dizziness. Can be absorbed through skin and may cause loss of oxygen-carrying capacity of blood.

Precautions

Avoid contact with skin, eyes and clothing. Wash thoroughly after handling. DO NOT breathe vapors. Use only with adequate ventilation. Keep container closed. Use impervious gloves, eye protection and if the TLV is exceeded or if used in a poorly ventilated area, use NIOSH/MSHA approved respiratory protection in accordance with applicable Federal, state and local regulations. Empty container may contain hazardous resides.

First Aid

In case of eye contact, flush thoroughly with water for at least 15 minutes. SEEK IMMEDIATE MEDICAL ATTENTION. In case of skin contact, wash affected areas with soap and water. If irritation persists, SEEK MEDICAL ATTENTION. Remove and wash contaminated clothing. If inhalation causes physical discomfort, remove to fresh air. If not breathing, give artifical respiration. If breathing is difficult, administer oxygen. SEEK IMMEDIATE MEDICAL ATTENTION. If swallowed, SEEK IMMEDIATE MEDICAL ATTENTION. Refer to Material Safety Data Sheet (MSDS) for further information.

VOC Content

0 g/L or 0 lbs/gal less water and exempt solvents.

For medical emergencies only,
Call ChemTrec (1-800-424-9300).

® = registered trademark
DEGADECK® = trademark of Evonik Röhm GmbH, Darmstadt / Germany

BASF Construction Chemicals, LLC – Building Systems

889 Valley Park Drive
Shakopee, MN, 55379

www.BuildingSystems.BASF.com

Customer Service 800-433-9517
Technical Service 800-243-6739

For professional use only. Not for sale to or use by the general public.

Form No. 1031118 4/09
Printed on recycled paper including 10% post-consumer fiber.

Product Data Sheet
Edition 8.2003
Identification no. 309
SikaPronto 19

Construction

SikaPronto® 19

Easy-to-use, high molecular weight methacrylate, crack healer/penetrating sealer

Description	SikaPronto 19 is a 2-component, rapid-curing, solvent-free, high molecular weight methacrylate, crack healer/penetrating sealer.
Where to Use	Use on grade, above and below grade on concrete and mortar. SikaPronto 19 seals surface of concrete from water and chlorides. For horizontal decks, slabs, patios, driveways, parking garages and other substrates exposed to foot and pneumatic-tire traffic.
Advantages	■ Penetrates cracks by gravity. ■ Structurally improves concrete surface. ■ Easy-to-use, 2-component system. ■ Does not produce a vapor barrier. ■ Low viscosity for easy, topical applications and excellent penetration into cracks. ■ Jobsite safe; not flammable. ■ Low odor - significantly less than most other methacrylates. ■ High bond strength. ■ Prolongs life of cracked concrete. ■ Flash point of 'A' Component is a high, safe-to-work-with 220°F (104°C). ■ As a penetrating sealer, SikaPronto 19 reduces water absorption and chloride-ion intrusion.

Typical Data *(Material and curing conditions @ 73°F (23°C) and 50% R.H.)*

Shelf Life	Component 'A': 9 months in original, unopened containers. Component 'B': 6 months in original, unopened containers.
Storage Conditions	Store dry at 40°-95°F (4°-35°C). **Condition material to 65°-75°F (18°-24°C) before using.** Storage at higher temperatures may cause material to pre-polymerize and will reduce shelf life.
Color	Light purple when liquid; light amber after cure.
Mixing Ratio	Plant-proportioned kit; mix entire unit.
Methacrylate Monomer Viscosity	25 cps maximum
Pot Life	Approximately 20 minutes.
Bulk Cure Time	6 hours** maximum
Traffic Time	12 hours** maximum

Flexural Properties (ASTM D-790):

1 day	Flexural Strength (Modulus of Rupture)	2,500 psi (17.2 MPa)

BOND STRENGTH (ASTM C-882): Hardened concrete to hardened concrete

2 day	**(dry cure)**	Bond Strength	2,100 psi (14.4 MPa)
14 day	**(moist cure)**	Bond Strength	2,300 psi (15.8 MPa)

Compressive Properties (ASTM D-695): Compressive Strength, psi (MPa)

	40°F* (4°C)*	**73°F* (23°C)***	**90°F* (32°C)***
1 hour	-	1,000 (6.8)	1,900 (13.1)
2 hour	-	2,300 (15.8)	2,700 (18.6)
1 day	1,800 (12.4)	2,900 (20.0)	3,500 (24.1)
7 day	3,500 (24.1)	3,100 (21.3)	4,300 (29.6)

*Material cured and tested at the temperatures indicated.
**Times vary based on temperature, humidity and exposure to sunlight.

Construction

Coverage	Typical coverage is 90-150 sq. ft./gal. for crack healing and surface sealing. Coverage varies with porosity and surface profile of substrate. Higher porosity will reduce coverage.
Packaging	1 gal. units, 4/ctn.; 4.5 gal. units.

How to Use

Surface Preparation	Substrate must be clean, sound and free of surface moisture. Remove dust, laitance, grease, oils, curing compounds, waxes, impregnations, foreign particles, coatings and disintegrated materials by mechanical means (i.e., blastcleaning). For best results, substrate should be dry.
Mixing	Empty entire contents of 'B' Component into pail containing 'A' Component. Mix for 3 minutes with a low-speed drill (400-600 rpm) using a Sika paddle. Mix only that quantity that can be placed within the pot life.
Application	SikaPronto 19 is applied to horizontal surfaces by roller, squeegee or broom. Spread material over area and allow to pond over cracks. Let material penetrate into cracks and substrate; remove excess leaving no visible surface film. For cracks greater than 1/8 in. (3 mm) wide, fill crack with oven-dried sand before applying SikaPronto 19. Seal cracks from underside, when accessible, to prevent leakage. A second treatment may be required on very porous substrates. Apply second treatment before broadcasting. After treatment, wait at least 20 minutes at 73°F (23°C); cover with light broadcast of a dry 8/20 or similar sand. Distribute evenly over the surface at a rate of 15 to 20 lbs. per 100 sq. ft. Do not exceed a delay of 2 hours at 73°F (23°C) before broadcasting. Allow to cure 12-16 hours at 73°F (23°C). Remove any loose sand and open to traffic. Consult Sika Technical Service for additional information.
Limitations	■ Do not thin. Addition of solvents will prevent proper cure. ■ Minimum ambient and substrate temperature 35°F (2°C). ■ Minimum age of concrete is 21-28 days depending on curing and drying conditions. ■ Sealed concrete surface may appear blotchy due to differential absorption. ■ Not designed to seal cracks subject to hydrostatic pressure at the time of application.
Caution	**Component 'A' - Irritant -** Skin, eye and respiratory tract irritant. Avoid contact. Avoid breathing vapors. Use only with adequate ventilation. Use of safety goggles and chemical resistant gloves is recommended. In case of high vapor concentrations or exceedance of PELs, use an appropriate NIOSH approved respirator. Wash thoroughly after use. Remove contaminated clothing. **Component 'B' - Irritant; Organic Peroxide -** Contains benzoyl peroxide. Skin and eye irritant. Avoid contact. Avoid breathing vapors. Use only with adequate ventilation. Use of safety goggles and chemical resistant gloves is recommended. In case of high vapor concentrations or exceedance of PELs, use an appropriate NIOSH approved respirator. Wash thoroughly after use. Remove contaminated clothing.
First Aid	**Eyes:** Hold eyelids apart and flush thoroughly with water for 15 minutes. **Skin:** Remove contaminated clothing. Wash skin thoroughly for 15 minutes with soap and water. **Inhalation:** Remove person to fresh air. **Ingestion:** Do not induce vomiting. **In all cases, contact a physician immediately if symptoms persist.**
Clean Up	Remove uncured material from tools and mixing equipment with water. Cured material can only be removed mechanically. In case of spillage, collect and/or absorb and dispose of in accordance with current, applicable local, state and federal regulations.

KEEP CONTAINER TIGHTLY CLOSED — KEEP OUT OF REACH OF CHILDREN
NOT FOR INTERNAL CONSUMPTION — FOR INDUSTRIAL USE ONLY
CONSULT MATERIAL SAFETY DATA SHEET FOR MORE INFORMATION

Visit our website at www.sikausa.com — **1-800-933-SIKA NATIONWIDE**

Regional Information and Sales Centers. For the location of your nearest Sika sales office, contact your regional center.

Sika Corporation
201 Polito Avenue
Lyndhurst, NJ 07071
Phone: 800-933-7452
Fax: 201-933-6225

Sika Canada Inc.
601 Delmar Avenue
Pointe Claire
Quebec H9R 4A9
Phone: 514-697-2610
Fax: 514-694-2792

Sika Mexicana S.A. de C.V.
Carretera Libre Celaya Km. 8.5
Corregidora, Queretaro
C.P. 76920 A.P. 136
Phone: 52 42 25 0122
Fax: 52 42 25 0537

QUALITY ISO 9001 9002 ACHIEVEMENT

Created: 04/02/07
Revised: 10/24/2008 (3)

Only use when recommended by the Regional Br. Const. Eng.
{[use for new or rehab. when crack width is .007 (just wide enough to see at five feet from the surface) - .025 inches, bigger cracks will require a more appropriate filler to be used first] [ACI states: the crack width of.025+ was selected because this is the size that the epoxies will fill easily and also the cracks are usually smaller below the surface]}

SB- BRIDGE DECK CRACK SEALER

SB-___.1 Description

Furnish and apply a protective methyl methacrylate or epoxy sealer to _____ of the roadway surface areas of Bridge No. _____, excluding the sidewalk, raised median and concrete railings. Perform this work in accordance with the applicable provisions of MnDOT 2433, the Plans, as directed by the Engineer, and the following:

SB-___.2 General

Apply a MnDOT approved, methyl methacrylate or epoxy sealer. Provide the Engineer with the sealer Manufacturer's written instructions for application and use, at least 30 calendar days before the start of the work.

SB-___.3 Materials

Furnish only one of the materials on the Department's "Approved/Qualified Product Lists of Bridge Crack Sealers" (http://www.dot.state.mn.us/products/index.html). For products not on the Department's prequalified list, provide information as required on the web site and as stated in the following tables.

Qualification Requirements for Epoxy Crack Sealers	
Viscosity, ASTM C 881	125 cps -
Gel Time, ASTM C 881	20 minutes minimum
14 Day Bond Strength, ASTM C882	1500 psi minimum
Gel Time (ASTM 2471)	60 minutes (max.)
Compressive Yield Strength , ASTM C 881	4000 psi 7 day minimum
Tensile Strength, ASTM C881	4,000 psi minimum
Tensile Elongation, (ASTM C881)	2.5 % minimum
Shear Bond Adhesion (ASTM C882)	>1500 psi

Qualification Requirements for MMA Resin	
Viscosity (Brookfield RVT)	25cps -
Gel Time, ASTM 2471	60 minutes maximum
Tack Free Time	5 Hours maximum at 72° F and 50 % R.H.
Tensile Elongation, ASTM D638	5% minimum
Shear Bond Adhesion, ASTM C882	>1500psi

The manufacturer of the selected product must directly ship a one quart sample of the sealer to the MnDOT Materials Lab (1400 Gervais Avenue; Maplewood, MN 55109) for quality assurance testing and IR scanning at least 30 days prior to the start of the work.

SB-___.4 Application Requirements

A. Surface Preparation

Clean all areas to be sealed by removing dirt, dust, oil, grease, curing compounds, waxes, laitance, or other contaminants by performing a light sweep sandblast that does not expose the aggregate. Collect all debris and other material removed from the surface and cracks, and dispose of it in accordance with applicable federal, state, and local regulations. Immediately before applying the sealer direct a 125 psi air blast, from a compressor unit with a minimum pressure of 365 ft^3 / min., over the entire surface to remove all dust and debris paying special attention to carefully clean all deck cracks. Use a suitable oil trap between the air supply and nozzle. Provide shielding as necessary to prevent dust or debris from striking vehicular traffic. Have the Engineer approve the prepared surface prior to applying the sealer.

Air dry a wet deck for a minimum of seventy-two hours before applying the sealer.

Cover all expansion joints in a manner that will prevent the sealer from contacting the neoprene seals but will allow sealer to penetrate the steel/concrete interface on each side of the joint. Secure the materials used to cover the neoprene seals with duct tape or another material approved by the Engineer.

B. Weather Limitations

Do not apply sealer materials during wet weather conditions or if adverse weather conditions are anticipated within 12 hours of the completion of sealer application. Do not mix or apply any of these products at temperatures lower or higher than those specified in their product literature. Apply the sealant at the coolest time of the day within these limitations. Application by spray methods will not be permitted during windy conditions, if the Engineer predicts unsatisfactory results.

C. Sealer Application

Do not thin or alter the sealer unless specifically required in the Manufacturer's instructions. Mix the sealer before and during its use as recommended by the Manufacturer. Distribute the sealant as a flood coat in a gravity-fed process by broom or roller, or with a spray bar near the surface so the spray pattern and coverage rates are reasonably uniform to the satisfaction of the Engineer. Do not allow running or puddling of the sealer to occur. Apply the sealant at a minimum rate of 100 sq. ft. / gallon and apply in two coats if running or puddling can not be controlled. Apply a second treatment on very porous substrates.

Broadcast to refusal an oven-dried 30 grit or similar sand into the wet, uncured resin.

Allow the sealant to dry according to the Manufacturer's instructions. Do not allow vehicular traffic onto the treated areas until the sealer has dried and the treated surfaces provide safe skid resistance and traction.

D. Test Section

Apply the sealant to a test area, of at least 50 sq. ft., on the shoulder of Bridge No. _____. The selected test area must contain a crack that is visible from five feet above the deck (.007 inches) but not be larger than .025 inches. The test section will be used to evaluate the application equipment, coverage rate, drying times, traffic control, etc. Propose the specific location and application time for the test section at least 5 days prior to applying the sealer. A technical representative from the sealer manufacturer must be present during application and drying of the test section.

Add a dissipating UV Dye to the sealant prior to placing it on the test area. This dye will help determine the crack penetration of the sealant. Within 30 days of placing the test panel, recover a core that is no greater than four inches in diameter and includes a sealed crack as determined above. Conduct independent certified laboratory tests for crack width and penetration depth of the sealer. Send results to Structural Concrete Engineer at the MnDOT Materials Lab (1400 Gervais Avenue; Maplewood, MN 55109). All the test results are for MnDOT informational purposes only.

Prior to application of the sealant, hold a meeting with the Manufacturer's Representative, the Engineer, and the Contractor to discuss all necessary safety precautions and application considerations.

SB-___.5 Method of Measurement

Measurement will be made to the nearest square foot of concrete area sealed based on surface area.

SB-___.6 Basis of Payment

Payment for Item No. 2433.618 "BRIDGE DECK CRACK SEALER" will be

made at the Contract price per square foot and shall be compensation in full for all costs of furnishing and applying the sealer to the bridge decks, as described above, including surface preparation, and all incidentals thereto.